Synthetic magnetism in quantum gases and photonic lattices

Dubček, Tena

Doctoral thesis / Disertacija

2017

Degree Grantor / Ustanova koja je dodijelila akademski / stručni stupanj: **University of Zagreb, Faculty of Science / Sveučilište u Zagrebu, Prirodoslovno-matematički fakultet**

Permanent link / Trajna poveznica:

Repository / Repozitorij:

University of Zagreb

Tena Dubček

SYNTHETIC MAGNETISM IN QUANTUM GASES AND PHOTONIC LATTICES

DOCTORAL THESIS

Zagreb, 2017.

University of Zagreb

FACULTY OF SCIENCE
DEPARTMENT OF PHYSICS

Tena Dubček

SYNTHETIC MAGNETISM IN QUANTUM GASES AND PHOTONIC LATTICES

DOCTORAL THESIS

Supervisors:

prof. dr. sc. Hrvoje Buljan

prof. dr. sc. Marin Soljačić

Zagreb, 2017.

Sveučilište u Zagrebu

PRIRODOSLOVNO - MATEMATIČKI FAKULTET
FIZIČKI ODSJEK

Tena Dubček

SINTETSKI MAGNETIZAM U KVANTNIM PLINOVIMA I FOTONIČKIM REŠETKAMA

DOKTORSKI RAD

Mentori:
prof. dr. sc. Hrvoje Buljan
prof. dr. sc. Marin Soljačić

Zagreb, 2017.

Acknowledgements

I would like to thank the world for being such an extraordinary place—hosting so many diverse intriguing phenomena that wait to be appreciated and comprehended, as well as all the nice people, in all the different beautiful places, whom I could join and who wanted to join me on this journey. Hrvoje and Marin—my supervisors, who showed me what a good physicist's journey is supposed to look like. Dario, Karlo, Bruno, Robert, Neven, Ticijana, Damir, Adi, Ido, Yichen, Li, Charles, Yi, Josue, Pri, Georgia, Scott, John, Max, Nick, Collin, Wolfgang, Marinko, Marija, Antonio, Katja, Boris, Ivica, and Davor—my collaborators in science. Agneza, Filip, Luka, Marko, Ivona, Jure, Nikola, Maritere, Gea and Bijesa—my collaborators in laughter. Ksenija, Marina, Marko and Ivan—who always knew how to solve my non-physics problems. All my friends in and from all different parts of the world—whom I don't even want to attempt to list. Ria and Lena—my everyday cuteness divergences. Dajana, Pavo, Goran, Davor—my crazy physicists' family. And, once again, Filip—my favorite physicist, my favorite friend. My favorite person.

Summary

Keywords: *synthetic magnetism, ultracold atoms, quantum gases, photonics, photonic lattices, topological matter, Weyl points, protected surface states, fractional statistics, anyons, laser assisted tunneling, grating assisted tunneling, conical diffraction, Tonks-Girardeau gas, pointlike interactions, evolution, synthetic Lorentz force, radiation pressure*

Many intriguing phenomena in modern physics are rooted in the coupling of electric charge to magnetic fields. However, it mostly includes quantum many-body systems, which makes these systems hard to address both experimentally—because of the rather extreme conditions they usually require, and theoretically—because of the exponential dependence of the required classical computer memory on the number of quantum system constituents. The solution is found by following Feynman's idea of the so-called quantum simulators. Namely, as new methods for synthetic magnetism are developed, controllable systems of neutral atoms and photons are governed to realize and simulate various fascinating phenomena, which are typically emergent only in elusive states of matter.

The contribution of the work presented in this thesis is twofold. The first part focuses on the role of synthetic magnetism in the research of topological phases [1, 2]. The latter are nowadays causing a lot of excitement, due to their fascinating emergent behavior, which opens the way for diverse technological applications. By taking advantage of tunable synthetic magnetic fields, we point out how topological phases that otherwise rely on complicated space groups and are thus hardly obtainable, can be realized in simple lattice geometries. Namely, we show that Weyl points, and all of the related phenomena, can be experimentally addressed in an experimentally viable ultracold atomic lattice with laser assisted tunneling [1]. We also consider the realization and detection of a state with fractional statistic in an ultracold atomic gas. We demonstrate how standard methods

and understanding have to be taken with caution when studying topological matter via quantum simulation and synthetic magnetism. Specifically, we point out that the momentum distribution, one of the key signatures of quantum states of matter, is not a proper observable for a system of anyons [2]. As a substitute, we propose to use the asymptotic single-particle density after expansion of anyons in free space from the state.

The second part of the thesis discusses our proposals of new methods for introducing synthetic magnetism in atomic and photonic systems [3–7]. We show that drawing analogies between different physical systems can yield new ideas in synthetic magnetism, which enables addressing intriguing topological phases and beyond. Namely, we propose a grating assisted tunneling scheme that introduces tunable synthetic magnetic fields in an photonic lattice [3], inspired by the laser assisted tunneling method for optical lattices. We also introduce an approach for the mapping of light propagation in dielectric structures and ultracold atomic dynamics to intriguing discrete models. By taking advantage of it, we also confirm the applicability of laser assisted tunneling for a Tonks-Girardeau gas in a 1D optical lattice [4]. Finally, we extend the concept of simulation to complex classical, rather than quantum, systems in the presence of magnetism. We propose a method for creating a synthetic Lorentz force in a classical ultracold atomic gas [5], which was recently experimentally realized through a collaboration with an experimental group [6, 7].

Contents

Introduction

"And I'm not happy with all the analyses that go with just the classical theory, because nature isn't classical, dammit, and if you want to make a simulation of nature, you'd better make it quantum mechanical, and by golly it's a wonderful problem, because it doesn't look so easy. Thank you."

Richard Feynman [8]

The collective behavior of a huge number of quantum particles can yield some of the most complex and unexpected phenomena in the world around us, such as superconductivity, superfluidity or Bose-Einstein condensation. Understanding and predicting the behavior of any strongly interacting many-body system is demanding: even when all single-particle governing laws are known, the big number of variables required for describing the whole system makes deducting its properties a formidable mathematical challenge. Luckily, in many of the cases, today's access to powerful computational resources allows physicists to extract relevant information without having to solve the equations analytically. Results obtained by numerically simulating many-body systems on computers greatly contribute to everyday's scientific advances. For a system of quantum particles, however, the number of degrees of freedom depends exponentially on the number of its constituents. The computer

memory required to describe and solve such an ensemble thus grows in the same manner, which is why the numerical approach is limited to a reduced number of particles.

1.0.1 Quantum simulators and synthetic magnetism

Quantum simulators

In 1982, Richard Feynman introduced the idea of using controllable physical systems to simulate desired quantum phenomena [8]. Based on the universality of quantum mechanics, he proposed the concept of quantum simulators as a solution for the problem classical computers face when dealing with quantum many-body systems. Feynman proposed to use a highly controllable quantum system that is carefully tailored in such a way to fully mimic (simulate) a target quantum many-body system, and its phenomena that would otherwise remain hidden and not understood.

Ultracold atomic gases and photonic systems with synthetic magnetism

The flexibility of ultracold atomic gases and photonic systems is remarkable [9–13]. Their effective dimensionality can range from one to three dimensions. Atoms in the dilute gases [9, 10] can have bosonic or fermionic statistics. Depending on the energy landscape created by magnetic fields and laser fields in their environment, they can be trapped in harmonic, periodic or distorted potentials. Interactions between atoms can be changed by using light scattering resonances. In photonic crystals [11], the photon behavior is governed by the crystal band structure in the same way as electrons' behavior in regular materials. By tailoring the low-loss dielectric structures through which light propagates, photons can mimic electron in various interesting states.

However, in any of the two systems, either ultracold atomic or photonic, there appear to be a missing ingredient. Both atoms and photons are electrically neutral particles, and as such cannot straightforwardly reproduce magnetic phenomena. On the other hand, a wide range of intriguing phenomena in modern physics, such as the gauge invariance or the quantum Hall and Aharonov-Bohm effects, find their roots precisely in the coupling of electromagnetic fields and charged particles. Furthermore, magnetism in general has historically shown to be an excellent guideline in the search of intriguing topologically ordered phases [14]. There is thus great excitement about finding solutions and introducing

artificial (*synthetic*) magnetism for the atoms and photons. The main idea consists in searching for environments in which the neutral atoms and photons are ruled by the same laws as charged particles in magnetic fields. The strategies for obtaining synthetic magnetic/gauge fields are closely related to the system at hand. It is diverse systems, and diverse schemes, that are simultaneously enabling a successful research of new interesting phases of matter. Every single new system or scheme, however, does it from a slightly different and new perspective, thus accelerating the research process.

1.0.2 A charge in an electromagnetic field

A classical charge in an electromagnetic field

In classical electrodynamics, the behavior of a charge q of mass m in an electromagnetic field is determined by the spatial and temporal dependence of the electric $\mathbf{E}(\mathbf{r}, t)$ and magnetic $\mathbf{B}(\mathbf{r}, t)$ fields. These fields can be expressed through a scalar $\phi(\mathbf{r}, t)$ and vector $\mathbf{A}(\mathbf{r}, t)$ potential,

$$\mathbf{E} = -\nabla\phi - \dot{\mathbf{A}} \tag{1.0.1}$$

$$\mathbf{B} = \nabla \times \mathbf{A}, \tag{1.0.2}$$

with $\dot{\mathbf{A}} \equiv \partial_t \mathbf{A}$. The choice of the potentials is not unique. Both the fields $\mathbf{E}$ and $\mathbf{B}$ are unchanged if a scalar function $\chi(\mathbf{r}, t)$ is used to simultaneously transform

$$\mathbf{A} \to \mathbf{A} + \nabla\chi \quad \text{and} \tag{1.0.3}$$

$$\phi \to \phi - \dot{\chi}. \tag{1.0.4}$$

The corresponding Lagrangian

$$L(\mathbf{r}, \dot{\mathbf{r}}) = \frac{1}{2}m\dot{\mathbf{r}}^2 - q\phi + q\dot{\mathbf{r}} \cdot \mathbf{A} \tag{1.0.5}$$

leads to an equation of motion that is only dependent on the fields, $m\ddot{\mathbf{r}} = q(\mathbf{E} + \mathbf{v} \times \mathbf{B})$. From the Lagrangian 1.0.5, it also follows that the canonical momentum $\mathbf{p}$ differs from

the kinetic momentum $\mathbf{\Pi}=m\dot{\mathbf{r}}$,

$$\mathbf{p} = \nabla_{\dot{\mathbf{r}}}L = \mathbf{\Pi} + q\mathbf{A}, \tag{1.0.6}$$

resulting in the Hamiltonian

$$H(\mathbf{r}, \mathbf{p}) = \mathbf{p}\dot{\mathbf{r}} - L = \frac{1}{2}m(\mathbf{p} - q\mathbf{A})^2 + q\phi. \tag{1.0.7}$$

A quantum charge in an electromagnetic field

For a quantum charged particle (q, m), the position $\mathbf{r}$ and canonical momentum $\mathbf{p}$ are associated with the operators $\hat{\mathbf{r}}$ and $\hat{\mathbf{p}}$. At the same time, the quantization rule

$$[\hat{r}_j, \hat{p}_k] = i\hbar\delta_{jk} \tag{1.0.8}$$

has to hold for any $j, k \in \{x, y, z\}$, which is satisfied for the operator $\hat{\mathbf{p}} = -i\hbar\nabla_{\mathbf{r}}$. We point out that, as a consequence of the fact that the kinetic momentum operator differs from the latter in terms of the vector potential $\mathbf{A}(\mathbf{r}, t)$, the Fourier analysis of wavefunctions $\psi(\mathbf{r}, t)$ that is typically used for extracting information about the momentum distribution (when $\mathbf{A} = 0$) will not be applicable here. The wave function $\psi(\mathbf{r}, t)$ corresponding to the Hamiltonian (Eq. 1.0.7) for a quantum particle is also gauge dependent. Specifically, any gauge transformation of the potentials in Eq. 1.0.3 is accompanied by a gauge transformation of the wave function

$$\psi(\mathbf{r}, t) \rightarrow \psi'(\mathbf{r}, t) = e^{i\frac{q}{\hbar}\chi(\mathbf{r})}\psi(\mathbf{r}, t). \tag{1.0.9}$$

Quantum electromagnetism and a geometric phase

Unlike the case for classical charges, where the potentials ϕ and $\mathbf{A}$ have no physical meaning, in quantum mechanics one can directly measure their presence even for particles that have never penetrated regions of non-zero field. Namely, the wave function of a quantum charged particle (q, m) traveling along a path $\mathcal{P}$ in a zero magnetic field $\mathbf{B} =$

$\nabla \times \mathbf{A} = \mathbf{0}$, but non-zero vector potential $\mathbf{A}$ acquires a phase shift

$$\varphi = \frac{q}{\hbar} \int_{\mathcal{P}} \mathbf{A} \cdot d\mathbf{r} \tag{1.0.10}$$

that can be observed through interference. This so-called Aharonov-Bohm phase [15] is only dependent on the geometry of the path, not on the velocity of the particle, and it thus represents an example of the so called *geometric phases*, which we additionally address in Section 2.0.2. First considered in 1959 by Aharonov and Bohm in the context of a charge moving in the presence of an infinite solenoid [15], this remarkable feature of quantum mechanics is nowadays of central importance in the studies related to synthetic magnetism.

Periodic quantum systems and electromagnetism: the Peierls substitution

The consideration of the effects of a gauge potential in free space can be expanded to systems in which an additional spatially periodic potential is present. This question is highly motivated by the studies of the effect of magnetism on crystal electrons, which in condensed-matter physics is solved by the well known *Peierls substitution* [16]. Specifically, in a two-dimensional deep periodic potential, the presence of a magnetic field, or vector potential, can be taken in account by assigning a complex value to the lattice tunneling matrix elements

$$-J|j+1,k\rangle\langle j,k| \rightarrow -Ke^{i\varphi_{j,k \rightarrow j+1,k}}|j+1,k\rangle\langle j,k|. \tag{1.0.11}$$

The Peierls substitution states that the phase $\varphi_{j,k \rightarrow j+1,k}$ is calculated from the vector potential

$$\varphi\left(\mathbf{r}_{j,k} \rightarrow \mathbf{r}_{j+1,k}\right) = \frac{q}{\hbar} \int_{\mathbf{r}_{j,k}}^{\mathbf{r}_{j+1,k}} \mathbf{A}(\mathbf{r}) \cdot d\mathbf{r}. \tag{1.0.12}$$

Clearly, as in the continuous case, there is a gauge freedom for the spatially discretized case, leading to infinite possible choices for the non-trivial phases φ. Nevertheless, the phases accumulated by a charge that travels around a lattice cell is gauge invariant, and corresponds to the magnetic field flux through the plaquette.

1.0.3 Synthetic magnetism for atoms: an overview

Historically, the first synthetic magnetic fields were implemented in rapidly rotating Bose-Einstein condensates, in which Coriolis forces play the role of the Lorentz force [17, 18]. This scheme is suitable for rotationally invariant trapping potentials.

An appealing idea with no symmetry constraints is to place the atomic gas in a specially tailored laser field that, due to the atomic interactions with light, acts as an artificial magnetic field for neutral atoms [19]. The mechanism is based on the analogy between the Aharonov-Bohm phase [15] accumulated when a charged quantum particle undergoes a closed loop in a magnetic field, and the Berry phase [20] accumulated when an atom adiabatically traverses a closed loop in the tailored laser field [19, 21]. During such an evolution, an instantaneous eigenstate $|n\rangle$ of the atom $|\psi_n(t)\rangle$ will, in addition to the standard dynamical phase, accumulate a geometric phase γ_n—the *Berry phase*

$$\gamma_n = \oint_C d\mathbf{r} \cdot \mathcal{A}^{(n)}(\mathbf{r}). \tag{1.0.13}$$

Here $\mathcal{A}^{(n)}(\mathbf{r})$ is a vector-valued function of the path coordinates $\mathbf{r}$ that plays the role of synthetic magnetic vector potential and is given by

$$\mathcal{A}^n(\mathbf{r}) = i\langle n, \mathbf{r}| \frac{\partial}{\partial \mathbf{r}} |n, \mathbf{r}\rangle. \tag{1.0.14}$$

We present a derivation, as well as the relation of geometric phases with holonomy and topology, in Section 2.0.2. The first implementation of synthetic magnetism by using laser-atom interactions was with spatially dependent Raman optical coupling between internal hyperfine atomic states in bulk BECs [22].

In optical lattices, methods of generating synthetic magnetic fields engineer the complex tunneling matrix elements between lattice sites [23–25]. The nontrivial phases of the complex tunneling parameters can thus be interpreted as Peierls phases [16] of the atoms hopping around the lattice. Methods include shaking of the optical lattice [23], laser assisted tunneling that realized staggered magnetic fields in optical superlattices [26] and the Harper Hamiltonian in tilted lattices [24, 25], and an all-optical scheme which enables flux rectification in optical superlattices [27].

1.0.4 Synthetic magnetism for photons: an overview

A number of experiments and proposals for the creation of synthetic gauge fields for photons have also been demonstrated [28–30, 30–40]. Often, they are related to ideas that have crossed into the optics arena from the matter-wave community, i.e. condensed matter and atomic systems. Topological phenomena potentially resulting from synthetic magnetism are, however, likely to be even more attractive: e.g due to the absence of heating by spontaneous emission, or the possibility to realize unidirectional backscattering immune states that are robust to imperfections [41–44].

The methods for generating synthetic magnetic fields are determined by the details of the specific systems. In systems of coupled optical resonators, the strategy is to tune the phase of the tunneling between coupled cavities [28–31]; e.g. by using link resonators of different length [28, 31] or time-modulation of the coupling [30]. Topological features, realized via synthetic gauge fields, were shown to arise in twisted [32, 33] or strained [34, 35] photonic lattices. Photonic topological insulators were also proposed in superlattices of metamaterials with strong magneto-electric coupling [36]. By modulating 1D photonic lattices along the propagation axis, one can choose the sign of the hopping parameter between neighboring sites [37]. Recently, artificial gauge fields for the photon fluids in materials with optical nonlinearities were also considered [39].

1.0.5 Tunable synthetic magnetism via periodic driving and modulation

We want to emphasize the role periodical driving and modulations can have in the development of synthetic magnetism presented in 1.0.3 and 1.0.4, and for enriching the physics of various systems, which is additionally confirmed by the work presented in this thesis (Sections 2.1, 3.1 and 3.2). An important concept in the consideration of periodically driven systems is the Floquet analysis [45–48]. It is based on the Floquet theorem for linear systems of differential equations with periodic coefficients [45], whose most known application in physics is in the Bloch theory of crystal bands. This approach has shown to be of great interest in various physical systems, from condensed matter to the above introduced photonic and cold-atomic systems [46].

In a periodically driven quantum system, the wave function $|\psi(t)\rangle$ obeys a time-

dependent Schrödinger equation

$$i\hbar\partial_t|\psi(t)\rangle=\hat{H}(t)|\psi(t)\rangle \qquad (1.0.15)$$

with $\hat{H}(t+2\pi/\omega) = \hat{H}(t)$, where ω is the driving frequency. Floquet analysis shows that the evolution results from the interplay of two ingredients: a linear phase evolution combined with micro-motion. Namely, the time-evolution operator describing the evolution $|\psi(t)\rangle=\hat{U}(t,t_0)|\psi(t_0)\rangle$ takes the form [48]

$$\hat{U}(t,t_0) \equiv \hat{U}_F(t)e^{-\frac{i}{\hbar}(t-t_0)\hat{H}_F}\hat{U}_F^\dagger(t_0). \qquad (1.0.16)$$

The operator $\hat{U}_F(t)$ describes the time-periodic component of the dynamics, the *micromotion*, and can be expressed as $\hat{U}_F(t)=e^{-i\hat{K}(t)}$ in terms of a time-periodic kick operator $\hat{K}(t)$. On the other hand, the linear phase evolution is described by a time-independent effective Hamiltonian $\hat{H}_F$ [47, 48]. The choice of the time-independent effective Hamiltonian, as well its corresponding time-periodic micromotion operator, is not unique, although always yielding the same stationary Floquet states, i.e. eigenstates of the time-evolution operator [48]. A special choice of the micromotion phase, obtainable by a time-independent unitary transformation $\hat{U} = \hat{U}_F^\dagger(t_0)$ of its operator $\hat{U}_F(t) \rightarrow \hat{U}_F(t)\hat{U} = \hat{U}_F(t)\hat{U}_F^\dagger(t_0) \equiv \hat{U}_F(t,t_0)$, yields an effective Hamiltonian that directly generates the stroboscopic evolution (in steps of the driving period), $\hat{H}_F \rightarrow \hat{U}^\dagger\hat{H}_F\hat{U} = \hat{U}_F(t_0)\hat{H}_F\hat{U}_F^\dagger(t_0) \equiv \hat{H}_{t_0}^F$. Here $\hat{H}_{t_0}^F$ is the so called *Floquet Hamiltonian*, whose corresponding micromotion operator $\hat{U}_F(t,t_0)$ becomes equal to identity once during each driving period. The corresponding time-evolution operator is given by [48]

$$\hat{U}(t,t_0) = \hat{U}_F(t,t_0)e^{-\frac{i}{\hbar}(t-t_0)\hat{H}_{t_0}^F}. \qquad (1.0.17)$$

There exists no straightforward procedure for deriving the effective Hamiltonian governing the linear phase evolution of a Floquet system. However, a systematic approximation is given by a high-frequency expansion of the two components of the time-evolution operator $\hat{U}(t,t_0)$:

$$\hat{H}_F \approx \sum_{\mu=1}^{\mu_{cut}} \hat{H}_F^{(\mu)} \qquad (1.0.18)$$

$$\hat{U}_F(t) \approx \exp\left(\sum_{\mu=1}^{\mu_{cut}} \hat{G}^{(\mu)}(t)\right),$$

with $\left[\hat{G}^{(\mu)}(t)\right]^\dagger = -\hat{G}^{(\mu)}(t)$ [48]. Up to the additional time-independent unitary transformation $\hat{U}$, it is known as the Floquet-Magnus expansion [46]. The expressions for different terms $\hat{H}_F^{(\mu)}(t)$ and $\hat{G}^{(\mu)}(t)$ are obtained by expanding the spectrum in the powers of the inverse frequency $(1/\omega)$, and incorporating the so-called Magnus expansion [49] into the Floquet theory. According to Magnus' theorem [49], if the convergence conditions hold, an unknown function $Y(t)$ satisfying $Y'(t)=A(t)Y(t)$ and $Y(0)=I$ can be written in the form $Y(t)=\exp(\Omega(t))$. Here $\Omega(t)$ is an infinite series of commutators, whose first terms are given by $\Omega(t)=\int_0^t A(t')dt'+\frac{1}{2}\int_0^t dt' \int_0^{t'} dt'' \left[A(t'), A(t'')\right]+...$ (see [50] for a pedagogical review).

Intimately related to these considerations of Magnus from the very beginning is the study of the so called Baker–Campbell–Hausdorff formula [50]. It gives C in terms of A, B and their multiply nested commutators when expressing $\exp(A)\exp(B)$ as $\exp(C)$, which can be often of interest when considering quantum dynamics. Namely,

$$
\begin{aligned}
C(A, B) &= \log\left(\exp(A)\exp(B)\right) \\
&= A + B + \frac{1}{2}[A, B] + \frac{1}{12}\left([A, [A, B]] + [B, [B, A]]\right) + ...
\end{aligned}
\tag{1.0.19}
$$

The Floquet-Magnus expansion is guaranteed to converge if the period-averaged operator norm of the Hamiltonian is much smaller than the driving energy [46]. It happens in systems where local Floquet Hamiltonians exist even at infinite times. In periodically driven interacting many-body systems, the periodic driving often leads to a chaotic dynamics, asymptotically resulting in heating to infinite temperatures and the loss of an effective Floquet Hamiltonian. Nevertheless, the high-frequency expansion might still provide a suitable approximation, at least up to a certain time span beyond which the system heats up [48]. In the limit where the driving frequency is much faster than all other natural frequencies of the system, the system has hard time absorbing energy from the drive, leading to virtual processes dressing the low-energy Hamiltonian, and one can define the Floquet Hamiltonian at least perturbatively.

In systems for which the governing Hamiltonian diverges in the limit $\omega \to \infty$, a high-

frequency expansion cannot be straight forwardly applied [47]. For example, this situation occurs in optical lattices that use a resonant restoration of the tunneling or are subjected to a strong time-modulated driving. It is solved by first applying a time-periodic unitary transformation $\hat{R}(t)$ of both the wave function $|\psi(t)\rangle$,

$$|\psi'\rangle = \hat{R}|\psi\rangle, \tag{1.0.20}$$

and the Hamiltonian $\hat{H}(t)$,

$$\hat{H}' = \hat{R}^\dagger \hat{H} \hat{R} - i\hbar \hat{R}^\dagger \frac{\partial}{\partial t} \hat{R}. \tag{1.0.21}$$

Such a transformation, which is reflected in a global shift of the quasimomentum [48], results in a periodically time-dependent Hamiltonian with no diverging terms. It allows for a significant progress in systems where $\hat{R}(t)$ and $\hat{H}'(t)$ can be computed explicitly [47], often by taking advantage of the Baker–Campbell–Hausdorff formula (Eq. 1.0.19). From there on, the standard methods based on the high-frequency expansion (Eq. 1.0.18) can be applied.

In cases where the driving strength is weak compared to the driving frequency ω and it changes at a rate much smaller than ω, any effects due to micro-motion can be disregarded [48]. In such cases, the tight-binding Hamiltonian $\hat{H}'(t)$ (Eq. 1.0.21) can be approximated by its time-independent cycle average[48]

$$\hat{H}' \approx \frac{1}{T} \int_0^T dt \hat{H}'(t) \equiv \hat{H}_{eff}, \tag{1.0.22}$$

which successfully describes the effective system behavior away from an oscillatory dynamics at the driving frequency. The result of this rotating-wave approximation can be related to Floquet theory. The time-independent cycle-averaged Hamiltonian $\hat{H}_{eff}$ constitutes an approximation of the effective Hamiltonian $\hat{H}_F \approx \hat{H}_{eff}$, whereas the unitary operator $\hat{R}(t)$ approximates the micro-motion operator $\hat{U}_F(t) \approx \hat{R}(t)$ [48].

An ultracold atomic gas with tunable synthetic magnetism obtained by the laser assisted tunneling method (1.0.3), which we return to several times throughout this thesis (Sections 2.1, 3.1 and 3.2), is an example of a physical system where Floquet analysis can lead to important conclusions. In what follows, we address this problem in the case of a one-

dimensional optical lattice, which can later easily be generalized.

In an optical lattice, atoms are subjected to a spatially periodic potential obtained through an interaction with laser fields tailored to form a standing wave. In the limit of a deep enough periodic potential (period d), particles (atoms) in such a system can be effectively described by the tight binding Hamiltonian

$$\hat{H}_0 = \sum_m (-J\hat{a}^\dagger_{m+1}\hat{a}_m + H.c.), \tag{1.0.23}$$

where $J \in \mathbb{R}$ denotes the effective tunneling matrix element. Here $\hat{a}^\dagger_m$ ($\hat{a}_m$) are the particle creation (annihilation) operators in the m-th minimum of the periodic potential, which satisfy the corresponding commutation relations. In order to introduce synthetic magnetism, i.e. nontrivial phases of the hopping elements, the tunneling between the neighboring sites is first suppressed by introducing a linear potential ω_m that makes the energies non-resonant. The tunneling is then restored by using a pair of Raman lasers of frequencies ω_1 and ω_2 and wave vectors $\mathbf{q}_1$ and $\mathbf{q}_2$, which result in a traveling wave perturbation $\sim \sin(\omega t - qx)$. Here the Raman frequencies are chosen to be resonant, $\omega \equiv \omega_1 - \omega_2$, and $q = (\mathbf{q}_1 - \mathbf{q}_2) \cdot \hat{\mathbf{x}}$. This perturbation can be seen as a time-periodic driving, and the new system is described by the Hamiltonian

$$\hat{H} = \sum_m \left(-J\hat{a}^\dagger_{m+1}\hat{a}_m + H.c.\right) + \sum_m \left(\frac{V_0}{2}\sin(\omega t - m\phi + \phi/2) + \omega m\right)\hat{a}^\dagger_m\hat{a}_m \tag{1.0.24}$$
$$\equiv \hat{H}_0 + \hat{H}_{drive}(t),$$

where V_0 measures the strength of the Raman driving and

$$\phi \equiv qd. \tag{1.0.25}$$

The frequency of the periodic driving ω is much faster than all other energy scales in the system. The high-frequency expansion of the Hamiltonian (1.0.24) can thus provide a suitable approximation at all experimentally relevant time-scales. However, as the Hamiltonian (1.0.24) diverges in the limit $\omega \to \infty$ because of the linear term, one has first to apply a time-periodic unitary transformation that removes the divergence (Eqs. 1.0.20

and 1.0.21). Namely, taking

$$R(t) = e^{i \int^t dt' \hat{H}_{drive}(t')} = e^{i \sum_m \left(-\frac{V_0}{2\omega} \cos(\omega t - m\phi + \phi/2) + \omega m t \right) \hat{a}_m^\dagger \hat{a}_m}$$

$$\equiv e^{i \sum_m \lambda_m(t) \hat{a}_m^\dagger \hat{a}_m}, \tag{1.0.26}$$

and making use of the Baker–Campbell–Hausdorff formula (Eq. 1.0.19) for evaluating the products of exponentials, yields a Hamiltonian with no diverging terms

$$\hat{H}'(t) = \hat{H}_0 + i \sum_k \left[\lambda_k(t) \hat{a}_k^\dagger \hat{a}_k, \hat{H}_0 \right] + \frac{i^2}{2!} \sum_{k',k} \left[\lambda_{k'}(t) \hat{a}_{k'}^\dagger \hat{a}_{k'}, \left[\lambda_k(t) \hat{a}_k^\dagger \hat{a}_k, \hat{H}_0 \right] \right] + \dots$$

$$= \sum_m \left(-J e^{i(\lambda_{m+1}(t) - \lambda_m(t))} \hat{a}_m^\dagger \hat{a}_m + H.c. \right)$$

$$= -J \sum_u \sum_m \left(\mathcal{J}_u \left(\frac{V_0}{\omega} \sin \frac{\phi}{2} \right) e^{-iu(\omega t - m\phi) + i\omega t} \hat{a}_{m+1}^\dagger \hat{a}_m + H.c. \right), \tag{1.0.27}$$

where $\mathcal{J}_u$ is the u-th Bessel function. The second line in Eq. 1.0.27 is a consequence of the commutation relations for the creation and annihilation operators $\hat{a}_m^\dagger$ and $\hat{a}_m$, which we have checked holds for both noninteracting bosons and bosons with contact interactions (Tonks-Girardeau gas in Section 3.2). The third line follows by making use of the Bessel generating function $e^{\frac{x}{2} \left(t - \frac{1}{t} \right)} = \sum_u \mathcal{J}_u(x) t^u$, and writing the exponential as an infinite series of Bessel functions. In the high-frequency limit $\omega \to \infty$, the stroboscopic evolution of the Hamiltonian in the rotating frame (Eq. 1.0.27) can now be straight forwardly obtained by using the rotating-wave approximation (Eq. 1.0.22), resulting in the effective Hamiltonian

$$\hat{H}_{eff} = -J \mathcal{J}_1 \left(\frac{V_0}{\omega} \sin \frac{\phi}{2} \right) \sum_m e^{i\phi m} \hat{a}_{m+1}^\dagger \hat{a}_m + H.c.$$

$$\equiv -\sum_m K e^{i\phi m} \hat{a}_{m+1}^\dagger \hat{a}_m + H.c. \tag{1.0.28}$$

Besides effectively rescaling the amplitude of the tunneling from J to $K \equiv J \mathcal{J}_1 \left(\frac{V_0}{\omega} \sin \frac{\phi}{2} \right)$, the combination of a linear tilt and Raman driving (Eq. 1.0.24) has also introduced a nontrivial phase for the tunneling matrix elements,

$$-J \quad \longrightarrow \quad -K e^{i\phi m}. \tag{1.0.29}$$

This is precisely what is needed for a synthetic magnetic field in the optical lattice, as motivated by the Peierls substitution (Eq. 1.0.11). The nontrivial phase ϕ, i.e. the

synthetic magnetic field, is determined by the angle between the two Raman lasers (Eq. 1.0.25), offering high tunability.

1.0.6 Outline

The contribution of the work presented in this thesis to the field of synthetic magnetism for neutral atoms and photons is twofold. In the first part, we explore interesting possibilities for the realization, research and discovery of new topological states of matter in quantum gases with synthetic magnetic fields: namely, Weyl fermions and semimetals [1], and systems with fractional statistics (anyons) [2]. Besides the self-evident fundamental motivation, these topological systems hold great potential for technological advances, e.g. through quantum computation. In the second part, we propose new methods for introducing synthetic magnetism, often inspired by analogies between different physical systems: the grating assisted tunneling scheme for optical lattices [3], the laser assisted tunneling in a Tonks-Girardeau gas [4], and a synthetic Lorentz force for a classical atomic gas [5–7]. We thus open the way to other studies of light propagation or particle dynamics in synthetic magnetic fields.

CHAPTER **2**

Topological matter via synthetic magnetism

Part of the work in this chapter is published in the following papers

- <u>T. Dubček</u>, C. J. Kennedy, L. Lu, W. Ketterle, M. Soljačić, and H. Buljan,
  Phys. Rev. Lett. **114**, 225301 (2015).

- <u>T. Dubček</u>, B. Klajn, R. Pezer, H. Buljan, and D. Jukić,
  Physical Review A Rapid Communication, accepted for publication.

2.0.1 Topological order

Phase transitions and Landau symmetry breaking theory

Matter, as the substance that has mass and takes up space in the world around us, has attracted human attention since antiquity. Throughout the history of natural sciences people have contemplated about the exact nature of matter, and its classification. It was Greek philosophers who introduced the idea of matter being built of discrete building blocks. Many centuries later, the development of condensed matter theory led to the classification by the different ways in which atoms are organized in materials, resulting in their different properties. Although always formed by atoms, many different orders and forms of materials could emerge, corresponding to the different symmetries in the organizations of the constituent atoms. The theory, concentrated on the different symmetries that are changed when materials change from one order to an other, could

account for all classically encountered forms of matter, such as solids, liquids, etc. For example, during a phase transition from liquid to crystal, the continuous translation symmetry of the liquid reduces to the discrete translation symmetry of the crystal—the higher symmetry is *spontaneously broken.* For a long time, it was believed that this phenomenological *Landau symmetry-breaking theory* [51, 52], with local order parameters, was indeed describing all possible orders in matter.

Towards topological order

A few decades ago, however, it started to appear that symmetry alone was not enough to completely characterize a material. With the discovery of the Berezinskii-Kosterlitz-Thouless transition [53, 54], and in the attempt to describe high temperature superconductivity [55] and the newly discovered quantum Hall states [56, 57] with robust quantized Hall conductivity [58], it became clear that a new kind of order needed to be introduced for distinguishing states that were different, but at the same time shared all the same (spatial and non-spatial) symmetries. Such phases, and the transitions between them, could not be defined by a local order parameter. Soon, with the advent of the so called spin-orbit-induced topological insulators [59–65], new topological quantum states started appearing.

Today, the study of topological aspects, and their interplay with symmetries, is widespread in the investigation of various electronic, and (interacting) bosonic and fermionic systems. Genuinely quantum mechanical, topological order is a type of order that characterizes gaped quantum phases of matter with a robust ground state degeneracy [14, 66]. Here gaped quantum phase denotes a class of ground states that can be continuously deformed into one another by varying local Hamiltonian parameters, while maintaining a non-zero gap for all excitations above the ground state [14, 66]. These states have wave functions that are topologically nontrivial. They are characterized by topological invariants such as the Chern or $\mathbb{Z}_2$ invariants [58, 59, 64, 66], which we define in Section 2.0.2. The *topological nontriviality*, i.e. the nontrivial topological properties of these states, not related to any local order parameter, can only be detected through the observation of emergent phenomena, e.g. protected surface states [66].

Intrinsic topological order

Only a part of the so called topological states whose quantum-mechanical wave functions are topologically non-trivial, possesses real intrinsic topological order [14, 66]. Phases with intrinsic topological order emerge in strongly interacting many-body systems [66]. Up to now, they are encountered only in fractional quantum Hall systems [67–69] and the so called quantum spin liquids [70, 71]. Microscopically, intrinsic topological order is reflected in long-range quantum entanglement [14]. The many-body states cannot be written as a product state. Macroscopically, it means the state is robust against any local perturbations in the Hamiltonian [14]. Intrinsic topological order and long-range quantum entanglement lead to striking emergent phenomena: fractional charge, fractional statistics and an emergent gauge theory [14]. Besides the interesting physics on the boundaries, intrinsic topological phases have fascinating low-energy bulk excitations. Topologically ordered states are of great technological interest, especially in the area of quantum computation and information technology [72–74], because the long-range entanglement and fractional statistics significantly reduce decoherence, as wave function phases are distributed over many particles.

Symmetry protected topological states

A somewhat more trivial kind of topological state, dependent on the specific symmetries that are present in the system, occurs in the so called *symmetry protected topological phases of matter* [66, 75]. They include insulating, superconducting, superfluid and nodal systems: topological insulators [64, 76], topological superconductors [77], Dirac and Weyl semimetals [78, 79], etc. In symmetry protected topological phases, the nontrivial topological properties are only protected against local deformations that do not break the global, continuous or discrete, symmetries (time reversal, spatial, pairing, chiral, etc.), thus the name *symmetry protected*. Despite having topologically non-trivial wave functions, the quantum entanglement in these states is only short-ranged[75]. A short-range entangled quantum state can be connected to a real space direct product state through smooth local deformations. Because of this, ideas originating from systems with no intrinsic topological order can be extended to single-particle quantum systems, e.g. an electron on a lattice in magnetic field, described by the Hofstadter-Harper Hamiltonian [80], or even classical

ones. Recent examples establishing a classical version of the underlying quantum description include photonic [81] and mechanical [82] systems inspired by electronic topological insulators.

The integer quantum Hall effect, whose discovery initiated the introduction of topological studies in physics, is somewhere between the two types of topological phases, thus characterized as *invertible* topologically ordered state [83]. Namely, integer quantum Hall states are simultaneously long-range entangled, but with no emergent fractionalized quasi-particles [66]. Nevertheless, all mentioned topological quantum phases, being intrinsic or not, can host protected gapless surface states that are often the main reason for the excitement around them [66].

2.0.2 Topology, holonomy and geometric phases

In mathematics, the field of topology is concerned with properties that are conserved under continuous deformations of certain objects, called *topological spaces* [84]. It deals with the basic aspects related to the construction of topological spaces and related fundamental concepts. Topology mostly developed as a field of study out of geometry, and is still closely related to the analysis of concepts such as space, dimension, and transformation. The conserved properties are expressed through the so called *topological invariants*, which are shared by all *homeomorphic* topological spaces, i.e. spaces that can be deformed into each other without "cutting and pasting" [84]. Examples of topological invariants include compactness, connectedness, orientability, as well as algebraic invariants such as the homology and homotopy groups [84]. Spaces with nonvanishing topological invariants are said to be topologically nontrivial and lead to topological protection. The differences between distinct topological phases cannot be detected by any local order parameter.

Topology and geometry: the Gauss-Bonnet theorem and topological invariants

An archetypal example of topological invariants is found in the so-called *Euler characteristic* χ of surfaces $\mathcal{S}$ in three-dimensional Euclidian spaces [84]. For surfaces of polyhedra, where it was classically defined, the Euler characteristic is given by

$$\chi = V - E + F, \tag{2.0.1}$$

where V, E, and F are respectively the numbers of vertices (corners), edges and faces in the given polyhedron. The Euler characteristic describes a topological space's shape or structure regardless of the way it is bent. For example, the surfaces of convex spherical polyhedra (tetrahedron, cube, octahedron, etc.) have Euler characteristic $\chi = 2$, while surfaces of toroidal polyhedra all have Euler characteristic $\chi = 0$. In Fig. 2.1(a,b), we show a few examples, and relation 2.0.1 can be verified explicitly by counting the total number of vertices, edges and faces in each of the polyhedra. A generalization of this formula for arbitrary surfaces is obtained by finding a polygonization of the surface. A sphere has thus the same Euler characteristic as spherical polyhedra, $\chi_{\mathrm{sphere}} = 2$. A torus, on the other hand, is characterized by $\chi_{\mathrm{torus}} = 0$. Another rather famous example is the Möbius band, with no vertices, 2 egdes and 2 faces, resulting in the Euler characteristic $\chi_{\mathrm{M\ddot{o}bius}} = 0$ (Fig. 2.1(c)).

In differential geometry, the topology of a surface, given by the Euler characteristic, is related to its geometry by the so called *Gauss-Bonnet theorem*,

$$\int_{\mathcal{S}} K da + \int_{\partial \mathcal{S}} k_g ds = 2\pi\chi(\mathcal{S}). \qquad (2.0.2)$$

Here K is the Gaussian (local) curvature, which is integrated over the whole surface $\mathcal{S}$, and k_g is the geodesic curvature of the boundary.

For closed surfaces, the second term on the L.H.S. of Eq. 2.0.2 vanishes ($k_g = 0$), and the Euler characteristic χ is thus given by the integral of the local curvature K. Interestingly, any continuous deformations (no cutting or pasting) of the surface will, although altering the details of K, result in the same integral $\int_{\mathcal{S}} K da$, and thus same χ. In other words, the Euler characteristic χ is a *topological invariant*—a quantity not sensitive to any local deformations of the surface. From this topological invariant, one can find the *genus*, i.e. the number of handles, of a closed two-dimensional surface,

$$g = \frac{1}{2}(2 - \chi). \qquad (2.0.3)$$

For example, a sphere has no holes, which is reflected in a vanishing $g_{\mathrm{sphere}} = 0$. A torus, on the other hand, has one hole, $g_{\mathrm{torus}} = 1$, and thus cannot be obtained from a sphere by any continuous deformation (Fig. 2.1(e)). This nonzero genus, $g \neq 0$, is reflected in the emergence of *topological protection* for closed loop living on the surface of the torus.

Namely, it is impossible to deform tiny loops on the surface into loops that thread the hole by any continuous transformations, and vice-versa. Loops on the surface of a torus that are closed by threading the hole, as is shown in Fig. 2.1(e), are (topologically) protected against any continuous deformation. This is in contrast with what happens on spherical surfaces, where arbitrary closed loops can always be continuously deformed into trivial (pointlike) ones. In mathematical words, the homotopy group of the torus has two elements, of which one is nontrivial, whereas the homotopy group for a sphere contains only the trivial element.

Topology and physics: towards topological protection of emergent phenomena

Many-body physical systems and phenomena can also be considered from a topological aspect. Phenomena characterized as topological include Lifshitz [85] and Kostelitz-Thouless phase transitions [53, 54], and the previously introduced topological quantum phases. The characteristics for which they are labeled as *topological* are rather diverse. Lifshitz transitions [85], for example, are continuous quantum phase transitions, not associated with symmetry breaking, but characterized by a change of the Fermi surface topology and its connectedness. -Berezinskii-Kostelitz-Thouless transitions [53, 54], on the other hand, are vortex unbinding transitions in which the standard Landau spontaneous symmetry breaking scenario with emergent Goldstone bosons is replaced by a mechanism that involves the creation of topological defects. The latter are finite energy distortion of the order parameter field, such as vortices and dislocations, that cannot be eliminated by any continuous change of the order parameter—they are topologically protected [53, 54].

However, without a doubt the most diverse and richest topology related phenomena occur in zero-temperature and gaped quantum states [66]. Different phases (various topological insulators, superconductors or semimetals) correspond to ground states characterized by different sets of topological invariants, and the transitions between them are called topological quantum phase transitions [66]. Their topological nature is reflected in the impossibility to describe them by local order parameters, and the rise of some sort of *topological protection.* Analogously to the example with the topological protection of closed loops threading the hole of a toroidal surface, topology can have a striking impact on the physics of emergent behavior. Generally, emergent phenomena occur when, in some regimes, the low-energy physics of complex many-body systems can be characterized
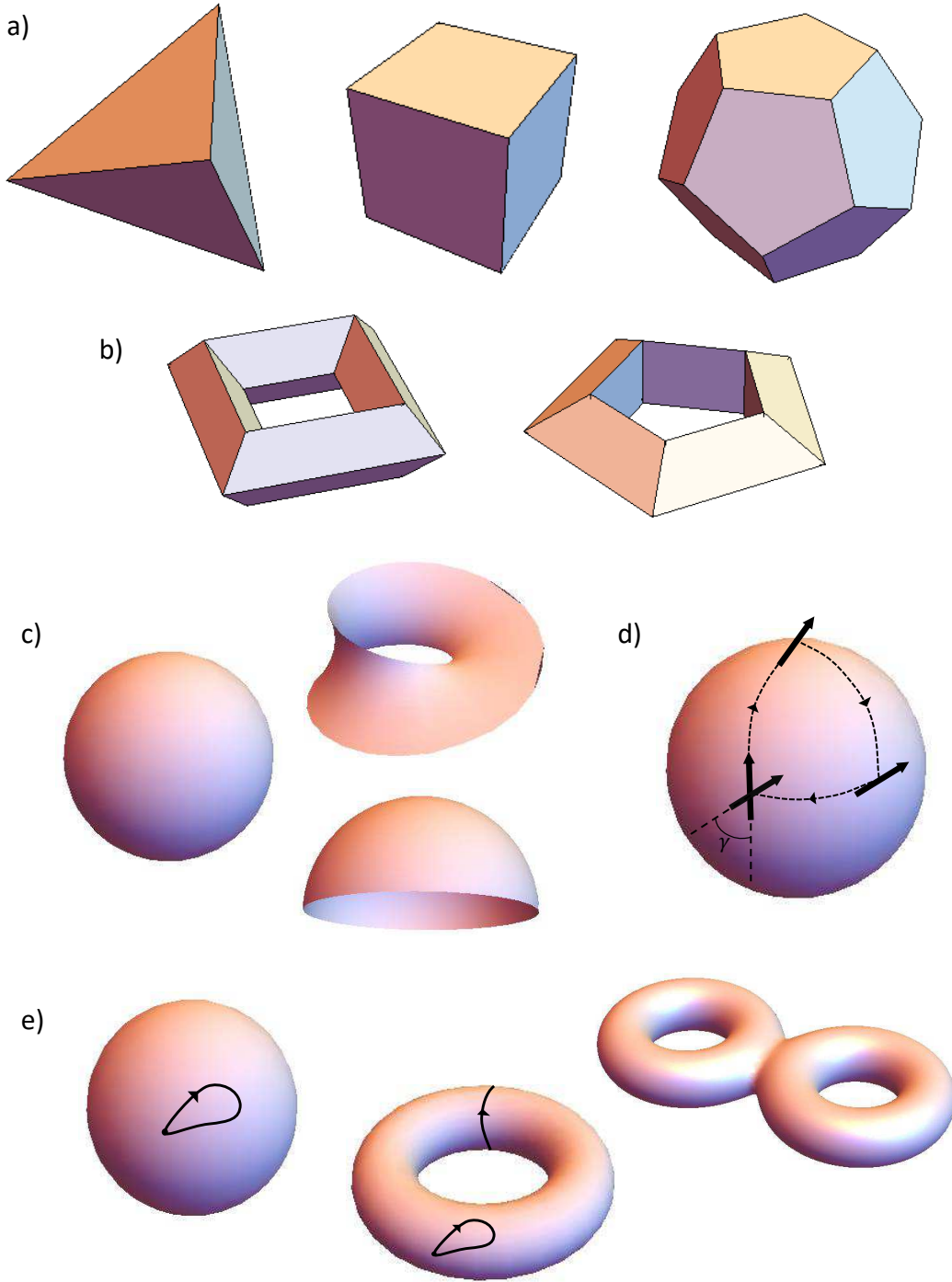
Figure 2.1: Topology and geometry.
(a) Spherical and (b) toroidal polyhedra, with Euler characteristics $\chi = 2$ and $\chi = 0$, respectively. (c) Geometrical objects with different Euler characteristics: $\chi_{\text{sphere}} = 2$, $\chi_{\text{cap}} = 1$ and $\chi_{\text{Möbius}} = 0$. According to the Gauss-Bonnet theorem, each Euler characteristic can be calculated either from polygonization of the surface, or by integrating the corresponding curvatures (Eq. 2.0.2). (d) Parallel transport of vector on a sphere. The vector direction in changed after its parallel transport along a closed loop. The resulting deflection angle is determined by the geometric path of the parallel transport (geometric phase). (e) Homotopy groups of objects with different topologies. Loops on the surface of a torus that are closed by threading the hole are (topologically) protected against any continuous deformation.

in terms of collective excitations (*quasiparticles*) [14, 66]. This is a consequence of the fact that the elementary particles are organized in a structure that breaks a continuous symmetry, resulting in the emergence of gapless Goldstone bosons [66]. The introduction of quasiparticles and their effective excitations offers a view with a more clear relation to macroscopic phenomena, yet these quasiparticles are generally not as robust as the fundamental counterparts. The scenario in topological quantum matter is rather different. In topological phases of matter, the low-energy field theory is a topological field theory—a field theory that is insensitive to the metric of space-time and is characterized by correlation functions that are topological invariants [66]. Due to this topological protection, the low-energy quasiparticles of a topologically ordered state are endowed with a robustness that is qualitatively similar to that usually enjoyed by fundamental particles. Moreover, while the collective excitations in topologically trivial matter are always scalar bosons, topologically ordered many-body systems allow for the emergence of excitations with fractional quantum numbers and fractional or even non-Abelian statistics [14, 66].

Parallel transport: geometrical and topological holonomy

Considerations of closed loops on surfaces with various curvatures and topologies can reveal even more if combined with the so called *parallel transport* of a tangent vector [84]. Namely, the vector is transported along the closed loop, always in the plane tangent to the surface of the closed surface and not allowed to rotate with respect to the normal. The way of transporting data such as vectors along a curve in a parallel and consistent manner defines the so called *connection* [84]. Depending on the characteristics of the surface, after completing the whole loop, it can happen that the vector points in a direction that differs from its initial orientation. This phenomenon is called a *holonomy* of the connection [84]. Two qualitatively different scenarios can happen, referred to as geometrical holonomy and topological holonomy.

For example, if a vector is transported parallel to the surface of a sphere around a closed loop (Fig. 2.1(d)), it will be eventually rotated by an angle with respect to the initial orientation that is equal to the solid angle subtended by the surface enclosed by the loop. Such a holonomy depends on the geometry of the path and represents the measure of the surface curvature, which is a geometrical property of the underlying space, and is thus called *geometrical holonomy* [84]. On the other hand, one can consider the parallel

transport of a tangent vector on a Mobius strip, whose curvature is zero everywhere. The resulting holonomy angle, unlike in the parallel transport on a sphere, does not depend on the details of the loop, but only on how many times the path circles the strip. Such a holonomy is due to the nontrivial topological properties of the underlying space and is called a *topological holonomy* [84]. Having a topological nature, a topological holonomy is robust against any deformations of the path that do not modify the winding number.

Holonomy in physics: the Berry phase

Geometric and topological holonomies have been identified in various physical systems as well. Historically, it started with a rather unsystematic approach that yielded several examples in both classical and quantum systems. They include the so-called Hannay angles for the rotation of a Foucault pendulum, the nontrivial phases of polarized beams passing through crystals [86], the phases of charged particle wave functions in vector potentials [15] and electron wave functions in molecular systems. Only relatively recently, following Berry's work [20], the concept of a phase factor has been recognized as a generic feature of quantum mechanics. In any quantum system with slowly varying external parameters that is subjected to a cyclic adiabatic evolution, the wave function accumulates a non-trivial geometrical phase that is dependent on the details of the evolution path—the *Berry phase* [20]. Interestingly, this phase factor for the wave function can be precisely understood as a holonomy in the Hermitian line bundle over the parameter space. The connection in such a bundle is naturally defined by the adiabatic theorem [87, 88]. Specifically, the adiabatic limit of the evolution of a wave vector describing the quantum state, along a specified path in parameter space, can be mapped to the parallel transport of a vector along a path on a curved surface. The Berry phase is technically an Abelian geometric phase, associated with adiabatic cyclic evolutions of non-degenerate pure quantum states. Later on, all these restrictions were removed, e.g. the concept generalized to non-adiabatic [89] and non-cyclic evolutions [90], possibly in mixed states [91] or degenerate ground states yielding non-Abelian phases [92]. The original Berry's case [20], however, already shows the big impact considerations of holonomies and the remarkably beautiful mathematical structure of the resulting phases in quantum mechanics.

Consider a quantum system described by a Hamiltonian $H = H(\mathbf{R})$ that depends on a set of parameters $\mathbf{R} = (R_1, R_2, ...)$ characterizing the environment [20, 66]. A

cyclic adiabatic evolution implies that the systems is described by a time-dependent set of parameters $\mathbf{R}(t)$, moving slowly along a certain closed path C in the parameter space. According to the adiabatic theorem, if the system starts in an eigenstate of $H(\mathbf{R}_0)$ described by $|\psi_n(0)\rangle = |n, \mathbf{R}_0\rangle$, it will remain in the instantaneous eigenstate corresponding to $E_n(\mathbf{R}(t))$ [20]. By solving the time-dependent Schrödinger equation, it follows that the instantaneous eigenstate $|n, \mathbf{R}(t)\rangle$ will accumulate two phases during such an evolution,

$$|\psi_n(t)\rangle = e^{i\gamma_n(t)} e^{-\frac{i}{\hbar} \int_0^t dt' E_n(\mathbf{R}(t'))} |n, \mathbf{R}(t)\rangle. \tag{2.0.4}$$

The second exponential represents the familiar dynamical phase. The additional phase $\gamma_n(t)$ is characterized by a phase angle $\gamma_n(t) = \int_0^t d\mathbf{R} \cdot \mathcal{A}^n(\mathbf{R})$. Here $\mathcal{A}^n(\mathbf{R})$ is a vector-valued function

$$\mathcal{A}^n(\mathbf{R}) = i\langle n, \mathbf{R}| \frac{\partial}{\partial \mathbf{R}} |n, \mathbf{R}\rangle, \tag{2.0.5}$$

called the *Berry connection* [66]. Although the Berry connection $\mathcal{A}^n(\mathbf{R})$ is a gauge-dependent quantity, its path integral over a closed path, i.e. the Berry phase angle γ_n, is gauge invariant [66]. Cyclic adiabatic quantum evolution can thus be regarded as the quantum version of geometrical holonomies, characterized by the Berry phase angle

$$\gamma_n = \oint_C d\mathbf{R} \cdot \mathcal{A}^n(\mathbf{R}). \tag{2.0.6}$$

The Berry connection can also be viewed as a synthetic electrodynamic vector potential, whose circulation along a closed loop C represents the synthetic magnetic flux through a surface bounded by C. Exploiting the analogy with electrodynamics, it is thus possible to introduce a gauge-invariant tensor $\Omega_{\mu\nu}^n(\mathbf{R}) = \nabla_\mu A_\nu^n(\mathbf{R}) - \nabla_\nu A_\mu^n(\mathbf{R})$, called the *Berry curvature tensor* [66]. For a three-dimensional parameter space, this reduces to the more intuitive situation $\Omega^n = \nabla \times \mathcal{A}^n(\mathbf{R})$. Physically, the Berry curvature can be thought of as the result of a residual interaction of the nth energy level with the other energy levels that were projected out as a result of the adiabatic approximation [66].

Geometric phases for electronic structures

The concept of geometric phases can be naturally adapted to electronic structures and Bloch bands in general [93, 94]. This can lead to a spectrum of interesting phenomena,

such as orbital magnetism or the Hall effects. The Brillouin zone is taken as the parameter space, with $H(\mathbf{R}) \to H(\mathbf{q})$. A slow cyclic variation of the wave vector $\mathbf{q}$ in the periodic Brillouin zone, which may be cause by an external field that enters the Hamiltonian as a time-dependent variation of $\mathbf{q} \to \mathbf{q} + \Delta\mathbf{q}(t)$ results in the wave function acquiring a geometric phase [93]. Additionally, if $\mathbf{q}$ and t are treated as independent parameters, $\mathbf{R} \to (\mathbf{q}, t)$, in cases where the eigenstates are explicitly time dependent, the geometric vector potential becomes time dependent, $\mathcal{A}^n(\mathbf{q}, t)$, and an additional geometric scalar potential arises. Just as expected from a synthetic magnetic field in momentum space, the simplest consequence of the existence of a nonvanishing Berry curvature is that it modifies the semiclassical equations of motion of a Bloch wavepacket. The anomalous velocity results from the changes in the electron distribution within the unit cell and the Berry phase is connected to the electron spatial location.

In systems with broken time-reversal symmetry, such as the paradigmatic quantum Hall effect, topological invariants are simply given by integrals of the Berry curvature over the Brillouin zone, giving rise to the so called (integer) Chern numbers [58, 66],

$$C = \frac{1}{2\pi} \int_{\partial BZ} d\mathbf{a} \cdot \mathbf{\Omega}^n(\mathbf{q}). \tag{2.0.7}$$

For time-reversal-invariant systems, $\mathbf{\Omega}(-\mathbf{q}) = -\mathbf{\Omega}(\mathbf{q})$ and all ordinary Chern numbers vanish by definition. Time-reversal-invariant systems of fermions are thus characterized by a new topological invariant, the Chern parity, i.e. the $\mathbb{Z}_2$ topological invariant ν [59, 64, 66, 95].

Mathematically, the $\mathbb{Z}_2$ topological invariant can be formulated in several ways [59, 64, 95], which tend not the be simple in the most general case. However, if the system has extra symmetry, calculations can be simplified a lot [64]. For example, in 2D spin crystals which conserve the perpendicular spin, time-reversal symmetry requires the relation between the Chern integers of up $n_\uparrow$ and down $n_\downarrow$ spins, $n_\uparrow + n_\downarrow = 0$, and the difference $n_\sigma = (n_\uparrow - n_\downarrow)/2$ defines the quantized spin Hall conductance. The $\mathbb{Z}_2$ is then given by [64, 95]

$$\nu = n_\sigma \mathrm{mod} 2. \tag{2.0.8}$$

In systems with inversion symmetry, on the other hand, the $\mathbb{Z}_2$ invariant ν is determined

from the Eq. [60, 64]

$$(-1)^\nu = \Pi_a \Pi_m \xi_m(\Lambda_a),$$ (2.0.9)

where $\xi_m(\Lambda_a)$ are the the parity eigenvalues of Bloch states, at special points Λ_a where $\mathbf{q}$ and $-\mathbf{q}$ coincide in the Brillouin zone.

2.0.3 Topological matter and (synthetic) magnetism

Magnetism has often shown to have a crucial role in the discovery and understanding of topological states of matter. The first recognized, and probably best known, example of topological order is in the fractional quantum Hall effect [67–69]. The quantum Hall effect, integer [56, 57] or fractional [67–69], shows up when 2D electrons at low temperatures are subjected to a magnetic field. This leads to a nonzero voltage V_{Hall} transverse to the direction of the current I_{channel}. The corresponding Hall conductance

$$\sigma = \frac{I_{\text{channel}}}{V_{\text{Hall}}} = \nu \frac{e^2}{h},$$ (2.0.10)

where e is the elementary charge and h is Planck's constant, is then extremely precisely quantized in terms of the so-called filling factor ν—the ratio of (quasi)particles to magnetic flux quanta. The striking feature of the quantum Hall effect is the persistence of the quantization as the electron density is varied. In the case of the integer quantum Hall effect, the factor ν is an integer number[56, 57]. Alternatively, in the case of the fractional quantum Hall effect, electrons can collectively bind magnetic flux lines into quasiparticles [67–69]. Interestingly, the corresponding excitations have a fractional elementary charge and fractional statistics—a topological order signature.

Later on, physicists tried to circumvent the necessity for the strong external magnetic fields, leading to the so called anomalous quantum Hall effect [96, 97]. Although the general mechanism is complicated with multiple contributions, the key ingredients responsible for the anomalous Hall effect are again related to magnetism, magnetization and spin-orbit coupling. The latter is a relativistic effect that can also be described through vector potentials, in general with non-commuting components (that is, non-Abelian). More generally, about a decade ago, spin-orbit coupling has also given rise to the appearance of a whole new field of symmetry protected topological phases. It is no accident: symmetries play an essential role in these systems and the existence of magnetic fields, as an archetypal exam-

ple of time-reversal symmetry interactions, can be an important guideline. Topologically ordered states yield emergent fractional statistics, charge and gauge theories [14, 66], which have all been closely related to magnetic phenomena since their very beginning. Finally, different topological phases are characterized by different Berry curvatures [14, 20, 66], which can be viewed as synthetic magnetic fields.

In this context, the recent advances in experiments on synthetic magnetic/gauge field for atoms and photons [19, 22, 40, 98] create an opportunity that should not be missed. Although the interest in topological order is nowadays spread among various areas in physics, and beyond, ultracold atomic gases and photonic systems are propelled as one of the most promising platforms for investigating these novel states of matter. Because of their high controllability, it is suddenly possible to carefully tailor the synthetic fields, and the resulting Berry curvature, thus moving the system towards desired topological orders.

2.0.4 Chapter outline

Below, we consider the realization and detection of two topological states in an ultracold atomic gas, as well as their striking properties and emergent phenomena: a system with Weyl points [1], and a system with fractional (anyonic) statistics [2]. Both realizations of Weyl and of anyonic systems have shown to be highly elusive, although of great interest both fundamentally and technologically. A viable and possibly simple scheme for their experimental realization in ultracold atomic gases, which exploits the advantages of atomic systems to contribute to the topological physics research across disciplines, is thus of great importance.

Weyl points are synthetic magnetic monopoles with a robust three-dimensional linear dispersion, identical to the energy-momentum relation for the not yet discovered relativistic Weyl fermions. In condensed matter, Weyl semimetals are a non-insulating symmetry protected topological phase. Materials with Weyl points are highly promising candidates, due to their striking properties such as the topologically protected "Fermi arc" surface states. By extending the experimentally viable laser assisted tunneling method for synthetic magnetic fields, we propose an accessible realization of Weyl points in a three-dimensional optical lattice [1]. We show that synthetic magnetism can break the ground for systems of high interest both in high energy and condensed matter physics.

Furthermore, we consider two-dimensional systems with intrinsic topological order, which give rise to emergent fractional (anyonic) statistics. Motivated by the search for a new realization and detection of such a state in an ultracold atomic gas, we point out at the striking characteristics of the particle correlations and the momentum distribution when statistics is fractional [2]. Namely, as wave functions for a system of anyons in two dimensions are not single-valued, the momentum distribution is not a proper observable. We propose to take advantage of the high controllability in the atomic gas, and use the information obtained by the free expansion of the initial state.

2.1 Weyl points in 3D optical lattices

As it is often with physical concepts, the interest for Weyl points originates from two directions in physics. Certainly, there are Weyl semimetals, the condensed matter version that can be found in gapless symmetry protected topological states of matter. For Weyl points to occur, the three-dimensional material has to possess translation symmetry-the symmetry protecting its topological nature. The time reversal and/or the inversion symmetry of the resulting lattice, however, need to be broken [99, 100], making the search for such materials challenging. Besides the earlier discussed fascinating general characteristics of topological materials, Weyl semimetals bring in some new unique aspects. The dispersions of the topological surface states intersect along the Fermi arcs. Their bulk low-energy electrons have a robust three-dimensional linear dispersion that is identical to the energy-momentum relation of the elusive relativistic massless fermions, the so called Weyl fermions, revealing the second reason for the interest in Weyl points. In relativistic quantum field theory there are three types of fermions: Dirac, Majorana, and Weyl fermions [101]. The latter two have never been observed in particle phyisics. It was conjectured that neutrinos could be Weyl fermions before the discovery of neutrino oscillations ruled out such a possibility. Weyl fermions are also related to the Adler-Bell-Jackiw chiral anomaly [102, 103]. A realization of a quantum system with emergent Weyl fermions thus opens the possibility to the study of a so called anomaly in a quantum field, i.e. the breaking of a conservation law of classical physics by quantum-mechanical effects. Finally, besides all the fundamental importance, we emphasize again the technological value of such a viable and possibly simple experimental scheme.

In the past decade, ultracold atomic gases and photonic systems have shown to be one of the most promising platforms for investigating topological states of matter [104, 105]. However, until recently, Weyl points were scarcely addressed in these fields. In photonics, the first prediction of a system with Weyl points considered a double gyroid photonic crystal with broken time-reversal and/or parity symmetry [100], which was soon followed by an experimental realization [106]. Around the same time, a few theoretical lattice models possessing Weyl points [107–109] and Weyl spin-orbit coupling [110] were studied in the context of ultracold atomic gases, owever, with no experimental realization. In this section, we propose the realization of the Weyl Hamiltonian for ultracold atoms by

a straightforward modification of the experimental system that was recently employed to obtain the Harper-Hofstadter Hamiltonian [24]. We show that, by using methods for generating synthetic magnetic fields and phase engineered hoppings, creating Weyl points is less demanding, possible away from the otherwise reduced number of space groups and points of symmetry in the Brillouin zone of the lattice in condensed matter systems [111, 112]. By including the third spatial dimension, the proposal anticipates the experimental exploration of nontrivial topology via synthetic magnetism in optical lattices with more than two dimensions.

2.1.1 Laser assisted tunneling in 2D: The Harper-Hofstadter Hamiltonian

One of the recent mathods for generating synthetic magnetic fields in optical lattices is the laser-assisted tunneling technique [24–26]. It is realized by coupling the lattice to two Raman lasers which, because of its spatial variation, makes the wave function of an atom tunneling from one lattice site to another acquire a nontrivial phase. The laser-assisted tunneling scheme requires only far off-resonant lasers and a single atomic internal state, and thus avoids heating by spontaneous emission. An early related proposal involved coupling of different internal states [113]. The scheme used in this proposal is based on the proposal introduced in Ref. [114], and later modified to enable generation of a homogeneous field [24, 25]. With this scheme, we can engineer both the amplitude and phase of the tunneling matrix elements in optical lattices. For example, if a cubic D-dimensional optical lattice has tunneling matrix elements J_d $(d = 1, \ldots, D)$, laser assisted tunneling can in principle change them to $K_d e^{i\Phi_d}$, where the phases depend on the position.

The presence or absence of symmetries play a crucial role in symmetry protected topological materials, such as the Weyl semimetals. The two-dimensional (2D) lattice realized in Ref. [24], which is our starting point, possesses both the time-reversal and inversion symmetry. Tunneling along the x direction is laser assisted, with the phase alternating between 0 and π, whereas hopping along y stays regular [see Fig. 2.2(a)]. The centers of inversion symmetry are denoted by orange crosses in Fig. 2.2(a). The time-reversal symmetry is a consequence of the fact that the accumulated phase per plaquette π is equivalent to a phase of $-\pi$. This system is a realization of the Harper Hamiltonian for $\alpha = 1/2$, where α is the flux per plaquette in units of the flux quantum [24, 25]. The

lattice has two sublattices (A-B) giving rise to pseudospin.

In quasimomentum representation, the Hamiltonian is

$$H_{\alpha=1/2}(\mathbf{k}) = -2\{J_y \cos(k_y a)\sigma_x + K_x \sin(k_x a)\sigma_y\}, \tag{2.1.1}$$

where σ_i denote Pauli matrices; it has two bands,

$$E_{\alpha=1/2} = \pm 2\sqrt{K_x^2 \sin^2(k_x a) + J_y^2 \cos^2(k_y a)}, \tag{2.1.2}$$

touching at two 2D Dirac points at $(k_x, k_y) = (0, \pm\pi/2a)$ in the Brillouin zone [115]. Here (K_x, J_y) denote the tunneling amplitudes, and (k_x, k_y) the Bloch wave vector.

2.1.2 Laser assisted tunneling in 3D: Line nodes and the Weyl Hamiltonian

Suppose that we construct a 3D lattice by stacking 2D lattices from Fig. 2.2(a), one on top of each other, with regular hopping (J_z) along the third (z) direction. This 3D lattice is described by the Hamiltonian

$$H_{LN}(\mathbf{k}) = -2\{J_y \cos(k_y a)\sigma_x + K_x \sin(k_x a)\sigma_y + J_z \cos(k_z a)\mathbb{I}\}, \tag{2.1.3}$$

where $\mathbb{I}$ is the unity matrix. The 2D Dirac points have become line nodes (LN) in the 3D Brillouin zone at which the two bands touch:

$$E_{LN} = -2J_z \cos(k_z a) \pm 2\sqrt{K_x^2 \sin^2(k_x a) + J_y^2 \cos^2(k_y a)}. \tag{2.1.4}$$

Note that both the inversion and the time-reversal symmetry are inherited from the $\alpha = 1/2$ Harper Hamiltonian. Furthermore, the system possesses the lattice translation symmetry, which is the only symmetry required for the protection of the Weyl symmetry protected topological state. In order to achieve Weyl points, we must break one of former two when adding the third dimension.

To achieve this goal, we propose to construct a 3D cubic lattice with laser assisted tunneling along both x and z directions as follows. First, tunneling along these directions is suppressed by introducing a linear tilt of energy Δ per lattice site, identical along x

and z. It can be obtained by a linear gradient potential (e.g., gravity or magnetic field gradient [24]) along the $\hat{x}+\hat{z}$ direction. The tunneling is restored by two far-detuned Raman beams of frequency detuning $\delta\omega = \omega_1 - \omega_2$, and momentum difference $\delta\mathbf{k} = \mathbf{k}_1 - \mathbf{k}_2$ [24]. For resonant tunneling, $\delta\omega = \Delta/\hbar$, and a sufficiently large tilt ($J_x, J_z \ll \Delta \ll E_{gap}$) [24], time-averaging over the rapidly oscillating terms yields an effective 3D Hamiltonian

$$H_{3D} = -\sum_{m,n,l} (K_x e^{-i\Phi_{m,n,l}} a^\dagger_{m+1,n,l} a_{m,n,l} + J_y a^\dagger_{m,n+1,l} a_{m,n,l}$$
$$+ K_z e^{-i\Phi_{m,n,l}} a^\dagger_{m,n,l+1} a_{m,n,l} + h.c.). \tag{2.1.5}$$

Here, $a^\dagger_{m,n,l}$ ($a_{m,n,l}$) is the creation (annihilation) operator on the site (m,n,l), and $\Phi_{m,n,l} = \delta\mathbf{k}\cdot\mathbf{R}_{m,n,l} = m\Phi_x + n\Phi_y + l\Phi_z$ are the nontrivial hopping phases, dependent on the positions $\mathbf{R}_{m,n,l}$. An inspection of Eq. (2.1.5) reveals that a wealth of energy dispersion relations can be achieved by manipulating the directions of Raman lasers $\delta\mathbf{k}$. Next, we choose the directions of the Raman lasers such that $(\Phi_x, \Phi_y, \Phi_z) = \pi(1,1,2)$, i.e. $\Phi_{m,n,l} = (m+n)\pi$ (modulo 2π). This is schematically illustrated in Fig. 2.2(b). It should be noted that a seemingly equivalent choice $(\Phi_x, \Phi_y, \Phi_z) = \pi(1,1,0)$, will not be operational, because a *nonvanishing* momentum transfer in the tilt direction is necessary for the resonant tunneling to be restored [24, 25, 115].

A sketch of the 3D lattice obtained with such a choice of phases is illustrated in Fig. 2.2. It can be thought of as an alternating stack of two types of 2D lattices, parallel to the xz plane, which are illustrated in Fig. 2.2(c,d); hopping between these planes is regular (along y). The 3D lattice has two sublattices (A-B). Another view is stacking of 2D lattices described by the Harper Hamiltonian $H_{\alpha=1/2}$ [Fig. 2.2(a)], such that the hopping along z has phases 0 or π, for $m+n$ even or odd, respectively. This breaks the inversion symmetry, and under application of Bloch's theorem,

$$H(\mathbf{k}) = -2\{J_y \cos(k_y a)\sigma_x + K_x \sin(k_x a)\sigma_y - K_z \cos(k_z a)\sigma_z\}. \tag{2.1.6}$$

Mathematically, the chosen phase engineering along z has replaced the identity matrix in H_{LN} with the Pauli matrix σ_z.
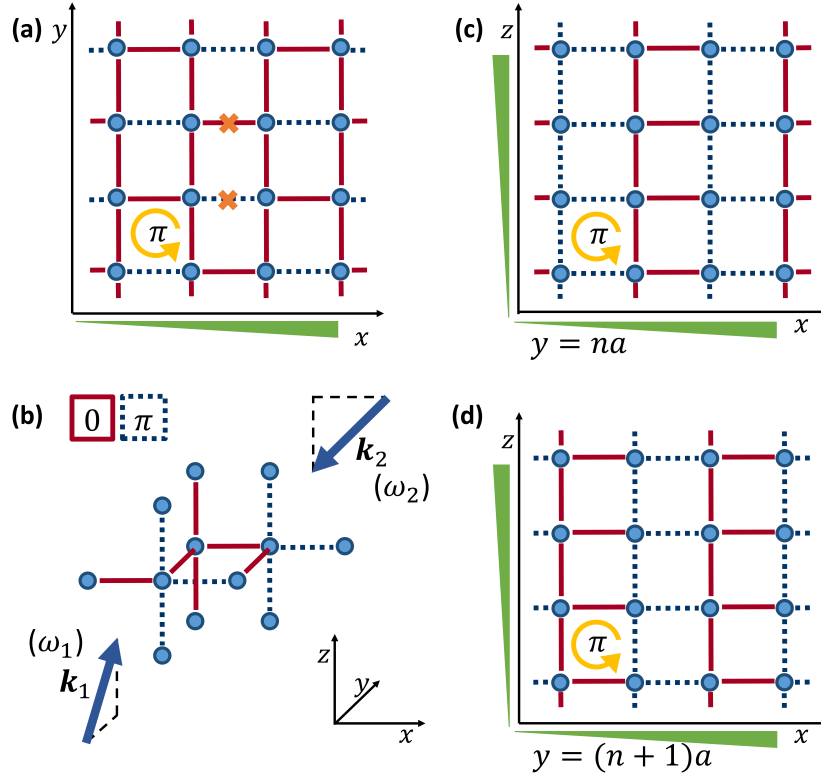
Figure 2.2: Sketch of the 3D cubic lattice with phase engineered hopping along x and z directions, which possesses Weyl points in momentum space. Dashed (solid) lines depict hopping with acquired phase π (0), respectively. (a) The xy planes of the lattice are equivalent to the lattice of the Harper Hamiltonian for $\alpha = 1/2$. Centers of inversion symmetry for this 2D lattice are denoted by orange crosses. Green triangles along the axes denote the tilted directions. (b) A pair of Raman lasers enabling laser assisted tunneling is sketched with arrows. The 3D lattice can be visualized as alternating stacks of 2D lattices parallel to the xz plane, which are shown in (c) and (d); the hopping between these planes (along y) is regular. The hopping along z is alternating with phase 0 or π, depending on the position in the xy plane [see (b), (c), and (d)], which breaks the inversion symmetry.

2.1.3 Topological synthetic magnetic monopoles

The energy spectrum of the Hamiltonian has two bands,

$$E(\mathbf{k}) = \pm 2\sqrt{K_x^2 \sin^2(k_x a) + J_y^2 \cos^2(k_y a) + K_z^2 \cos^2(k_z a)}, \qquad (2.1.7)$$

which touch at four Weyl points within the first Brillouin zone at

$$(k_x, k_y, k_z) = (0, \pm\pi/2a, \pm\pi/2a). \qquad (2.1.8)$$

Fig. 2.3 depicts the energy spectra in the first Brillouin zone, the Weyl points, and their chiralities. The dispersions around the Weyl points are locally linear and described by the anisotropic Weyl Hamiltonian $H_W(\mathbf{q}) = \sum_{i,j} q_i \nu_{ij} \sigma_j$ [116], where $\mathbf{q} = \mathbf{k} - \mathbf{k}_W$ is the displacement vector from the Weyl point (located at $\mathbf{k}_W$) in momentum space. Here $[v_{ij}]$ is a 3×3 matrix, with elements $v_{xy} = -2K_x a$, $v_{yx} = \pm 2J_y a$, $v_{zz} = \pm 2K_z a$, and zero otherwise. The topological nature of the system is reflected in the possibility to assign (positive and negative) chirality, defined as $\kappa = \mathrm{sign}(\det[v_{ij}])$, to the Weyl points [100].

Weyl points are monopoles of the synthetic magnetic field in momentum space. In order to verify this property of our energy nodes, we have calculated the gauge field, i.e. Berry connection

$$A(\mathbf{k}) = i\langle u(\mathbf{k})|\nabla_{\mathbf{k}}|u(\mathbf{k})\rangle, \qquad (2.1.9)$$

and the synthetic magnetic field, i.e. Berry curvature

$$\mathbf{\Omega} = \nabla_{\mathbf{k}} \times \mathbf{A}(\mathbf{k}). \qquad (2.1.10)$$

The obtained Berry curvature is depicted in the insets of Fig. 2.3, clearly demonstrating that what we have proposed is a construction of topological synthetic magnetic monopoles in momentum space of a 3D optical lattice.

These monopoles are robust to any perturbation that adds a σ_i term ($i = x, y, z$) in the Hamiltonian. The only way for Weyl points to disappear is when two of them with opposite chirality annihilate. This topologically protected nature of Weyl points can be probed in the proposed setup by adding a tunable A-B sublattice energy offset in the same fashion as in Ref. [117], such that the on-site energy at sites with $m + n$ odd (even) is ϵ

$(-\epsilon)$. This adds an $\epsilon\sigma_z$ term to the Hamiltonian in Eq. 2.1.6, and shifts the Weyl points parallel to the z-axis by tuning ϵ, as illustrated in Fig. 2.3(a). By making this term large enough ($\epsilon = \pm 2K_z$), one can drive the annihilation of the Weyl points pairwise either at $(k_x = 0, k_y = \pm\pi/2a, 0)$ for $\epsilon = -2K_z$, or at the edge of the Brillouin zone for $\epsilon = 2K_z$, and open up a gap in the system.

2.1.4 Topological surface states and Fermi arcs

Weyl semimetals imply the existence of intriguing topological surface states that come in the form of 'Fermi arcs' in momentum space [99]. Topological effects such as Berry curvature have been experimentally observed in ultracold atomic systems [27, 117]. However, surface states are difficult to detect with light scattering methods because one has to distinguish them from the bulk signal (e.g., see [118] and references therein). Nevertheless, it is illustrative to show Fermi arcs and surface states in our model. In Fig. 2.4(a) we take a slab of our lattice cut orthogonally to the $\hat{x} - \hat{y}$ direction (infinite along the $\hat{z}$ and $\hat{x} + \hat{y}$ directions), and in Fig. 2.4(b) we plot the energy spectrum of this slab $E(\mathbf{k})$, where $\mathbf{k} = k_{\parallel}(\hat{x} + \hat{y})/\sqrt{2} + k_z\hat{z}$. The Weyl points are now connected with 'Fermi arcs' in momentum space (shown with dashed lines). The states on the arcs are surface states [99], as can be seen from the inset in Fig. 2.4(b) (only states from one of the surfaces are shown). Surface states closer to the Weyl points spread more into the bulk than those in the center of the arcs. The Fermi arcs belong to two energy dispersion sheets of surface states, each one corresponding to one of the slab surfaces. The two sheets are located adjacent to the energy dispersion of bulk states [99]; one sheet is on the bottom (the other is on the top) of the upper (lower, respectively) band. These two sheets intersect at Fermi arcs.

2.1.5 Experimental detection of Weyl points

We now propose schemes for the experimental detection of Weyl points that are applicable for both ultracold bosons and fermions. In order to verify that we have points at which the two bands touch in the 3D Brillouin zone, one can accelerate the initially prepared ultracold atomic cloud from the ground state position in momentum space towards the Weyl point using a constant force, and observe the crossover to the second band which can be revealed by time-of-flight measurements. By pushing the cloud in directions which
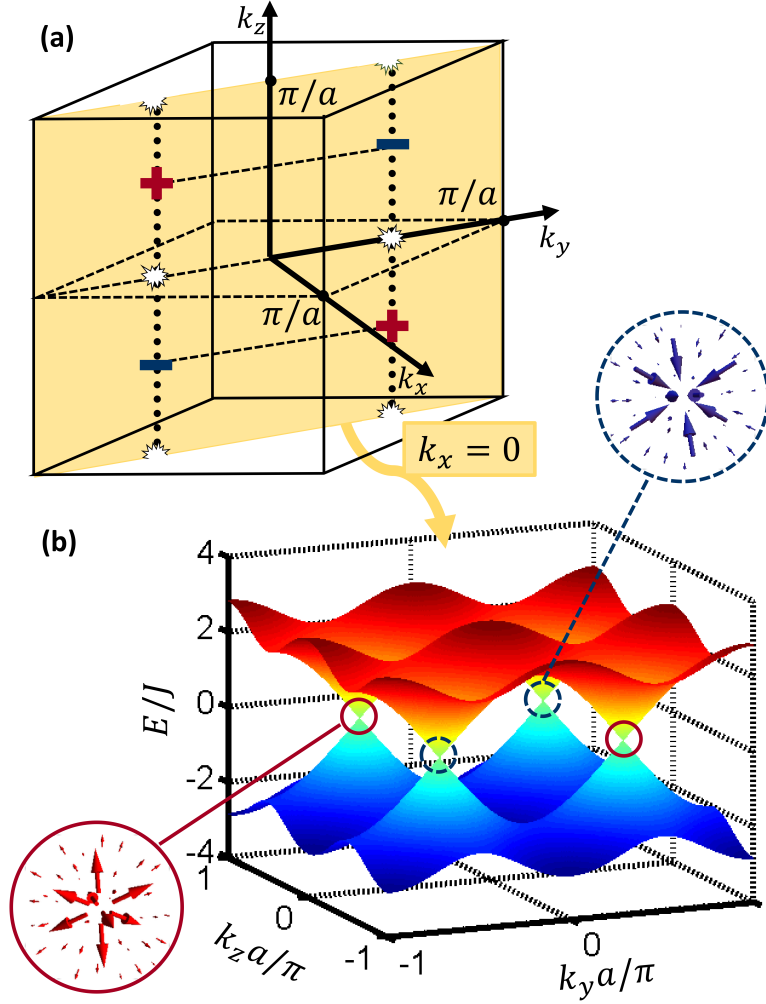
Figure 2.3: Sketch of the first Brillouin zone of the lattice depicted in Fig. 2.2, energy spectrum and Weyl points. (a) The positions of the Weyl points in the Brillouin zone and their chiralities are indicated with $+$ and $-$ signs. If a tunable A-B sublattice energy offset is introduced, Weyl points move along dotted lines, and can annihilate at points denoted with stars (see text). (b) Energy spectrum in the $k_x = 0$ plane [shaded plane in (a)], shows linear dispersion in the proximity of the Weyl points. The insets show the Berry curvature of two Weyl points, demonstrating that they are synthetic magnetic monopoles in momentum space.
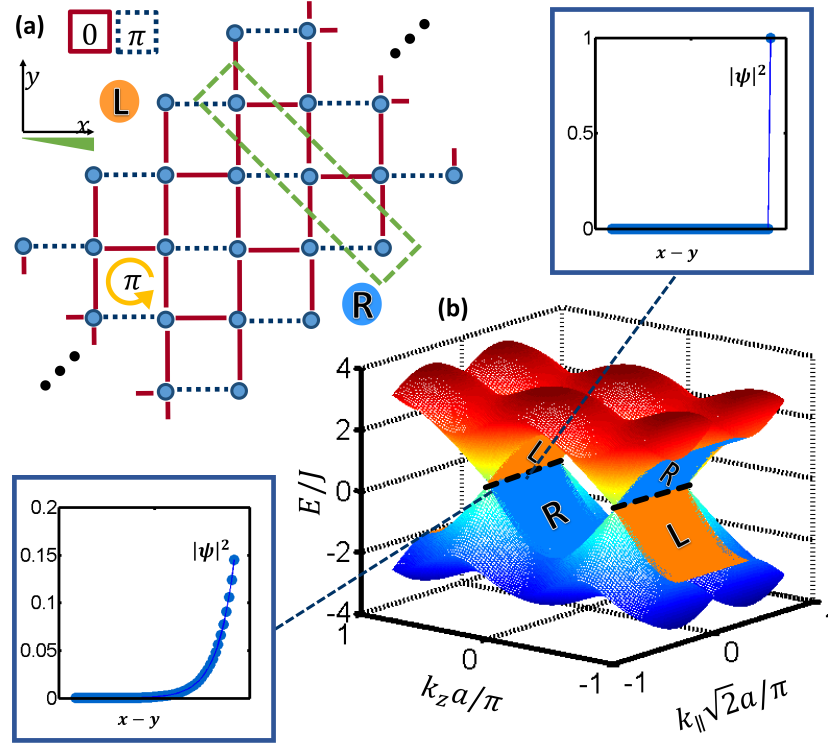
Figure 2.4: Surface states and Weyl points. (a) A slab of finite-width is cut from the 3D lattice along planes orthogonal to the $\hat{x} - \hat{y}$ direction; cross section in the xy plane is sketched. The two sides of the slab are indicated with letters L and R. (b) Energy spectrum of the slab. The two dispersion sheets of surface states (corresponding to the two surfaces of the slab) are denoted with R (blue) and L (orange). The intersections of the two sheets are Fermi arcs (denoted with dashed lines). The arcs connect Weyl points of opposite chiralities. The insets show examples of the profile of the Fermi arc surface states across the slab, as indicated by the green dashed box in (a).

would 'miss' the Weyl point, Bloch oscillations would be observed within the lowest band. Such a scheme was recently used to detect Dirac points in a honeycomb optical lattice [119], and also to probe the topological phase transition in the Haldane model [117]. Two points are worth emphasizing here. First, Weyl points are robust and would not be destroyed by an additional small force [99, 105]. Second, the trajectory of the gas being pushed would not be deflected in our lattice, because we have a time-reversal symmetric Hamiltonian.

The second scheme to observe the Weyl points is Bragg spectroscopy [120]. By using an additional pair of Raman lasers, i.e., a two-photon Raman transition, one can couple states of the Hamiltonian (Eq. 2.1.6) with a given energy and momentum difference, and induce excitations from the lower band to the upper band to probe the band-structure [120]. This scheme would reveal the existence of Weyl points with very high resolution as it would not change the internal atomic state, and therefore not be sensitive to Zeeman shifts.

The proposed methods are applicable for both bosons and fermions. Here we discussed atoms in a single spin state, however, a mixture of spin states provides another degree of freedom to explore new phenomena, e.g., see [121]. By using single spin fermions, the Weyl semimetal phase could be achieved by adjusting the particle density, i.e., the Fermi level to the energy of the Weyl points.

The realization of Weyl points with ultracold atoms would open a new frontier of research in Weyl physics, with potential to exploit unique atomic physics methods of state preparation and diagnostics. As an example, consider a BEC which is initially formed in the ground state of the band structure (e.g., see [122]), and then, by applying a potential tilt for a finite duration, placed (in quasi-momentum space) at a Weyl point. This state is a superposition of eigenstates from the vicinity of the Weyl point, and would start expanding in our 3D lattice. If we assume isotropic dispersion around Weyl points ($K_x \approx J_y \approx K_z$), the magnitude of the group velocity $\hbar^{-1}|\nabla_{\mathbf{k}} E(\mathbf{k})|$ is uniform. In this case, the BEC has unique expansion in a form of a spherical shell with radius $\sim \hbar^{-1}|\nabla_{\mathbf{k}} E(\mathbf{k})|t$ (the shell would have structure depending on the initial excitation).

$$\sim$$

We pointed out that Weyl points, and all the related exciting phenomena, can be

experimentally addressed in the setup that was recently employed to obtain the Harper Hamiltonian [24, 25]. Both Weyl fermions in quantum field theory and Weyl semimetals as a symmetry protected topological state have shown to be elusive, mostly because of the strict requirements on the space groups and symmetries they impose. By phase engineered hopping methods such as laser assisted tunneling, which are developed for atomic systems, these requirements are circumvented. By including such a tunable synthetic magnetism in the design of quantum systems, this concept can open a new frontier in the research of complex and puzzling topological matter. Moreover, as in topological phases interactions can have a significant impact, our result on the applicability of laser assisted tunneling in the presence of strong interactions [4], presented in the next section, additionally strengthens this possibility.

2.2 Fractional statistics in an expanding atomic gas

Quantum states with intrinsic topological order are characterized by long-range entanglement [66]. Unlike symmetry protected topological states that require the presence of symmetry constraints (e.g. the Weyl semimetals encountered in Section 2.1), phases with intrinsic topological order do not rely on any symmetry protection. Indeed, the presence of long-range entanglement in these systems leads to the emergent quantum order. Namely, the bulk of systems with intrinsic topological order hosts fascinating behavior in the form of exotic quantum quasiparticles [66].

In two-dimensional systems, the emergent particles, called anyons, have fractional statistics. Anyonic statistics interpolates between bosons and fermions [123, 124]. The paradigmatic realization of anyons is found in the fractional quantum Hall effect (FQHE) [67, 96], where localized quasiparticle excitations have a fractional elementary charge [96] and statistics [125, 126]. Quantum spin-liquids, realizing the Kitaev model [70], are the other known system that realizes anyonic quasiparticles [71]. While the fundamental motivation for exploring anyons is self-evident, the so-called non-Abelian anyonic excitations hold potential for technological advances, as they could be used for robust topological quantum computation [72] (for review see Ref. [73]).

Some of the intriguing quantum mechanical implications of fractional statistics were pointed out decades ago [123, 124], giving a simpler intuitive picture of anyons as composite particles [123], and anyons arising from merely statistical considerations [124]. A lot more, however, still needs to be understood and discovered. Experiments with ultracold atomic gases seem to be a perfect playground for exploring anyonic physics, because of the quality in preparation, manipulation, and detection of numerous intriguing quantum states [9]. Again, synthetic magnetic fields in these systems [98] enable physicists to tinker with topology and, because of the possibility to explore 2D systems [127], statistics as well. In an early paper, Paredes *et al.*, inspired by the FQHE, proposed the realization of a 1/2-Laughlin state in a bulk rotating gas [128]. Different schemes were later proposed with atoms in optical lattices [129–131]. Ultracold atoms with two hyperfine levels in non-Abelian potentials could yield ground states with non-Abelian anyonic excitations [132], while bosons in Floquet-driven optical lattices may effectively exhibit fermionic statistics [133]. The one-dimensional (1D) version of anyons [134–142] has also aroused interest,

especially in 1D optical lattices [139–142]. Such particles were proposed to emerge from occupation dependent hopping amplitudes, which could be realized with laser-assisted tunneling [139, 141], or Floquet modulations [142]. Other proposals include lattices of polar molecules [143], photonics lattices [144] and circuit-QED systems [145].

An undoubtedly important ingredient that needs to be investigated in this context is the detection of the anyonic quantum state. Detection schemes that have been addressed rely on braiding [128, 130, 146, 147], the pair-correlation function [131], and precision spectroscopy [148]. Free expansion, or time-of-flight method, is among the most used detection techniques from the atomic physics toolbox [9], which could be of interest for systems where bosons are converted into anyons by manipulating with their interaction (as in [139]), or by introducing them as impurities in a background of topological states (e.g., [130, 131, 149]). Up to now, however, expansion studies exist only for 1D systems [137].

We study the expansion of Abelian anyons in 2D. Typically, in systems of ultracold bosons or fermions, free expansion provides the momentum distribution of the initial quantum state [9]. Namely, the confining potential is turned off abruptly and, in cases where interactions can be neglected, a given state expands according to its momentum distribution, which is defined as the diagonal of the reduced single-particle density matrix (RSPDM) represented in a basis of kinetic momentum eigenstates. The momentum distribution is a valuable characteristic of any quantum state and was, for example, of paramount importance as a signature of Bose-Einstein condensation [150], and the onset of Fermi degeneracy in a trapped atomic gas [151]. We point out that, however, in a system of anyons, the momentum distribution is not a proper observable. We think of anyons as Wilczek's composite particles [123], consisting of a charge and an infinitely thin magnetic flux. As the magnetic field is non-vanishing at the position of the composite particle in any gauge, it follows that orthogonal component of the kinetic momentum operator do not commute on all space and cannot be diagonalized in the same basis. Nevertheless, this can be remedied by turning definitions around. We define the quasimomentum distribution for anyons as the asymptotic limit of the single-particle density of an anyonic gas freely expanding from an initially localized state, which reduces to the standard definition in the case of bosons or fermions. As an example, we calculate an exact time-dependent wave function, which for $t<0$ describes an eigenstate of N anyons in a harmonic trap, and for $t>0$ describes expansion of anyons after the trap is suddenly turned off at $t=0$. We find

the solution by employing a scaling transformation [152, 153], and the quasimomentum distribution via Monte-Carlo integration. For $N=2$ particles, we find that the asymptotic single-particle density corresponds to the projection coefficients of the initial state onto two-anyon eigenstates in free space, which underpins our conjecture. In addition, we point out that anyonic statistics can be extracted from the pair-correlation function: the two-particle correlations at short interparticle distances scale as a power-law with the statistical parameter α in the exponent.

2.2.1 A multi-valued wavefunction and momentum distribution

An anyonic wavefunction ψ describing expansion from an eigenstate in a harmonic trap obeys the Schrödinger's equation $i\frac{\partial}{\partial t}\psi=H\psi$, with the Hamiltonian

$$H = \sum_{i=1}^{N}\left[-\frac{1}{2}\nabla_i^2 + \frac{1}{2}\omega(t)^2 r_i^2\right].\tag{2.2.1}$$

Here, $\omega(t<0)=1$ and $\omega(t\geq0)=0$. The symmetry of the wavefunction is anyonic, i.e.

$$\psi(\ldots,\mathbf{r}_i,\ldots,\mathbf{r}_j,\ldots,t)=e^{im\pi\alpha}\psi(\ldots,\mathbf{r}_j,\ldots,\mathbf{r}_i,\ldots,t),\tag{2.2.2}$$

where $\mathbf{r}_i=x_i\hat{\mathbf{x}}+y_i\hat{\mathbf{y}}$ are the particle positions, and $m\in\mathbb{Z}$ depends on how they are braided during the exchange. The anyonic wave function is a multi-valued function of the positions $\{\mathbf{r}_i\}$ (e.g., see [126] for a discussion). For N bosons and fermions, the RSPDM,

$$\rho(\mathbf{r},\mathbf{r}',t)=N\int\psi^*(\mathbf{r},\mathbf{r}_2,...,\mathbf{r}_N,t)\psi(\mathbf{r}',\mathbf{r}_2,...,\mathbf{r}_N,t)d\mathbf{r}_2...d\mathbf{r}_N,\tag{2.2.3}$$

furnishes one-body observables such as the momentum distribution, which is given by its Fourier transform:

$$n(\mathbf{k},t)=(2\pi)^{-2}\int\rho(\mathbf{r},\mathbf{r}',t)e^{i\mathbf{k}\cdot(\mathbf{r}-\mathbf{r}')}d\mathbf{r}d\mathbf{r}'.\tag{2.2.4}$$

For anyons, the single-particle density, i.e., the diagonal $\rho(\mathbf{r},\mathbf{r},t)$ of the RSPDM is uniquely defined, as it is not phase-dependent; therefore, $\rho_D(\mathbf{r},t)\equiv\rho(\mathbf{r},\mathbf{r},t)$ is a legitimate observable. However, the off-diagonal elements of the anyonic RSPDM depend on the wave function phase and are not single-valued. Consequently, $n(\mathbf{k},t)$ is not single-valued and therefore it cannot be used as a definition of momentum distribution for anyons. We note in passing

that for 1D anyons this problem does not exist as the wavefunction and consequently the RSPDM are single valued [135–139].

2.2.2 Wilczek's composite particles

A more physical insight in the question of anyonic momentum distribution is obtained if we think of anyons as Wilczek's composite particles (CP) consisting of a point charge q and an infinitely thin magnetic flux tube with magnetic flux Φ, so that $\alpha{=}{-}q\Phi/2\pi$ [123]. The Hamiltonian describing such composite particles includes pairwise vector potential interactions:

$$H_{CP} = \sum_{i=1}^{N} \left[-\frac{1}{2} \left(\nabla_i + i\alpha \sum_{j\neq i} \frac{\hat{\mathbf{z}} \times \mathbf{r}_{ij}}{r_{ij}^2} \right)^2 + \frac{1}{2}\omega^2(t)r_i^2 \right], \qquad (2.2.5)$$

where $\mathbf{r}_{ij}{=}\mathbf{r}_i{-}\mathbf{r}_j$. The corresponding wavefunction $\psi_{CP}(\mathbf{r}_1, \ldots, \mathbf{r}_N, t)$ is bosonic or fermionic (here we assume bosonic symmetry for ψ_{CP}). The vector potential interactions can be gauged out from the Hamiltonian H_{CP} to obtain H [123, 154], that is, the wavefunction ψ_{CP} is related to the anyonic wavefunction ψ by a gauge transformation

$$\psi\left(\mathbf{r}_1, ..., \mathbf{r}_N, t\right) = \prod_{i<j}^{N} e^{i\alpha\phi_{ij}} \psi_{CP}\left(\mathbf{r}_1, ..., \mathbf{r}_N, t\right), \qquad (2.2.6)$$

where ϕ_{ij} is the relative angle between two particles in the xy-plane. The RSPDM $\rho_{CP}(\mathbf{r}, \mathbf{r}', t)$ of the wavefunction ψ_{CP} is uniquely defined, and it can be used to obtain one-body observables, by properly accounting the gauge. For example, the Fourier transform of $\rho_{CP}(\mathbf{r}, \mathbf{r}', t)$ yields the canonical rather than the kinetic momentum distribution because of the presence of vector potential interactions. In order to obtain the kinetic momentum distribution, one should first find a basis of eigenstates of the kinetic momentum operators. However, this is not possible because the x and y components of these operators do not commute at the positions of the particles where the flux is present:

$$[p_{x,i}^a, p_{y,i}^a] = -i2\pi\alpha \sum_{j\neq i} \delta(\mathbf{r}_i{-}\mathbf{r}_j), \qquad (2.2.7)$$

where $p_{x,i}^a\hat{\mathbf{x}}{+}p_{y,i}^a\hat{\mathbf{y}} \equiv -i\nabla_i{+}\alpha \sum_{j\neq i} \hat{\mathbf{z}}{\times}\mathbf{r}_{ij}/r_{ij}^2$. Therefore, unlike the case for bosons or fermions, the kinetic momentum distribution for anyons is not a proper observable. In order to remedy this situation, we study the expansion of anyons from an initially localized

state, to find an appropriate observable that corresponds to the momentum distribution, which reduces to the usual definitions when the statistical parameter α approaches 0 for bosons or 1 for fermions.

2.2.3 Free expansion of two anyons

For clarity, we first discuss the free expansion of two anyons released from a harmonic trap. When $N=2$, the Schrödinger equation $i\frac{\partial}{\partial t}\psi=H\psi$ can be rewritten in center-of-mass $\mathbf{R}=(\mathbf{r}_1+\mathbf{r}_2)/2\equiv(R,\theta)$ and the relative $\mathbf{r}=\mathbf{r}_1-\mathbf{r}_2\equiv(r,\phi)$ coordinates. The ground state for two anyons in a harmonic potential is given by [123, 124, 154],

$$\psi(\mathbf{R},\mathbf{r},t=0)=\mathcal{N}_2 r^{|\alpha|}e^{i\alpha\phi}e^{-R^2-\frac{r^2}{4}}, \tag{2.2.8}$$

where $\mathcal{N}_2$ is the normalization constant. Equation (2.2.8) already shows two important characteristics of fractional statistics $(0<|\alpha|<1)$, with all their implications: the wavefunction cannot be written as a product of single-particle wavefunctions, and it is not single-valued. At $t=0$, the trap is turned off and two anyons start expanding. The expansion dynamics can be found by decomposing the wavefunction (2.2.8) into two-anyon eigenstates in free space, which are given by [15]

$$\phi_{KkMm}(\mathbf{R},\mathbf{r})=e^{iM\theta}J_{|M|}(KR)e^{i(m+\alpha)\phi}J_{|m+\alpha|}(kr), \tag{2.2.9}$$

up to normalization, with the corresponding energy $E_{Kk}=K^2/4+k^2$. The principal quantum numbers are $\{K,k\}\in[0,\infty\rangle$, and the angular quantum numbers are $\{M,m\}\in\mathbb{Z}$. Because the initial ground state is rotationally invariant, only eigenstates with $M=m=0$ are present in the expansion; therefore, we omit M and m in further notation. The time-dependent wavefunction during free expansion of two anyons is

$$\psi(\mathbf{R},\mathbf{r},t>0)=\int dKdkKka_{Kk}\phi_{Kk}e^{-iE_{Kk}t} \tag{2.2.10}$$
$$\propto\frac{1}{(1+it)^2}\left(\frac{r}{1+it}\right)^{|\alpha|}\exp\left[-\frac{R^2+r^2/4}{1+it}+i\alpha\phi\right],$$

where the coefficients a_{Kk} are the projection coefficients of the initial wavefunction (2.2.8) on eigenstates in free space (2.2.9):

$$a_{Kk} \propto k^{|\alpha|} e^{-\frac{K^2}{4} - k^2}. \tag{2.2.11}$$

We identify $|a_{Kk}|^2$ with the quasimomentum distribution of two anyons.

That this definition is natural is underpinned by the following observations: (i) the quasimomentum distribution does not change during free expansion; (ii) this definition reduces to the standard one when the statistical parameter α approaches 0 for bosons or 1 for fermions; (iii) the asymptotic form of the single-particle density $\rho_D(\mathbf{r}, t{\to}\infty)$ has the same shape as $|a_{Kk}|^2$. Observation (i) is evidently true, observation (ii) follows from the fact that eigenstates for bosons and fermions in free space are built from plane waves (properly symmetrized), and we have verified (iii) to hold explicitly. The generalization of Eq. 2.2.10 to the case of N anyons would read $\psi(t{>}0) = \int d\beta a_\beta \phi_\beta e^{-iE_\beta t}$. However, a definition of the single-particle quasimomentum distribution from the projection coefficients a_β is unclear, as we do not know which quantum numbers β, define eigenstates ϕ_β of N anyons in free space. These eigenstates are complex many-body wavefunctions, because a system of anyons is a genuine many-body problem with all its inherent difficulties, even though Hamiltonian H appears as to describe noninteracting particles. The fact is that vector potential interactions between particles from H_{CP}, when gauged out to obtain H, remain hidden in the anyonic symmetry of the wavefunction ψ. Nevertheless, we can *define* the quasimomentum distribution for N anyons as the asymptotic single-particle density, after expansion in free space. This definition obviously obeys observation (ii) above, although the connection with projection coefficients a_β is not yet clear.

2.2.4   Free expansion of an anyonic gas

Let us now consider expansion of N anyons from the harmonic trap. The generalization of wavefunction (2.2.8) for $N{>}2$ does not yield the ground state in a harmonic oscillator. In order to gain understanding of the expansion dynamics of anyons, we assume that initially the system is in its eigenstate, given by [154]

$$\psi(\{\mathbf{r}_i\}, t{=}0) = \mathcal{N}_N \prod_{i<j} r_{ij}^{|\alpha|} e^{i\alpha\phi_{ij}} e^{-\sum_{k=1}^{N} \frac{|\mathbf{r}_k|^2}{2}}. \tag{2.2.12}$$
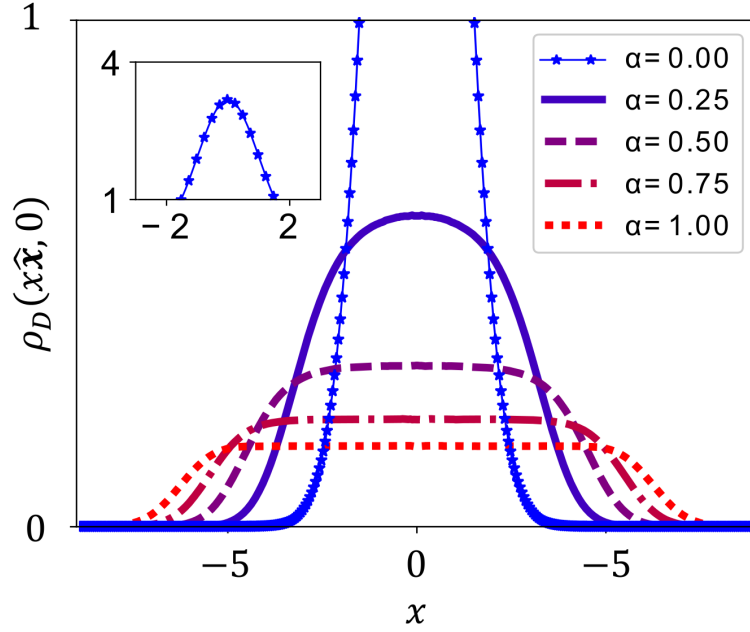
Figure 2.5: The profile of the single-particle density $\rho_D(x\hat{\mathbf{x}}, 0)$ of the wavefunction (2.2.13), which we identify as quasimomentum distribution (see text), for $N = 20$ and different values of α, obtained via Monte-Carlo integration. The inset shows the peak of the bosonic density at $\alpha = 0$. The single-particle density at any time $t > 0$ is given by $\rho_D(\mathbf{r}, t) = b^{-2}\rho_D(\mathbf{r}/b, 0)$.

We can obtain the dynamics of the system for $t \geq 0$ by employing the scaling transformation [152, 153]:

$$\psi(\{\mathbf{r}_i\}, t>0) = \frac{1}{b^N}\psi(\{\frac{\mathbf{r}_i}{b}\}, 0)e^{i\frac{\dot{b}}{2b}\sum_k^N |\mathbf{r}_k|^2}e^{-iE_N\tau(t)}. \tag{2.2.13}$$

Here $b=\sqrt{1 + t^2}$ is the time dependent scaling factor, $E_N=N+\alpha N(N-1)/2$ the eigenstate energy and $\tau(t)=\int^t \frac{dt'}{b^2(t')}$ a scaled time. The evolution of the single-particle density is self-similar

$$\rho_D(\mathbf{r}, t) = \frac{1}{b^2}\rho_D(\frac{\mathbf{r}}{b}, 0). \tag{2.2.14}$$

Consequently, the shape of the asymptotic single-particle density is the same as the initial single-particle density. In Fig. 2.5 we plot its profile for $N = 20$, for different values of the statistical parameter α. We see that on the bosonic side, the form is narrower and sharper, and it gets flatter and broader on the fermionic side, as one would expect from the quasimomentum distribution.

2.2.5 Correlations of particles with fractional statistics

Another observable that depends on the statistical parameter α, and can be used to obtain information on the anyonic character of the system is the pair correlation function [131]. The pair correlation function

$$g(\mathbf{r}_1, \mathbf{r}_2, t) = N(N-1) \int |\psi(\mathbf{r}_1, \mathbf{r}_2, \ldots, \mathbf{r}_N, t)|^2 d\mathbf{r}_3 \ldots d\mathbf{r}_N \qquad (2.2.15)$$

is illustrated in Fig. 2.6 for different values of α and N, at t=0 (it changes trivially with time due to the self-similarity of the evolution). One particle is fixed at $\mathbf{r}_2 = \hat{\mathbf{x}}$, and we show g as a function of the position of the second particle, $\mathbf{r}_1$. In Fig. 2.6(a) we show g for N=5: two particles are uncorrelated only in the bosonic limit ($\alpha = 0$), coinciding with the case with no repulsive statistical interactions at any distances [155, 156]. In Fig. 2.6(b), the angle ϕ_1 parametrizes the position of the moving particle, $\mathbf{r}_1 = \cos\phi_1\hat{\mathbf{x}} + \sin\phi_1\hat{\mathbf{y}}$. Suppose that we perform expansion of two anyons from a harmonic trap. If we detect one anyon at an angle $\phi_2 = 0$, one may ask what is the probability of detecting the second anyon at some other angle ϕ_1? The plot in Fig. 2.6(b) for $N = 2$ provides information on what we may expect from such an experiment. Bosons would be completely uncorrelated with probability independent of ϕ_1, fermions anti-correlated with the peak of the probability at $\phi_1 = \pi$, and anyons ranging in between these two cases, depending on α. From the structure of the wavefunction (2.2.13) it follows that for small interparticle distances, the pair correlation function scales as

$$g \propto |\mathbf{r}_1 - \mathbf{r}_2|^{2|\alpha|}. \qquad (2.2.16)$$

This can be seen from the plot in Fig. 2.6(b). It was recently pointed out that in topologically ordered states, the low energy onset of spectral functions scales as a power law with the statistical parameter in the exponent [157].

2.2.6 Ideas for implementation

One possible route to implement free expansion of anyons in ultracold atomic gases is by building upon the proposals in Refs. [128, 131, 149]. Suppose that one implements a system proposed in Ref. [128], where one first introduces a system of hard-core bosons
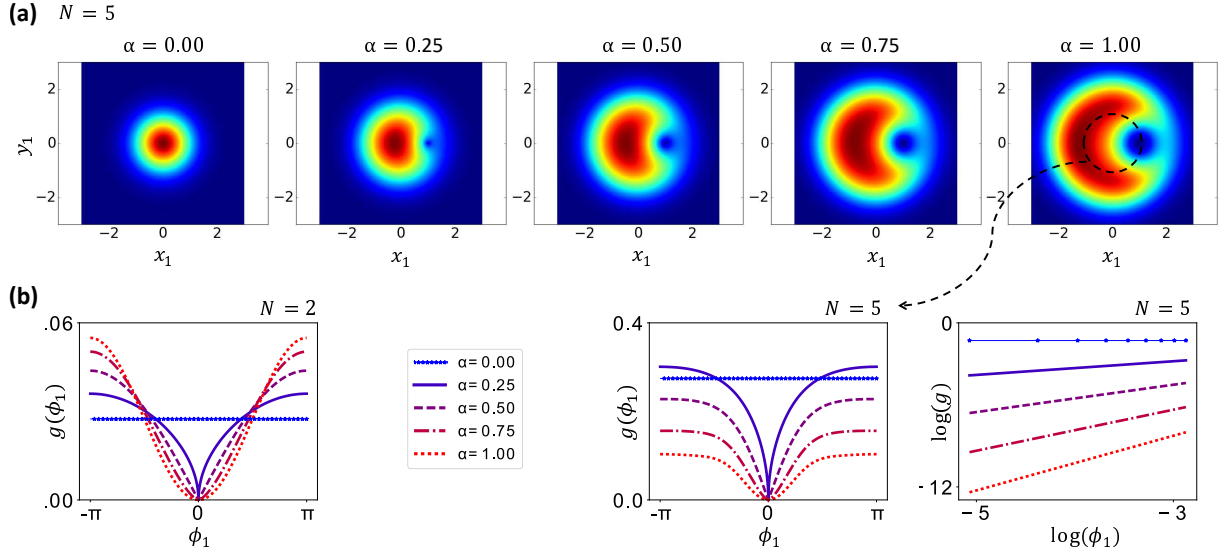
(a) $N = 5$

(b)

Figure 2.6: Pair correlations of anyons. (a) Pair correlation function $g(\mathbf{r}_1, \mathbf{r}_2 = \hat{\mathbf{x}})$ for different values of the statistical parameters α. (b) Dependence of g on the distance between particles $|\mathbf{r}_1 - \mathbf{r}_2| = |(\cos\phi_1 - 1)\hat{\mathbf{x}} + \sin\phi_1\hat{\mathbf{y}}|$ as a function of N and α. See text for details.

in a synthetic magnetic field, which is represented by a bosonic version of the Laughlin wavefunction for electrons in the quantum Hall regime [128]. Next, instead of creating quasihole fractionalized excitations with lasers [128], suppose that one introduces a few bosonic atoms of another species, which have hard-core repulsive interactions with the original bosons. These newly introduced bosons would behave as anyons, and their expansion in the presence of background of the original bosons would reveal the quasimomentum distribution discussed here. Such a system of test particles immersed in a fractional quantum Hall like state was discussed in Refs. [131, 149].

$\sim$

We have pointed out that the momentum distribution, one of the key signatures of various quantum states of matter, is not a proper observable for a system of anyons. When statistics is fractional, which can be thought of as the presence of specific vector interactions, orthogonal components of kinetic momentum do not commute on all space, and the corresponding RSPDM cannot be diagonalized in the same basis. As a substitute for the momentum distribution of a spatially localized anyonic state, we proposed to use the asymptotic single-particle density after expansion of anyons in free space from the state.

This definition reduces to the standard one when the statistical parameter approaches that for bosons or fermions. We also presented examples of expansion dynamics obtained by exact calculations, which underpin our proposal. Furthermore, we have demonstrated that two-particle correlations of this state scale as a power-law with the statistical parameter in the exponent. Finally, we have proposed a possible implementation of this system with ultracold atomic gases.

Historically, the momentum distribution played a crucial role as key signature in experimental realizations of new quantum states with ultracold atoms, such as the Bose-Einstein condensated [150] and Fermi degenerated [151] trapped atomic gases. Nowadays, when an increasing attention is attracted by topologically ordered states of matter because of their amazing emerging phenomena, understanding their signatures is more than crucial. In this context, fractional quantum numbers are among the most exciting emerging phenomena. Our work stresses out how standard methods and understanding have to be taken with caution when studying topological matter via quantum simulation and synthetic magnetism. We show how ultracold atomic systems can help identifying intriguing aspects associated with extracting observables from topological systems with emergent fractional statistics.

The quest for synthetic magnetism

Part of the work in this chapter is published in the following papers

- T. Dubček, K. Lelas, D. Jukić, R. Pezer, M. Soljačić, and H. Buljan,
  New J. Phys. **17**, 125002 (2015).

- K. Lelas, N. Drpić, T. Dubček, D. Jukić, R. Pezer, and H. Buljan,
  New J. Phys. **18**, 095002 (2016).

- T. Dubček, N. Šantić, D. Jukić, D. Aumiler, T. Ban, and H. Buljan,
  Phys. Rev. A **89**, 063415 (2014).

- N. Šantić, T. Dubček, D. Aumiler, H. Buljan, and T. Ban,
  Sci. Rep. **5**, 13485 (2015).

- N. Šantić, T. Dubček, D. Aumiler, H. Buljan, and T. Ban,
  Opt. Soc. Am. B **34**, 1264 (2017).

3.0.1 The many faces of (synthetic) magnetism

The beginning of mankind's interest in magnetism dates back to the ancient era, when people first discovered lodestones, naturally magnetized pieces of magnetite, was attracting iron. Throughout centuries, surgeons and sailors from ancient Greece and China exploited what these materials could offer, while philosophers were astonished by the phenomenon. Comprehending it, however, was not an easy task. In the 19th century, several discoveries

happened, mainly by the work of H. C. Ørsted, A.-M. Ampère, C. F. Gauss; J.-B. Biot, F. Savart, and M. Faraday. This finally enabled the complete understanding of magnetism, and its unification with electricity and optics through J. C. Maxwell's classical theory of electromagnetism [158]. Many fascinating phenomena, such as charge distributions, electric circuits, optical rays or ultraviolet radiations, finally had a good explanation. At the beginning of 20th century, this motivated A. Einstein's theory of special relativity. It showed the theory for magnetism and magnetic fields cannot be separated from the kinematic properties of the system. With the advent of quantum mechanics, furthermore, the classical theory had to be adapted for systems where quantum behavior is important. Still today, it is a field in which new questions arise, and new answers and explanations have to be brought up.

The many different characteristics, behaviors and phenomena magnetism and magnetic interactions can cause are striking. Various materials have diverse magnetic properties that lead to different ways they are analized and used. Magnetism is also closely related realizations of interesting physical concepts, such as geometrical and topological phases [66]. It plays an important role in the fundamental foundations of quantum electrodynamics, electroweak and gauge theories [159]. Although always the same interaction, magnetism appears to have endless possible appearances and faces. Not all of which are completely understood yet.

As quantum simulations contribute to the study and comprehension of intriguing magnetic phenomena through synthetic magnetism, a clear guideline emerges. The flexibility that systems as ultracold gases or photonic lattices can offer must not be neglected. Depending on the system at hand, finding a suitable scheme that enables the study of a specific targeted concept or phenomenon is crucial. It can be in bulk or ordered systems, with strong interactions or noninteracting particles, methods based on kinematics or interactions with light. As each method has its own advantages and limitations, different approaches often tackle complementary aspects.

3.0.2 Chapter outline

In this chapter, we consider and propose new methods that enable the realization of synthetic magnetism in photonic and atomic systems.

By drawing analogies between an optical and a photonic lattice, we introduce a grating assisted tunneling scheme for tunable synthetic magnetic fields in one- and two-dimensional photonic lattices [3]. The resulting lattices possess Dirac points in k-space, whose signature we show to be a conical diffraction pattern. We explicitly show that, in two dimensions, the lattice with grating assisted tunneling can realize the Harper-Hofstadter Hamiltonian, traditionally achieved by using magnetic fields or spin-orbit interactions coupled to charged particles.

Additionally, we show that in one dimension the laser assisted tunneling method can also generate synthetic magnetic fields in systems with strong interactions, namely the Tonks-Girardeau gas [4].

Finally, we propose the realization of a synthetic Lorentz force in a classical cold atomic gas [5]. Unlike standard methods for synthetic magnetism in quantum degenerated gases, based on the adiabatic motion of atoms, here the force arises from radiation pressure. The theoretical proposal is followed by two collaborations with an experimental group, which yielded the experimental demonstration of the idea [6, 7]. The introduced synthetic Lorentz force opens the possibility to mimic classical charged gases in magnetic fields in cold-atom experiments.

3.1 Grating assisted tunneling in photonic lattices

The excitement about about topological states of matter is spread among many different fields. Besides all the fundamental reasons that make these fascinating novel states of matter so attractive, much of the interest arouses because of the technological advances their striking phenomena could enable. Nowadays, it is clear that light science and optical technologies play a central role in the quality of life and the development of society. The possibility to manipulate and control light by designing topological states is thus extremely appealing, making topological photonics a rapidly growing field [28–31, 33, 34, 36, 37, 41–44, 100, 105, 160], for review see [105]. An extremely motivating topological aspect of topological photonic systems are the topologically protected surface states. In these systems, it is reflected in the existence of unidirectional states guiding light [41–44], which are immune to backscattering and robust to imperfections. They may thus serve as novel waveguides and for building integrated photonic devices. The first experimental observations of such edge states were in the microwave domain, in magneto-optical photonic crystals [44], theoretically proposed in Refs. [41–43]. In the optical domain, imaging of topological edge states was reported in Floquet topological insulators, implemented in modulated honeycomb photonic lattices [33], and in the two-dimensional array of coupled optical-ring resonators [31].

Incidentally, synthetic magnetism offers unique tools for achieving these novel topological photonic states and phases. It is thus important to develop methods for obtaining synthetic magnetic/gauge fields depending on the system at hand. Different strategies based on modulation, magneto-electric coupling or tailored geometries have been realized in coupled optical resonators, photonic crystals and metamaterials. However, a viable scheme for an arbitrary design of the phases of the complex tunneling matrix elements in optical lattices, which possess a great potential for exploring photonic topological effects, have been insufficiently addressed. In this section, we introduce one such scheme, termed *grating assisted tunneling*, and propose its implementation in optically induced photonic lattices [161–165]. The method is inpired by the earlier mentioned laser assisted tunneling scheme, which was implemented in optical lattices with ultracold atoms [24–26]. We show that drawing analogies between the behavior of different controllable physical systems can lead to new ideas and significant advances. As the ultracold atomic system with heating

from spontaneous emission is replaced by a photonic system where this is absent, many of the results obtained with ultracold gases become perhaps even more feasible when adapted to a photonic environment. The proposed method realizes tunable synthetic magnetic fields in an optical lattiece. We demonstrate the emergence of synthetic magnetic fields by directly comparing the evolution in the continuous photonic lattices with grating assisted tunneling, and the dynamics in discrete lattices with non-trivial hopping phases. Namely, we show that one- and two-dimensional square photonic lattices with grating assisted tunneling can yield a conical diffraction pattern, which constitutes the realization of the Harper-Hofstadter Hamiltonian.

3.1.1 A photonic lattice

We consider the paraxial propagation of light in a photonic lattice defined by the index of refraction $n = n_0 + \delta n(x, y, z)$ ($\delta n \ll n_0$), where n_0 is the constant background index of refraction, and $\delta n(x, y, z)$ describes small spatial variations, which are slow along the propagation z-axis. The slowly varying amplitude of the electric field $\psi(x, y, z)$ follows the (continuous) Schrödinger equation:

$$i\frac{\partial \psi}{\partial z} = -\frac{1}{2k}\nabla^2 \psi - \frac{k \delta n}{n_0}\psi; \tag{3.1.1}$$

here, $\nabla^2 = \partial^2/\partial x^2 + \partial^2/\partial y^2$, and $k = 2\pi n_0/\lambda$, where λ is the wavelength in vacuum. From now on we will refer to $\delta n(x, y, z)$ as the potential or index of refraction. In the simulations we use $n_0 = 2.3$, corresponding to the systems that were used to implement the optical induction technique [162, 163], and $\lambda = 500$ nm.

3.1.2 The grating assisted tunneling method

For clarity, let us first present the grating assisted tunneling method in a 1D photonic lattice. If the potential is a periodic lattice, $\delta n_L(x) = \delta n_L(x+a)$, where a is the lattice constant, and if the lattice is sufficiently 'deep', the propagation of light can be approximated by using a discrete Schrödinger equation [165, 166]:

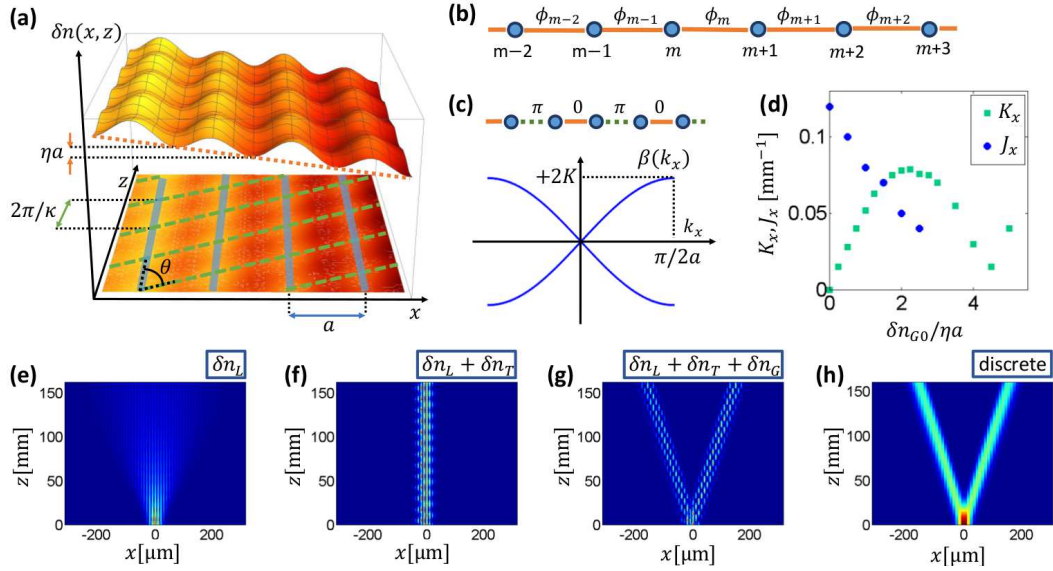$$i\frac{d\psi_m}{dz} = -(J_x \psi_{m-1} + J_x \psi_{m+1}), \tag{3.1.2}$$

Figure 3.1: Illustration of the grating assisted tunneling scheme. (a) Sketch of the spatial dependence of the index of refraction $\delta n_L(x,z) = \delta n_L + \delta n_T + \delta n_G$, which creates a synthetic magnetic field in a photonic lattice. A 1D photonic lattice $[\delta n_L = \delta n_{L0} \cos^2(\pi x/a)]$ is superimposed with a linear gradient index in the x direction ($\delta n_T = -\eta x$, orange dotted line), and an additional small grating potential $[\delta n_G = \delta n_{G0} \cos^2((q_x x - \kappa z)/2)]$, at a small angle ($\theta$ is on the order of $1°$) with respect to the z axis. In the xz plane we plot the projection of δn_L (blue bold lines), and the grating (green dashed lines). (b) A discrete lattice with complex tunneling matrix elements between sites, $K_x e^{i\phi_m}$, and spatially dependent phases ϕ_m, can model the system in (a). (c) A particular choice of θ (see text), yields a lattice with $\phi_m = \pi m$, and a dispersion with a 1D Dirac cone at $k_x = 0$. (d) The amplitude of the tunneling K_x as a function of the strength of the grating δn_{G0} (green squares). The tunneling amplitude J_x versus δn_{G0} for a system without the tilt. (e,f,g) Numerical simulation of the evolution of a wavepacket that initially excites modes close to $k_x = 0$ in the continuous 1D photonic lattice. (e) Diffraction in a periodic photonic lattice δn_L. (f) Propagation in the tilted system, $\delta n_L + \delta n_T$, shows that the tunneling (diffraction) is suppressed. (g) The tunneling is restored by an additional grating potential with $q_x = \pi/a$. (h) Propagation of the wavepacket in the corresponding discrete model illustrated in (c).

where J_x quantifies the tunneling between adjacent waveguides and $\psi_m(z)$ is the amplitude at the mth lattice site, i.e., waveguide. To create a synthetic magnetic field, we adopt the strategy to tune the phase of the tunneling between lattice sites. For this 1D lattice, we seek a scheme which effectively renormalizes J_x to get $K_x \exp(i\phi_m)$, where ϕ_m denotes the phase for tunneling from site m to site $m + 1$. The scheme is illustrated in Fig. 3.1. In Fig. 3.1(a) we show the potential $\delta n(x, z)$, which can be modeled as a discrete lattice with complex tunneling parameters $K_x \exp(i\phi_m)$ shown in Fig.3.1(b).

Let us gradually explain the idea behind the variation of the index of refraction as in Fig. 3.1(a). In Fig. 3.1(e), we show the propagation of intensity in a continuous 1D model in the lattice potential

$$\delta n_L(x) = \delta n_{L0} \cos^2(\pi x/a), \tag{3.1.3}$$

with $\psi(x, 0) = \sqrt{I} e^{-x^2/(3a)^2}$; $\delta n_{L0} = 4 \times 10^{-4}$, $a = 10$ μm. We see the usual diffraction pattern for a spatially broad excitation covering several lattice sites [165]. Next, suppose that we introduce a linear gradient of index of refraction along the x direction

$$\delta n_T(x) = -\eta x \tag{3.1.4}$$

in addition to the lattice potential, such that $\delta n = \delta n_L(x) + \delta n_T(x)$. For a sufficiently large tilt, the tunneling is *suppressed*. This can be seen from Fig. 3.1(f) which shows the propagation of intensity in a tilted potential with $\eta = 0.1\delta n_{L0}/a$; the tilt should be smaller than the gap between the first two bands. Finally, let us introduce an additional small grating potential at a small angle θ with respect to the z axis,

$$\delta n_G(x, z) = \delta n_{G0} \cos^2((q_x x - \kappa z)/2), \tag{3.1.5}$$

such that

$$\delta n(x, z) = \delta n_L(x) + \delta n_T(x) + \delta n_G(x, z). \tag{3.1.6}$$

This total potential $\delta n(x, z)$ is illustrated in Fig. 3.1(a). The 'frequency' κ is determined by the angle θ of the grating with respect to the z-axis, which is chosen such that $\kappa = \eta a k/n_0$ and the grating forms a z-dependent perturbation resonant with the index offset between neighboring lattice sites ηa (Fig. 3.1(a)). The grating *restores* the tunneling along the x-axis, hence the term *grating assisted tunneling*. Restored tunneling is seen in Fig. 3.1(g)

which shows diffraction for identical initial conditions as in Figs. 3.1(e) and (f); the grating parameters are $q_x = \pi/a$ and $\delta n_{G0} = 0.1\delta n_{L0}$.

However, the diffraction pattern is drastically changed. In order to interpret it, we point out that, for resonant tunneling where $\kappa = \eta ak/n_0$ and a sufficiently large tilt ($J \ll \eta$), z-averaging over the rapidly oscillating terms shows that the system can be modeled by an effective discrete Schrödinger equation (e.g., see [24] for ultracold atoms):

$$i\frac{d\psi_m}{dz} = -(K_x e^{i\phi_{m-1}}\psi_{m-1} + K_x e^{-i\phi_m}\psi_{m+1}), \qquad (3.1.7)$$

where $\phi_m = \mathbf{q} \cdot \mathbf{R}_m = q_x ma$. In Fig. 3.1(g) we used $q_x = \pi/a$, i.e., $\phi_m = m\pi$. Such a discrete lattice is illustrated in Fig. 3.1(c); its dispersion having a 1D Dirac cone at $k_x = 0$. For a wavepacket that initially excites modes close to $k_x = 0$, the diffraction in the discrete model (Eq. 3.1.7) yields the so-called (1D) conical diffraction pattern [37, 167], as illustrated in Fig. 3.1(h). The initial conditions for propagation in the discrete model corresponds to the initial conditions in the continuous system, $\psi_m(0) = \sqrt{I}e^{-(m/3)^2}$, and $K_x = 0.053$ mm^{-1}. Thus, we interpret the diffraction pattern in Fig. 3.1(g) as 1D conical diffraction, a signature of the discrete model depicted in Fig. 3.1(c). A comparison of the discrete [Fig. 3.1(h)] and the realistic continuous model [Fig. 3.1(g)], clearly shows that we can use grating assisted tunneling to tune the phases of the tunneling parameters in the discrete Schrödinger equation, thereby realizing synthetic magnetic fields.

Before proceeding to 2D systems, we discuss the amplitude of the tunneling matrix elements K_x as a function of the strength of the grating δn_{G0}. Figure 3.1(d) shows K_x (green squares) and J_x (blue circles) versus δn_{G0}, where J_x corresponds to the potential which includes the lattice and the grating, but no tilt. The amplitudes J_x and K_x are obtained by comparing the diffraction pattern of the discrete with the continuous model, and adjusting J_x and K_x until the two patterns coincide, as in Figs. 3.1(g) and (h). Our results in Fig. 3.1(d) are in agreement with those in ultracold atoms [e.g., see Fig. 3(a) in Ref. [24]].

3.1.3 Grating assisted tunneling in 2D and the Harper-Hostadter Hamiltonian

The extension of the scheme to 2D lattices is straightforward. We consider a square lattice, $\delta n_L = \delta n_{L0}(\cos^2(\pi x/a) + \cos^2(\pi y/a))$, the tilt in the x direction, $\delta n_T(x) = -\eta x$, and the grating which has the form $\delta n_G(x, y, z) = \delta n_{G0} \cos^2((q_x x + q_y y - \kappa z)/2)$. Propagation of light in the total potential $\delta n(x, y, z) = \delta n_L(x, y) + \delta n_T(x) + \delta n_G(x, y, z)$ can be modeled by the discrete Schrödinger equation (the derivation is equivalent to that in Ref. [24] for ultracold atoms):

$$i\frac{d\psi_{m,n}}{dz} = -\ (K_x e^{i\phi_{m-1,n}}\psi_{m-1,n} + K_x e^{-i\phi_{m,n}}\psi_{m+1,n}$$
$$+\ J_y \psi_{m,n-1} + J_y \psi_{m,n+1}), \tag{3.1.8}$$

where $\phi_{m,n} = \mathbf{q} \cdot \mathbf{R}_{m,n} = q_x ma + q_y na$. Note that the tunneling along y does not yield a phase because there is no tilt in the y direction; the tunneling amplitude along y depends on the depth of the grating, as illustrated in Fig. 3.1(d) with blue circles.

In order to demonstrate that the propagation of light in the continuous 2D potential $\delta n(x, y, z)$ is indeed equivalent to the dynamics of Eq. 3.1.8, we compare propagation in the discrete model (Eq. 3.1.8), with that of the continuous equation (Eq. 3.1.1). The lattice parameters are $\delta n_{L0} = 4 \times 10^{-4}$, $a = 13$ μm; the tilt is given by $\eta = 0.1\delta n_{L0}/a$; the grating is defined by $\delta n_{G0} = 0.17\delta n_{L0}$ and $q_x = -q_y = \pi/a$, which yields $\phi_{m,n} = (m-n)\pi$, and κ is chosen to yield resonant tunneling. The discrete lattice which corresponds to this choice of phases is illustrated in Fig. 3.2(a). It has two bands,

$$\beta = \pm 2\sqrt{K_x^2 \sin^2(k_x a) + J_y^2 \cos^2(k_y a)} \tag{3.1.9}$$

(β is the propagation constant), touching at two 2D Dirac points at $(k_x, k_y) = (0, \pm\pi/2a)$ in the Brillouin zone [115], as depicted in Fig. 3.2(b). Suppose that the incoming beam at $z = 0$, excites the modes which are in the vicinity of these two Dirac points. Around these points, for a given $\hat{\mathbf{k}} = \mathbf{k}/k$, the group velocity, $\nabla_{\mathbf{k}}\beta(k_x, k_y)$, is constant. Thus, the beam will undergo conical diffraction, which has been thoroughly addressed with Dirac points in honeycomb optical lattices [167]. To demonstrate this effect, we consider the

propagation of a beam with the initial profile given by

$$\psi(x, y, 0) = \sqrt{I} \cos(y\pi/2a) \exp(-(x/3a)^2 - (y/3a)^2) \qquad (3.1.10)$$

in the 2D potential $\delta n(x, y, z)$ (the cosine term ensures that we excite modes close to the two Dirac points). In Fig. 3.2(c) we show this beam after propagation for $z = 162$ mm. The two concentric rings are a clear evidence of conical diffraction [167, 168]. We also compare this with the propagation in the discrete model (Eq. 3.1.8), with tunneling phases plotted in Fig. 3.2(a); $K_x = 0.11$ mm^{-1}, $J_y = 0.14$ mm^{-1}. The results of the propagation in the discrete model are shown in Fig. 3.2(d). It is evident that for our choice of the tilt and the grating, we have effectively realized the lattice plotted in Fig. 3.2(a). This is in fact a realization of the HHH for $\alpha = 1/2$, where α is the flux per plaquette in units of the flux quantum [24, 25].

We emphasize that the spatial phase between the periodic lattice potential δn_L and the grating δn_G is a relevant parameter. This point has recently been examined in detail in the context of ultracold atoms [169]. To translate it to our system, suppose that in our 1D system, we shift the grating along the x-direction, such that $\delta n_G = \delta n_{G0} \cos^2((q_x x - \kappa z + \xi)/2)$. This simply shifts the phases in the discrete lattice [shown in Fig. 3.1(c)] such that ϕ_m is replaced by $\phi_m + \xi$, which moves the 1D Dirac point in k_x-space by $\Delta k_x = \xi/a$. We have numerically verified that this indeed happens.

3.1.4 Proposal for experimental realization

For the experimental implementation of the scheme, we propose the so-called optical induction technique in photosensitive materials, which can be implemented in photorefractives [161–165]. In these systems, both the lattice $\delta n_L(x, y)$ and the grating potential $\delta n_G(x, y, z)$ can be obtained in a straightforward fashion by using interference of plane waves in the medium [165]. The lattice constant a, the grating parameter $\mathbf{q}$, and hence the hopping phase $\phi_{m,n} = \mathbf{q} \cdot \mathbf{R}_{m,n}$, are tunable by changing the angle between the interfering beams. This could enable manipulation of the phases of the tunneling matrix elements in real time [163].

The most challenging part of the implementation appears to be creation of the linear tilt potential. To observe the conical diffraction effects, one needs a linear gradient over the
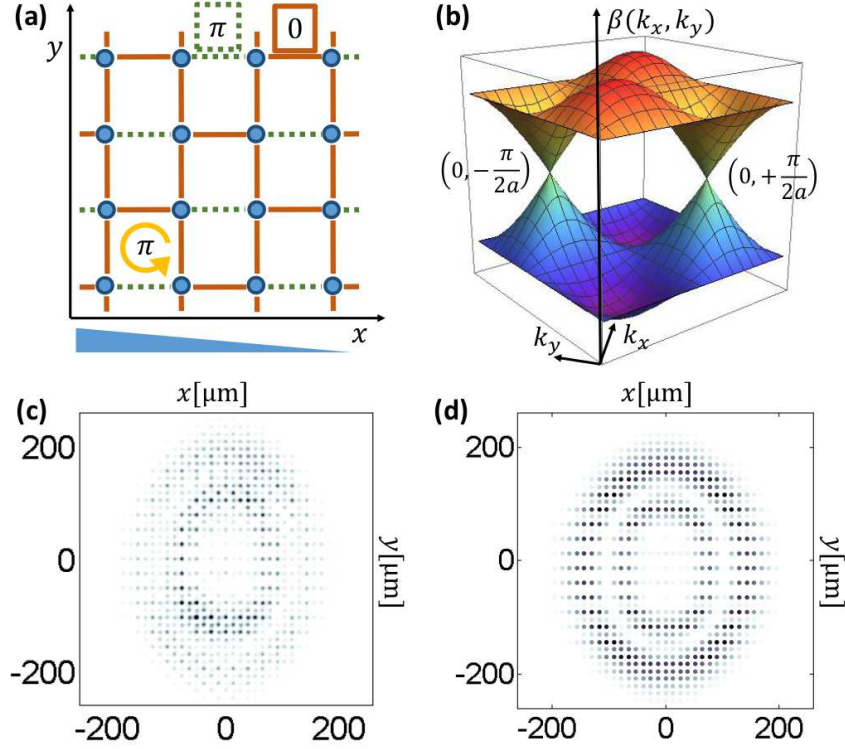
Figure 3.2: Grating assisted tunneling and conical diffraction in a square photonic lattice. (a) Sketch of the 2D lattice with grating assisted tunneling along the x direction. The resulting nontrivial hopping phases π and 0 are denoted with dashed and solid lines, respectively. A wavepacket that makes one loop around the plaquette accumulates the phase π. (b) The lattice possesses two 2D Dirac cones at $(k_x, k_y) = (0, \pm\pi/2a)$ in the dispersion $\beta(k_x, k_y)$, where β is the propagation constant. (c) Intensity of a beam, which initially excites modes in the vicinity of the Dirac points, after propagation for $z = 162$ mm. The intensity has two concentric rings corresponding to the conical diffraction pattern. (d) Simulation of the diffraction pattern in the discrete model corresponding to the lattice in (a), which also exhibits conical diffraction (see text for details).

~ 20 lattice sites, which implies a total index tilt $\Delta n = 20\eta a \sim 20 \times 0.1 \delta n_{L0} \sim 8 \times 10^{-4}$. In principle, the linear tilt could be achieved by using a spatial light modulator. Another possibility which could create a linear tilt is to use crystals with linear dependence of the index of refraction on temperature, and a temperature gradient across the crystal.

However, it should be emphasized that if one uses a superlattice for δn_L, rather than the linear tilt potential, as in Ref. [26] for ultracold atomic gases, the grating assisted tunneling scheme proposed here would straightforwardly yield *staggered* synthetic magnetic fields for photons. The achievement of such staggered fields is straightforward with optically induced lattices proposed here.

$$\sim$$

We have proposed a grating assisted tunneling scheme that introduces tunable synthetic magnetic fields in an optical lattice, inspired by laser assisted tunneling in lattices of quantum gases. Such a possibility is yet another manifestation and consequence of the many faces interesting physical phenomena can have. Once again, it emphasizes the value of Feynman's idea of universal quantum simulation, and the search for systems that are governed by the same laws. Nevertheless, as each of the systems possesses its own advantages and limitations, making every new contribution to synthetic magnetism valuable. For example, the absence of heating from spontaneous emission in photonics, present in atomic systems, could result in even more feasible results, such as the potentially resulting topological characteristics leading to backscattering immune light propagation.

We have confirmed the validity of the proposed grating assisted tunneling method for synthetic magnetism by a direct comparison of the light propagation in such a continuous system and the evolution in a discrete model with nontrivial hopping phases. This approach can open the way for mapping the light propagation in tailored dielectric structures to intriguing discrete models, such as the Harper-Hofstadter Hamiltonian.

3.2 Laser assisted tunneling in a Tonks-Girardeau gas

The introduction of interaction into quantum systems can lead to strongly correlated quantum many-body states. Interactions can significantly enrich the underlying physics and induce interesting consequences. In the context of topological matter, for example, interactions have been shown to influence the transitions between different topological phases [14, 66]. However, the prediction of the behavior of these systems is extremely demanding. It is in these cases that quantum simulations and synthetic magnetism appear to be the only way to the comprehension and characterization of such systems. The recent experimental progress of the control of ultracold atomic gases has given rise to a powerful tool for the coherent manipulation of many-body states and their dynamics, where interactions between particles can be accurately adjusted by using light scattering resonances. The introduction of synthetic magnetism, however, raises an important question, especially in the case of optical lattices. In the latter, synthetic magnetic fields are essentially obtained by periodic driving [23, 24, 26]. Interactions are known to induce thermalization during the time-evolution of most quantum systems, as conjectured by the eigenstate thermalization hypothesis [170]. With the addition of periodical driving, which can potentially be an infinite source of energy, the system can thermalize to an effectively infinite temperature [171–175]. Therefore, the combination of interactions and periodical driving may have substantial consequences on the applicability of standard methods for synthetic magnetism in quantum systems. In this chapter, we investigate the laser assisted tunneling method for creating synthetic magnetic fields in a Tonks-Girardeau gas. We start by introducing the consequences of interactions and periodic driving in quantum many-body systems. We then consider the impact it can have on synthetic magnetism in strongly interacting one-dimensional Bose gases, showing that the stroboscopic dynamics of a Tonks–Girardeau gas with laser assisted tunneling effectively realizes the ground state of 1D hard-core bosons on a discrete lattice with nontrivial hopping phases.

3.2.1 Periodically driven interacting systems

Unlike most noninteracting quantum systems, whose trajectories in phase space typically stay confined by the strict constraints of motion (the so called *localization*), interacting

systems are likely to thermalize to the usual thermal state. At long times, no matter how far from equilibrium the state in which the system is initially prepared is, the system is ergodic and can be accurately described using equilibrium statistical mechanics. In accordance with the so called *eigenstate thermalization hypothesis*, this can be seen as a consequence of the thermal distributions being encoded in each many-body eigenstate [176]. In a periodically driven, i.e. Floquet, interacting system, the driving perturbation can be strong enough to mix exponentially many eigenstates of the undriven Hamiltonian together. This leads to a thermalization scenario that is independent on the initial state. It is in contrast to what happens with no interactions present, when the extensive number of conserved quantities exponentially reduces the number of states that are being mixed. Furthermore, due to the lack of energy conservation in nonintegrable Floquet systems, as energy is periodically pumped in by the driving, it is believed that the system approaches a state described by an infinite-temperature ensemble [172, 177].

Although an intuition about transitions between phases with significantly different long-time scenarios can be built from the paragraph above, there exist many possible exceptions. For example, the introduction of disorder that is strong enough can effectively reduce the size of the phase space, via segmentation into local subspaces, and lead to a localized and nonergodic behavior in an interacting many-body system (*many-body localization*). In periodically driven interacting systems that are mappable to free systems, on the other hand, happens an extensive reduction of the eigenstates that get mixed together, leading again to localization [177]. Moreover, even systems that approach effectively infinite temperatures at infinite times can, if the time-scale relevant for the experiment is shorter than the heating time t_h, approach a prethermalized Floquet steady state before heating up.

An optical lattice with laser assisted tunneling, in which the tunneling suppressed by a linear tilt is resonantly restored by a time-periodic potential (ω), is an example of a Floquet system. When no interactions are present, the corresponding high-frequency effective Hamiltonian directly corresponds to the target Hamiltonian with synthetic magnetic fields, at all times that are experimentally relevant (a few hundred milliseconds). It is important to investigate whereas the addition of interactions will still allow such a mapping of the Floquet Hamiltonian. We address this problem in the context of a one-dimensional gas with contact interactions, the Tonks-Girardeau gas, on an optical lattice. Due to

the reduced dimensionality, this many-body system promises to show enhanced quantum effects. It is also strongly related to the one-dimensional hard-core version of anyons [137]. In order to check the applicability of the standard laser assisted tunneling method, we directly compare the quantum dynamics of a continuous Tonks-Girardeau system with the periodic driving, with the ground state of hard core bosons on a discrete lattice with complex hopping parameters.

3.2.2 Tonks-Girardeau gas and laser assisted tunneling

We consider N identical bosons in 1D interacting via pointlike interactions, described by the Hamiltonian

$$\hat{H} = \sum_{i=1}^{N} \left[-\frac{\hbar^2}{2m} \frac{\partial^2}{\partial x_i^2} + V(x_i, t) \right] + g_{1D} \sum_{1 \leq i < j \leq N} \delta(x_i - x_j). \tag{3.2.1}$$

In the strongly interacting Tonks-Girardeau regime [178], with infinitely repulsive contact interactions $g_{1D} \to \infty$, the interaction term in the Hamiltonian in Eq. 3.2.1 can be replaced by a boundary condition for the many-body wave function

$$\Psi_B(x_1, x_2, \ldots, x_N, t) = 0 \text{ if } x_i = x_j, \tag{3.2.2}$$

satisfied by an antisymmetric many-body wave function describing a system of noninteracting spinless fermions in 1D [178]. One can thus express the exact (static or time-dependent) solution for the Tonks-Girardeau model via the famous Fermi-Bose mapping [178, 179], as

$$\Psi_B(x_1, x_2, \ldots, x_N, t) = \prod_{1 \leq i < j \leq N} \text{sgn}(x_i - x_j) \Psi_F(x_1, x_2, \ldots, x_N, t) , \tag{3.2.3}$$

where ψ_F denotes the solution for the noninteracting spinless fermionic case. By knowing the many-body wave function describing the Tonks-Girardeau gas in an external potential (ψ_B) or the noninteracting fermionic 1D gas (ψ_F), one can obtain the reduced single particle density matrix (RSPDM), defined as

$$\rho_{\{B,F\}}(x, y, t) = N \int dx_2 \ldots dx_N \, \Psi^*_{\{B,F\}}(x, x_2, \ldots, x_N, t) \Psi_{\{B,F\}}(y, x_2, \ldots, x_N, t) \tag{3.2.4}$$

The RSPDM makes available, at least in principle, the expectation values of all one-body

observables for the system, such as the single-particle density

$$\rho_{\{B,F\}}(x,x,t) = \sum_{m=1}^{N} |\psi_m(x,t)|^2 \tag{3.2.5}$$

and the momentum distribution

$$n_{\{B,F\}}(k,t) = \frac{1}{2\pi} \int dx dy \, e^{ik(x-y)} \rho_{\{B,F\}}(x,y,t). \tag{3.2.6}$$

The single particle density $\rho_B(x,x,t)$ is identical for the Tonks-Girardeau gas and the noninteracting Fermi gas [178], and are thus straightforward to obtain. On the other hand, the momentum distributions are significantly different on the two sides of the Fermi-Bose mapping [180]. While the procedure is standard for noninteracting spinless fermions, for the continuous Tonks-Girardeau model it can be efficiently calculated as outlined in Ref. [181].

A Tonks-Girardeau gas in an optical lattice with laser assisted tunneling can be described by the Hamiltonian in Eq. 3.2.1, with a time- and space-dependent potential

$$V(x,t) = V_L(x) + V_T(x) + V_R(x,t). \tag{3.2.7}$$

Here, the spatially periodic $V_L(x) = V_L \cos^2(\pi x/D)$ accounts for the lattice. Atoms can tunnel between its adjacent minima with an effective hopping parameter J. $V_T(x) = \alpha x/D$ introduces the tilt potential, which suppresses the tunneling between neighboring sites for α large enough, if no $V_R(x,t)$ is present. The spatially and time-periodic $V_R(x,t) = V_R \cos^2\left[(qx - \omega t)/2\right]$ describes the potential arising from the two Raman lasers, with a difference in frequency ω and wave vectors q. This restores the tunneling for $\hbar\omega = \alpha$, and introduces effective nontrivial phases of the hopping parameters. In the regime $J \ll \alpha D$ when the tilt completely suppresses the standard tunneling, for noninteracting systems, the combination $V_T(x) + V_R(x)$ is responsible for laser-assisted tunneling.

3.2.3 Hard core bosons and complex tunneling matrix elements

A continuous model of the Tonks-Girardeau gas in the potential in Eq. 3.2.7, in the case of a deep optical lattice, can be approximated by a discrete Hamiltonian with kinetic (hopping) terms, on-site interactions, tilt and periodic drive. The evolution of

such a discrete Hamiltonian is determined by the high-frequency expansion [47, 182], explained in Section 3.2.1. Because of the tilt potential, the Hamiltonian is divergent in the limit of $\omega \to \infty$, which can be removed by applying a time-dependent unitary transformation into a rotating frame. In the case of resonant driving ($\hbar\omega = \alpha D$), as a results of this transformation, the kinetic, tilt and drive terms become an effective kinetic term with complex hopping matrix elements. The on-site interaction term, however, is not affected for any strength of the interaction energy U and any lattice dimension. In other words, the Tonks-Girardeau gas in the continuous potential (Eq. 3.2.7) can be approximately described with a Hamiltonian of hard core bosons (HCB) on a discrete lattice with nontrivial hopping phases:

$$\hat{H} = -K \sum_{m=1}^{M} \left[e^{i\phi_m} \hat{b}_{m+1}^{\dagger} \hat{b}_m + h.c \right], \quad \hat{b}_m^{\dagger 2} = \hat{b}_m^2 = 0, \quad \left\{ \hat{b}_m, \hat{b}_m^{\dagger} \right\} = 1, \tag{3.2.8}$$

where the hopping phase is given with $\phi_n = qDn$ and K is the effective hopping amplitude.

The ground state properties of the HCB Hamiltonian (Eq. 3.2.8) can be obtained by using the Jordan-Wigner transformation [183–185]

$$\hat{b}_m^{\dagger} = \hat{f}_m^{\dagger} \prod_{\beta=1}^{m-1} e^{-i\pi \hat{f}_\beta^{\dagger} \hat{f}_\beta} \quad \hat{b}_m = \prod_{\beta=1}^{m-1} e^{i\pi \hat{f}_\beta^{\dagger} \hat{f}_\beta} \hat{f}_m, \tag{3.2.9}$$

which maps the HCB Hamiltonian (Eq. 3.2.8), to the Hamiltonian for discrete noninteracting spinless fermions:

$$\hat{H} = -\sum_{m=1}^{M} \left[K e^{i\phi_m} \hat{f}_{m+1}^{\dagger} \hat{f}_m + h.c \right], \tag{3.2.10}$$

where $\hat{f}_m^{\dagger}$ and $\hat{f}_m$ are the creation and annihilation operators for spinless fermions.

3.2.4 Continuous vs. discrete

In order to confirm the appropriateness of mapping the effective Hamiltonian of a Tonks-Girardeau gas in an optical lattice with laser assisted tunneling to that of hard-core bosons in a lattice with synthetic magnetism, i.e. when strong interactions are present, we directly compare the evolution and observables for the continuous and discrete system. We consider a discrete lattice with $M = 40$ sites, corresponding to $M = 40$ lattice sites of the
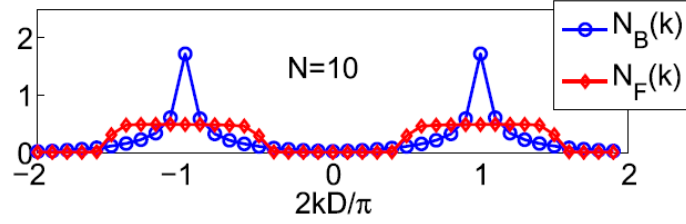
Figure 3.3: Ground state momentum distribution of hard core bosons $N_B(k)$ and non-interacting spinless fermions $N_F(k)$ in the discrete lattice with hopping phases $\phi_m = m\pi$. [4]

optical lattice potential $V_L(x)$. By choosing the angle between the Raman beams [24, 25] to yield $q = \pi/D$ in the time-dependent potential $V_R(x,t)$, we select a particular phase of the hopping parameters, $\phi_n = n\pi$. For this choice of the hopping phase, the discrete lattice has alternating hopping matrix elements, $K(-1)^n$, for tunneling from site n to site $n+1$. We estimate the effective hopping amplitude to be $K = 0.012E_R$, by comparing the expansion of a Gaussian wave packet in the continuous and the evolution in the discrete systems. The method is inpired by a similar procedure we have presented in the previous section for a photonic system.

Specifically, we compare the ground state momentum distribution of hard core bosons $N_B(k)$ and noninteracting spinless fermions $N_F(k)$ in the discrete lattice with hopping phases $\phi_m = m\pi$, with the momentum distributions for Tonks-Girardeau bosons in the continuous Wannier-Stark-ladder potential with periodic driving $n_B(k,t)$ and for free fermions $n_F(k,t)$, respectively, at different times. The comparison for the same number of particles clearly shows that the distributions for the continuous systems overlap at all stroboscopic instants in Fig. 3.4, and are also in agreement with the results for a discrete model guided by the effective Hamiltonian in Fig. 3.3. The occupancies of natural orbitals are also in agreement at stroboscopic times, additionally strengthening the result about the applicability of laser assisted tunneling in a Tonks-Girardeau gas.

$\sim$

We have considered laser assisted tunneling, a powerful method for creating tunable synthetic magnetic fields and tailoring the phases of complex matrix elements in lattices of
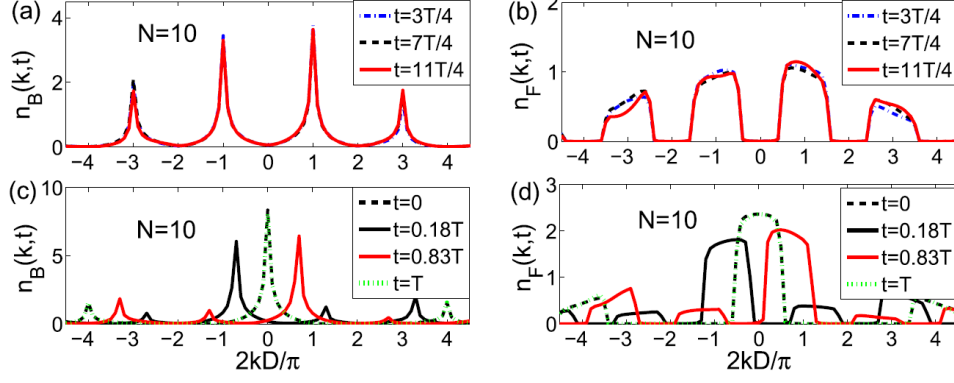
Figure 3.4: Time dependence of the momentum distributions of Tonks-Girardeau bosons in the continuous Wannier-Stark-ladder potential with periodic driving $n_B(k,t)$ and of free fermions $n_F(k,t)$, at different times. [4]

ultracold atoms, in a system with strong contact interactions. Namely, we have confirmed its applicability for a Tonks-Girardeau gas in a 1D optical lattice. Although interactions are present, the high-frequency approximation of the continuous effective Hamiltonian, describing the stroboscopic evolution in such a system, can be mapped to that of 1D hard-core bosons on a discrete lattice with nontrivial hopping phases. Additionally, we have directly compared the evolution of observables, such as momentum distribution and natural orbitals, in the continuous and discrete systems, obtaining excellent agreement at stroboscopic times.

Once again, we have shown that numerical 'experiments', confirming a direct mapping of continuous systems to discrete models, can open the way to the study of states where simple approximations are not necessarilly applicable. For example, a similar study could be performed for interactions of (finite) modulated strength [186, 187], potentially resulting in new intriguing correlated many-body phases.

3.3 Synthetic Lorentz force in classical atomic gases

In many of the complex many-body systems it is particularly the *quantum* nature of its constituents that has a key role in the striking phenomena they give rise to. Consequently, there has been a lot of interest in the interest in the study of quantum degenerate matter, which also motivated the search for physical systems that can be used as quantum simulators, such as quantum degenerate atomic gases. Most methods for synthetic magnetism have been, accordingly, designed to rely on an adiabatic evolution in the ultracold quantum degenerate system. It is thus possible to simulate, understand and predict the behavior of complex quantum systems and related magnetic phenomena, which would have hardly been possible even by using the most powerful super-computers. The latter can, nevertheless, be valid for some systems that do not fall in the category of quantum degenerate matter. Examples include complex astrophysical objects, such as stars or globular clusters, and plasmas, such as those in tokamak fusion reactors. However, *classical* (rather than quantum degenerate) cold atomic gases have been circumvented in the quest for synthetic magnetism, even though they could simulate in a controllable fashion, and in tabletop experiments, versatile complex classical systems.

In classical atomic gases, any scheme for synthetic magnetism must be operational on atoms moving with fairly large velocities (at least up to ~ 0.5 m/s), which is why standard methods relying on adiabatic dynamics are limited. In addition, because of the relatively large volumes they occupy in magneto-optical traps, the synthetic force in classical gases has to be fairly uniform and strong in volumes of at least few cubic millimeters. On the other hand, because of the higher temperatures, schemes do not need to be limited by avoiding spontaneous emission. With these guidelines in mind, we propose a method for creating a synthetic Lorentz force based on the Doppler effect and radiation pressure [5]. The theoretical proposal is followed by a collaboration with experimentalists at the Institute of physics in Zagreb, yielding the experimental confirmation of the synthetic Lorentz force [6, 7]. In this section, we briefly review the main concepts and the results of this collaboration.

3.3.1 Doppler force and two-step two-photon absorption

Atomic clouds trapped in optical molasses and magneto-optical traps are cooled down by using the so called Doppler cooling [188] . The standard Doppler cooling force arises when the laser field interacting with the cloud is red detuned compared to the atomic resonance frequency, as is sketched in Fig.3.5(a). Due to the Doppler effect, an atom has a higher probability of absorbing a photon if it is moving towards the light source. Every absorption changes the momentum of the atom along the laser propagation axis. On the other hand, spontaneously emitted photons yield random kicks. Cycles of absorption and emission result in a viscous damping force $\mathbf{F}_D(\mathbf{v}) \approx -\alpha \mathbf{v}$ for small velocities. This force is collinear with the atom's velocity.

In order to obtain a synthetic Lorentz force, we construct a laser-atom system in which the Doppler effect and radiation pressure result in a force orthogonal to the atom's velocity, for example $F_y(v_x)$. The simplest configuration yielding such a dependence is sketched in Fig. 3.5(b). A three-level atom interacts with two orthogonal laser beams in the $x - y$ plane (linearly polarized along z). The laser ω_{12} is detuned by $\delta_{12} = \omega_{12} - (E_2 - E_1)\hbar^{-1}$, whereas ω_{23} is detuned by δ_{23}. The resulting force for such a configuration is shown in Fig. 3.5(c,d). The absorption of ω_{23} photons, which results in F_y, is the second step in the two-step two-photon absorption process: $|1\rangle \rightarrow |2\rangle \rightarrow |3\rangle$. The probability for two-step absorption depends on the Doppler shifted detuning values $\delta_{12} - k_{12}v_x$ and $\delta_{23} - k_{23}v_y$, which provides the desired dependence of F_y on v_x. The maximum in F_y is expected for atoms with velocity $(v_x = \delta_{12}/k_{12}, v_y = \delta_{23}/k_{23})$, where each step is resonant.

3.3.2 Synthetic Lorentz force in a cold ^{87}Rb cloud

The idea for constructing the synthetic Lorentz force is general and potentially applicable to various atomic species. For concreteness, we theoretically consider such a force in a cold cloud of ^{87}Rb atoms, the same species in which the experimental realizations take place later on. The force can be calculated by using density matrices and the Ehrenfest theorem, yielding its dependence on the atomic velocity $\mathbf{F}(\mathbf{v})$. For example, in Fig. 3.5(c,d) we show the force resuting from a simple three-level scheme. The details of the dependence of such a force are determined by the specific characteristics of the system and scheme, e.g. atomic state decay rates and laser detunings or intensities. By taking
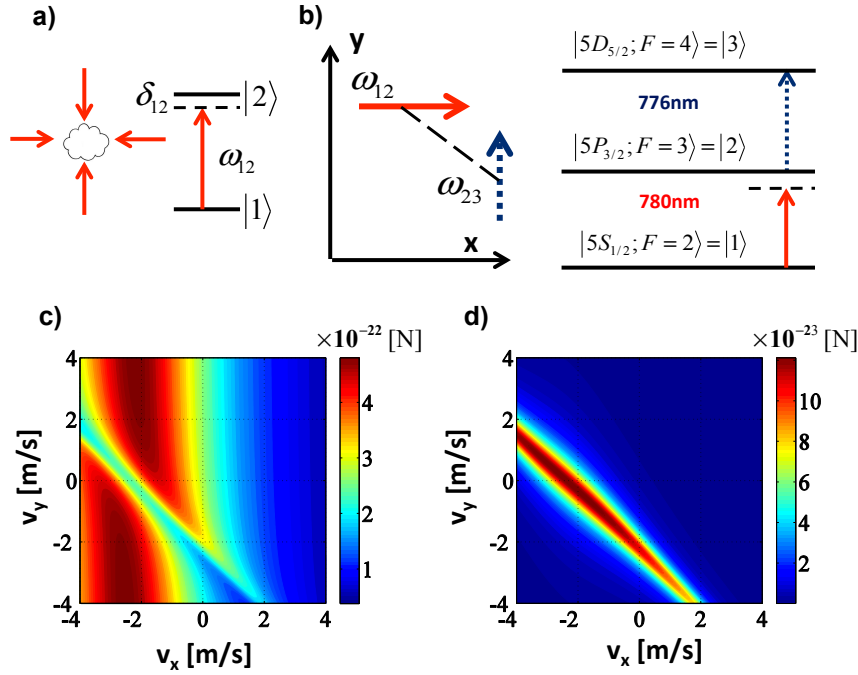
Figure 3.5: Sketch of the main idea for constructing the synthetic Lorentz force. (a) Illustration of the setup for the standard Doppler cooling force (using two-level atoms). (b) The idea for the synthetic Lorentz force in the simplest three-level system that can be realized with ^{87}Rb atoms. The dashed line indicates that two-step absorption of $\omega_{12} + \omega_{23}$ yields F_y . The force components (c) F_x and (d) F_y calculated as a function of the atomic velocity.

advantage of the multi-level structure of atoms, including new atomic states that are coupled by additional pairs of laser, and properly adjusting the detunings, it is therefore possible to taylor a synthetic Lorentz force.

Because of the small velocities of the cold atoms, an excellent approximation is often given by the Taylor expansion of the force in velocity up to the linear term:

$$\begin{bmatrix} F_x \\ F_y \end{bmatrix} = \begin{bmatrix} F_{x0} \\ F_{y0} \end{bmatrix} + \begin{bmatrix} \alpha_{xx} & 0 \\ 0 & \alpha_{yy} \end{bmatrix} \begin{bmatrix} v_x \\ v_y \end{bmatrix} + \begin{bmatrix} 0 & \alpha_{xy} \\ \alpha_{yx} & 0 \end{bmatrix} \begin{bmatrix} v_x \\ v_y \end{bmatrix}$$

$$= \mathbf{F}_0 + \mathbf{F}_D(\mathbf{v}) + \mathbf{F}_{SL}(\mathbf{v}). \qquad (3.3.1)$$

The third term $\mathbf{F}_{SL}(\mathbf{v})$ is a general form of the synthetic Lorentz force with components perpendicular to the velocity components: $F_{SL,x} = \alpha_{xy}v_y$, $F_{SL,y} = \alpha_{yx}v_x$. The force on a standing atom is $\mathbf{F}_0$. The components of the standard Doppler force are $F_{D,x} = \alpha_{xx}v_x$, and $F_{D,y} = \alpha_{yy}v_y$. Because the matrix representing $\mathbf{F}_D$ is diagonal, it can be formulated through a scalar potential in velocity space. When $\alpha_{xy} = -\alpha_{yx}$, $\mathbf{F}_{SL}$ takes the form of the
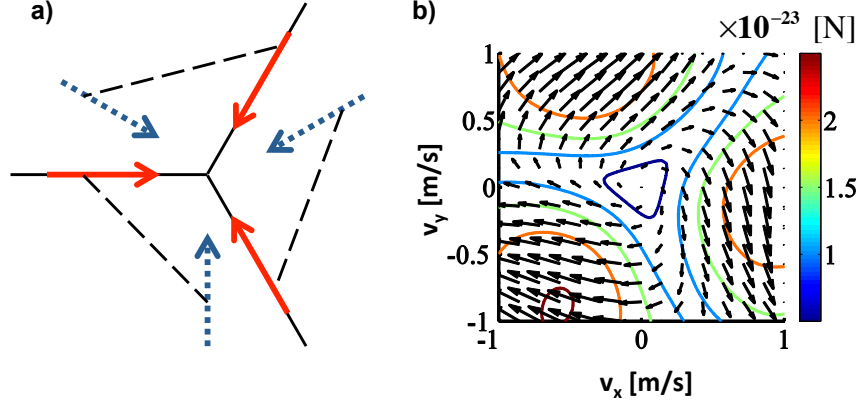
Figure 3.6: The tripod configuration of the three two-step excitations arms for ^{87}Rb, and the obtained force. (a) Red solid arrows depict first-step excitations (red detuned), and blue dotted arrows depict second steps (blue detuned). Black dashed lines connect beams that correspond to one arm. (b) Contour lines and length of the arrows correspond to the magnitude of the force $|F(v)|$.

standard Lorentz force: $\mathbf{F}_{SL} = \mathbf{v} \times \mathbf{B}^*$, where $\mathbf{B}^* = \alpha_{xy}\hat{\mathbf{z}}$. This can be achieved by using a tripod configuration of three two-step excitation arms, as we show in Fig. 3.6.

The above presented prediction of the synthetic Lorentz force is made for individual atoms. In order to be able to observe it experimentally, one has to know its impact on a cold atomic cloud containing a huge number ($\sim 10^9$ [188]) of atoms. We propose two scenarios, in which the signature of the synthetic Lorentz force can be found in the center-of-mass motion (CM), and in the shape of the atomic cloud. Both of them were recently experimentally realized [6, 7], yielding a final confirmation of the idea.

In the first case [6], the cold atomic cloud is initially displaced from the center of the trap by a bias field, which causes its acceleration along the x-axis towards the center. When in the center, the magneto-optical-trap cooling laser and all real magnetic fields are turned off, leaving the cloud under the influence of only the synthetic Lorentz force. The motion of the cloud is imaged with a camera. By looking at the trajectories, shown in Fig. 3.7, we can see that the cloud travels along the x-axis by inertia, whereas it accelerates along the y-axis due to the synthetic Lorentz force.

In the second case [7], the cold atomic cloud is initially rotationally asymmetrical. As the cloud is released from a magneto-optical trap, i.e. cooling lasers are turned off, the evolution of its shape is observed under the influence of thermal expansion and the applied synthetic Lorentz force. The signature of the synthetic Lorentz force is an angular deflection during the expansion of the cloud. We theoretically discuss the expansion of
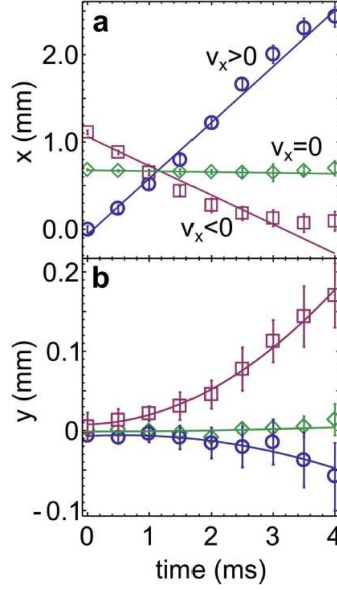
Figure 3.7: Experimental measurements of the synthetic Lorentz force [6]: the trajectories of the CM of the atomic cloud in the presence of the synthetic Lorentz force. (a) $x(t)$, and (b) $y(t)$ for three different initial velocities, $v_x = 0.6\text{m/s} > 0$ (circles), $vx = -0.3\text{m/s} < 0$ (squares), and $v_x = 0\text{m/s}$ (diamonds); the initial component of $v_y = 0$ in all measurements. Accelerating motion along y is the signature of the transverse force F_y, which depends on the orthogonal velocity v_x.

the cloud by employing the Fokker-Planck equation [188]

$$\frac{\partial P(\mathbf{x}, \mathbf{v}, t)}{\partial t} + \mathbf{v} \cdot \nabla_r P = \frac{-1}{m} \nabla_v \cdot [(\mathbf{F}_D + \mathbf{F}_{SL})P] + \frac{D}{m^2} \nabla_v^2 P, \qquad (3.3.2)$$

where $P(\mathbf{x}, \mathbf{v}, t)$ is the distribution of particles in the phase space and D is the diffusion constant. In Fig. 3.8, we show the comparison of experimental and theoretical results for the atomic density distributions after a 4ms expansion of the asymmetrical cloud for three different laser configurations. Unlike the case when only first-step beams are present, figures (b,c), the influence of the two-step absorption and the synthetic Lorentz force can be seen through the deflection in figures (e,f,h,i).

We point out that, due to unavoidable experimental imperfections and additional limitations of experiments, an initial theoretical framework often has to be extended in order to successfully account for the experimental situation. For example, not all transitions between the atomic states that participate in creating the synthetic Lorentz force are closed, meaning that over time the population will leak into other states. This can lead to a significant modification of the system evolution, and is experimentally accounted for by the introduction of additional lasers that repump the population in the targeted
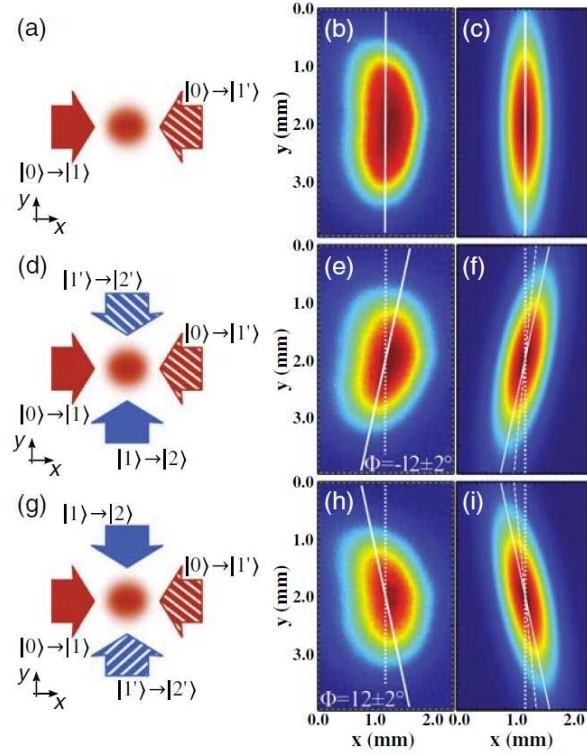
Figure 3.8: Experimental measurements of the synthetic Lorentz force [7]: Atom density distributions after time-of-flight of 4 ms for three different configurations, (a, d, g). The corresponding experimental, (b, e, h), and numerical results, (c, f, i), are show in the same row. (b, c) Density distribution with only the first-step beams present. (e, f, h, i) Density distributions with all four beams present, hence under the influence of the synthetic Lorentz force. Note that the two second-step beams have switched places from (d) to (g). The deflection angles of the major axes are indicated with full white lines. In panels (f) and (i) a dashed line indicates what the deflection angle would be without the synthetic Lorentz force term in Eq. 3.3.1.

cycle. On the other hand, the lasers driving the transitions have a finite linewidth, which we introduce in the simulations by convolving the force in velocity space with a Gaussian.

$\sim$

By proposing a method for creating a synthetic Lorentz force in classical atomic gases, we open the way to the study of complex classical, rather than quantum degenerate, systems of charged particles in magnetic fields, such as astrophysical objects or plasma. The idea is based on the Doppler effect and radiation pressure in two-step two-photon transitions, yielding a force orthogonal to the atomic velocity. A collaboration with the experimental group at the Institute of Physics in Zagreb has recently yielded the experimental proof of the method for a cold atomic cloud in a magneto-optical trap [6, 7], once again emphasizing the importance of collaborations between theoretical and experimental studies.

CHAPTER 4

Conclusions

A wide spectrum of intriguing phenomena in modern physics, such as the quantum Hall or Bohm-Aharonov effects, gauge invariance and topological phases, is rooted in the coupling of electric charge to magnetic fields. However, it mostly includes quantum many-body systems, which noticeably makes the research and understanding harder. On one hand, phenomena in which the quantum nature of a system is essential are hard to experimentally address, because they often require matter subjected to quite extreme conditions. For example, extremely high magnetic fields and low temperatures, or highly complicated structural designs. On the other hand, quantum many-body systems are nearly impossible to theoretically address or simulate on classical computers, due to the needed computer memory exponential dependence on the number of constituents.

The recognition of such a puzzling situation is certainly not new. It was in 1982. that Feynman proposed the brilliant solution involving the concept of controllable quantum simulators [8]. Only more recently, however, following the experimental advances in the control of systems as ultracold atomic gases [9, 10] and photonic structures [11–13], Feynman's idea is finally brought to reality. As new methods for synthetic magnetism are developed, neutral atoms and photons are governed to realize and simulate various fascinating phenomena, typically emergent only in elusive states of matter. Still, many significant aspects of correlated quantum many-body phases are yet to be discovered and understood.

The contribution of the work presented in this thesis is twofold. The first part focuses on the role of synthetic magnetism in the research of topological phases [1, 2]. The latter are nowadays causing a lot of excitement, due to their fascinating emergent behavior, which opens the way for diverse technological applications. As a consequence of a rather

special quantum order - the topological order, phenomena such as protected surface states or excitation with fractional quantum numbers emerge. Arguably their key aspect is the robustness, particularly of interest in the context of quantum computation. We have considered two systems in which highly elusive topological emerging phenomena occur, and their relation to (synthetic) magnetism. By taking advantage of tunable synthetic magnetic fields, we have pointed out how topological phases that otherwise rely on complicated space groups and are thus hardly obtainable, such as Weyl semimetals, can be realized in simple lattice geometries. Namely, we have shown that Weyl points can be experimentally addressed in an experimentally viable ultracold atomic lattice with laser assisted tunneling [1]. As expected, this resulted in emergent surface states in the form of Fermi arcs. Moreover, the consideration of laser assisted tunneling in the presence of pointlike strong interactions, presented in the second part of the thesis, introduces a general pathway for investigating the possibility of realizing exotic topological phases with interacting ultracold atomic gases in synthetic magnetic fields. We have also considered the realization and detection of a state with fractional statistic in an ultracold atomic gas. We have demonstrated how standard methods and understanding have to be taken with caution when studying topological matter via quantum simulation and synthetic magnetism. Ultracold atomic systems can emphasize the intriguing aspects associated with extracting relevant observables from systems with fractional statistics. Specifically, we have pointed out that the momentum distribution, one of the key signatures of quantum states of matter, is not a proper observable for a system of anyons because orthogonal components of kinetic momentum do not commute [2]. As a substitute for the momentum distribution of a spatially localized anyonic state, we have proposed to use the asymptotic single-particle density after expansion of anyons in free space from the state, which is justified by the correct bosonic/fermionic limits and examples of expansion dynamics obtained by exact calculations.

The second part of the thesis discusses our proposals of new methods for introducing synthetic magnetism in atomic and photonic systems [3–7]. We have shown that drawing analogies between different physical systems can yield new ideas in synthetic magnetism, which enables addressing intriguing topological phases and beyond. Namely, we have proposed a grating assisted tunneling scheme that introduces tunable synthetic magnetic fields in a photonic lattice [3]. It is inspired by laser assisted tunneling in lattices of

quantum gases, nevertheless without problems due to heating by spontaneous emission. We have confirmed the validity of the proposed grating assisted tunneling method by a direct comparison of the light propagation in the continuous system, which realizes conical diffraction, and the evolution in a discrete model with nontrivial hopping phases. We stress out that this approach can open the way for a general mapping of light propagation in tailored dielectric structures to intriguing discrete models, such as the Harper-Hofstadter Hamiltonian. In an atomic environment, such an approach enabled our investigation of the applicability of laser assisted tunneling in the presence of strong interactions, and we have confirmed its applicability for a Tonks-Girardeau gas in a 1D optical lattice [4]. Although the high-frequency approximation yields the correct effective Hamiltonian for the stroboscopic evolution in this specific example, our work emphasizes how direct mapping of continuous systems to discrete models via numerical 'experiments' can open the way to the study of states where simple approximations are not necessarily applicable. Finally, we have extended the concept of simulation to complex classical, rather than quantum, systems in the presence of magnetism. Examples include complex astrophysical objects and stars. We have proposed a method for creating a synthetic Lorentz force in a classical ultracold atomic gas, based on the Doppler effect and radiation pressure in two-step two-photon transitions that yield a force orthogonal to the atomic velocity [5]. The theoretical proposal was followed by a collaboration with an experimental group, which yielded the experimental proof of the method for a cold atomic cloud in a magneto-optical trap [6, 7].

....

Prošireni sažetak

1 Uvod

Kolektivno ponašanje velikog broja kvantnih čestica dovodi do nekih od najsloženijih i zanimljivih pojava, kao što su supravodljivost, suprafluidnost ili Bose-Einesteinova kondenzacija. Međutim, razumijevanje i predviđanje razvoja kvantnih višečestičnih sustava izuzetno je zahtjevno, čak i u slučajevima kada su svi zakoni koji vladaju jednočestičnim ponašanjem poznati. S jedne strane, eksperimentalna dostupnost zanimljivih pojava u kvantnim sustavima znatno je otežana ekstremnim uvjetima koje takva stanja zahtijevaju (npr. niske temperature). S druge strane, uobičajen pristup prema kojem se višečestični sustavi numerički simuliraju na klasičnim računalima nije primjenjiv u slučajevima u kojima je kvantna priroda sustava izražena. Naime, broj stupnjeva slobode kvantnih sustava čestica eksponencijalno je ovisan o njihovom broju. Računalna memorija koja je potrebna za opisivanje i rješavanje toga sustava, dakle, eksponencijalno raste s brojem čestica u sustavu. Zbog toga je numerički pristup u slučaju kvantnih pojava ograničen na sustave s malim brojem čestica.

Richard Feynman je 1982. godine uveo ideju korištenja kontrolabilnih fizikalnih sustava za simuliranje željenih kvantnih pojava [8]. Kao rješenje problema s kojim se klasična računala susreću u slučajevima kvantnih višečestičnih sustava, predložio je koncept *kvantnih simulatora*. Točnije, Feynman je predložio korištenje visoko kontrolabilnih kvantnih sustava koji su pažljivo prilagođeni na način da u potpunosti oponašaju (simuliraju) željeni kvantni višečestični sustav, te njegove pojave koje bi u protivnom ostale skrivene i nerazjašnjene.

U tom kontekstu, posljednjih godina veliku pozornost privlači fleksibilnost ultrahlad-

nih atomskih plinova i fotoničkih sustava [9–13]. Njihova efektivna dimenzionalnost može se kretati od jedne do tri dimenzije. Atomi u ovim rijetkim hladnim plinovima [9, 10] mogu pripadati bozonskoj ili fermionskoj statistici. Zbog raznolike prostorne ovisnosti energije, podrijetlom od okolnih magnetskih polja i laserske svjetlosti, atomi mogu biti zatočeni u harmoničkim, periodičkim ili iskrivljenim potencijalima. Međudjelovanje između atoma moguće je namjestiti korištenjem raspršenja svjetlosti. U fotoničkim kristalima [11], ponašanje fotona određeno je strukturom kristalnih vrpci na isti način kao i elektronsko ponašanje u uobičajenim materijalima. Krojenjem dielektričnih struktura kroz koje se svjetlost propagira, fotonima se može oponašati elektrone u raznolikim zanimljivim stanjima.

Međutim, i atomi i fotoni električki su neutralne čestice, te kao takve ne mogu izravno reproducirati magnetske pojave. S druge strane, široki raspon intrigantnih pojava u modernoj fizici, kao što su baždarna invarijantnost ili kvantni Hallov i Aharonov-Bohm efekt, proizlaze upravo iz vezanja elektromagnetskih polja i nabijenih čestica. Postoji stoga veliko zanimanje za pronalazak umjetnih (*sintetskih*) magnetskih polja za atome i fotone, odnosno okruženja u kojem se neutralni atomi i fotoni ponašaju po istim zakonima kao nabijene čestice u magnetskim poljima. U klasičnim sustavima, radi se ponajprije o Loretzovoj sili. U kvantnim sustavima, kao ključne značajke izdvajaju se pojava geometrijskih faza (Aharonov-Bohm faza [15] i Peierlsova substitucija [16]).

Pristup i način stvaranja sintetskog magnetskog/baždarnog polja usko je vezan uz konkretan sustav o kojemu se radi. Prva sintetska magnetska polja za atome dobivena su pri brzoj rotaciji Bose-Einstein-kondenziranih atomskih plinova, korištenjem analogije između Coriolisove i Loretzove sile [17, 18]. U narednim godinama, pokazano je da se umjetna magnetska polja za neutralne atome mogu dobiti iz njihovog međudjelovanja sa svjetlošću u posebno krojenim laserskim poljima [19, 21, 22]. U tom slučaju, mehanizam se temelji na analogiji Aharonov-Bohmove faze [15] pri gibanju nabijene čestice u magnetskom polju, i Berryjeve faze [20] pri adijabatskom gibanju atoma u laserskom polju [19, 21, 22]. U optičkim rešetkama, metode za stvaranje sintetskih magnetskih polja uključuju kompleksne matrične elemente tuneliranja između čvorova rešetke [23–27]. Netrivijalne faze kompleksnih matričnih elemenata tuneliranja atoma, dobivene primjerice trešnjom ili tzv. laserski potpomognutim tuneliranjem, pri tom se interpretiraju kao Peierlsove faze [16]. Sličan pristup, te analogija s Peierlsovim fazama matričnih elemenata tuneliranja, za

stvaranje sintetskih magnetskih polja koristi se i u fotoničkim sustavima [28–30, 30, 31, 31–37, 39, 40].

2 Topološka materija pomoću sintetskog magnetizma

Dijelovi ovoga poglavlja objavljeni su i u sljedećim radovima:

- T. Dubček, C. J. Kennedy, L. Lu, W. Ketterle, M. Soljačić, and H. Buljan,
  Phys. Rev. Lett. **114**, 225301 (2015).

- T. Dubček, B. Klajn, R. Pezer, H. Buljan, and D. Jukić,
  Physical Review A Rapid Communication, prihvaćeno.

Magnetizam se povijesno pokazao i kao odlična nit vodilja u potrazi za tzv. *topološkim fazama*. Topološko uređenje vrsta je uređenja koje se pojavljuje u kvantnim fazama tvari s energetskim procjepom i robusnom degeneracijom osnovnog stanja [14, 66]. Topološka stanja odlikuju se značajkama koje su topološki netrivijalne. Značajke su nevezane za lokalne parametre uređenja, odnosno zaštićene su od lokalnih deformacija, i moguće ih je detektirati isključivo kroz pojavu proizlazećih fenomena, kao što je pojava zaštićenih rubnih stanja [66]. Faze s intrinsičnim topološkim uređenjem pojavljuju se u jako međudjelujućim kvantnim višečestičnim sustavima, a dosad su uočene u necjelobrojnom kvantnim Hallovim sustavima [67–69], te u kvantnim spinskim tekućinama [70, 71]. U ovim stanjima prisutna je dugodosežna kvantna prepletenost, a osim rubnih stanja u njihovoj unutrašnjosti pojavljuju se pobuđenja necjelobrojnog naboja i statistike [14]. Nešto trivijalnija vrsta topoloških stanja pripada tzv. *simetrijski zaštićenim topološkim fazama* [66, 75], koje uključuju topološke izolatore, topološke supravodiče, Diracove i Weylove polumetale. U ovim sustavima, topološka netrivijalnost zaštićena je isključivo od lokalnih deformacija koje ne ruše prisutnu globalnu simetriju, te oni nisu okarakterizirani dugodosežnom kvantnom prepletenošću.

2.1 Weylove točke u 3D optičkim rešetkama

U relativističkoj kvantnoj teoriji polja postoje tri vrste fermiona: Diracovi fermioni, Majoranini i Weylovi fermioni. Weylovi fermioni, koji su opisani tzv. Weylovim hamiltonijanom $H_{\text{Weyl}} = \vec{\sigma} \cdot \vec{k}$, gdje je $\vec{\sigma}$ vektor Paulijevih matrica i $\vec{k}$ trodimenzionalni impuls, nisu

nikad opaženi u fizici elementarnih čestica. Posljednjih godina javilo se veliko zanimanje za Weylove polumetale—simetrijski zaštićene topološke sustave, u kojima se niskoenergetski elektroni ponašaju kao Weylovi fermioni. U ovim materijalima javljaju se zaštićena rubna stanja, čije se disperzije sijeku na tzv. Fermijevim lukovima. Osim fundamentalnog značaja Weylovih fermiona i pripadnih pojava kao što je Adler-Bell-Jackiw kiralna anomalija, topološka rubna stanja Weylovih polumetala značajna su i s aspekta eventualne primjene za kvantna računala [72–74]. Za realizaciju Weylovih fermiona, međutim, potrebno je udovoljiti simetrijskim zahtjevima, odnosno imati narušenje vremenske i/ili prostorne obrativosti. Zbog toga je potraga za takvim sustavima poprilično zahtjevna. Prvi sustav u kojemu su Weylove točke predložene [100] i realizirane [106] bio je žiroidni fotonički kristal. Slijedile su realizacije u čvrstostanjskim sustavima [111, 112], a javilo se i nekoliko prijedloga u onim hladnoatomskim [107–110]. U svakome od primjera, radilo se o sustavima s kompliciranim geometrijskim značajkama.

U ovom radu predlažemo korištenje kontrolabilnosti i fleksibilnosti kvantnih plinova sa sintetskim magnetskim poljima, odnosno eksperimentalno dostupnu realizaciju Weylovog hamiltonijana u jednostavnoj kubičnoj optičkoj rešetci s laserski-potpomognutim tuneliranjem [1]. Laserski-potpomognuto tuneliranje [24, 25] jedna je metoda za stvaranje sintetskih magnetskih polja i uvođenja netrivijalnih faza kompleksnih matričnih elemenata tuneliranja u optičkim rešetkama. Dvodimenzionalna varijanta ovoga sustava relativno je nedavno korištena u realizaciji Harper-Hofstadterovog hamiltonijana. Rad donosi prijedlog za njegovu izravnu trodimenzionalnu generalizaciju, u čijoj se disperziji predviđa pojava Weylovih točaka—točaka u kojima se dvije vrpce sijeku linearno u sva tri smjera. Ukazujemo kako hladni atomski plinovi pružaju jedinstvenu mogućnost za eksperimetalno opažanje ovakve disperzije, kroz slobodnu ekspanziju u obliku sfernih ljuski. Weylove točke predstavljaju sintetske magnetske monopole u Brillouinovoj zoni, što je direktno potvrđeno izračunom Berryijeve zakrivljenosti. Razmatranjem rešetke koja je konačna duž jednog smjera u prostoru, pokazujemo pojavu rubnih stanja. Izračunom njihove disperzije, eksplicitno dobivamo oblik Fermijevih lukova u trodimenzionalnoj Brillouinovoj zoni predloženog sustava. Konačno, dajemo konkretne prijedloge za potvrdu svi navedenih karakteristika u eksperimentalnoj realizaciji, korištenjem dvije uobičajene tehnike za hladne atomske plinove: Braggova spektroskopija [120], te akceleracija oblaka u smjeru Weylove točke i prijelaz u višu vrpcu [119].

2.2 Necjelobrojna statistika u hladnom atomskom plinu

Postojanje dugodosežne kvantne prepletenosti u sustavima s intrinsičnim topološkim uređenjem vodi do pojave egzotičnih kvantnih kvazičestičnih pobuđenja u njihovoj unutrašnjosti [66]. U dvodimenzionalnim sustavima, čestice koje se pojavljuju opisane su necjelobrojnom statistikom i nazivaju se *anyoni*. Paradigmatična realizacija anyona javlja se u necjelobrojnom kvantnom Hallovom efektu [67, 96], gdje lokalizirana kvazičestična pobuđenja imaju necjelobrojni naboj i statistiku. Kvantne spinske tekućine drugi su primjer sustava koji realizira anyonske kvazičestice kroz realizaciju Kitaevog modela [70, 71]. Statistika anyona interpolira između one bozonske i fermionske, zbog čega se pri zamjeni dvaju čestica u višečestičnoj valnoj funkciji ψ pojavljuje netrivijalna faza $\psi(\ldots,\mathbf{r}_i,\ldots,\mathbf{r}_j,\ldots,t){=}e^{im\pi\alpha}\psi(\ldots,\mathbf{r}_j,\ldots,\mathbf{r}_i,\ldots,t)$, gdje je $0 < \alpha < 1$ tzv. statistički parametar, a $\mathbf{r}_i$ dvodimenzionalne koordinate čestica. Na neke od intrigantnih kvantno-mehaničkih posljedica necjelobrojne statistike ukazano je već prije nekoliko desetljeća [123, 124], kroz intuitivnu sliku kompozitnih čestica, no dio ih ostaje nerazjašnjen još i danas. Sintetski magnetizam i ultrahladni atomski plinovi, te kontrolabilnost i fleksibilnost koje pružaju, postavljaju se vrlo perspektivan put za proučavanje problema anyona [128–133]. Realizacija jednodimenzionalne varijante anyona u optičkim rešetkama također je privukla pozornost[139–142]. U kontekstu novih eksperimentalnih realizacija anyonskih sustava, neosporno bitan sastojak jest njihova detekcija.

U ovome radu razmatramo slobodnu ekspanziju Abelovih anyona u 2D [2]. Slobodna ekspanzija jedna je od najkorištenijih metoda za detekciju u hladnim atomskim plinovima i optičkim rešetkama [9]. U uobičajenim sustavima ultrahladnih bozona i fermiona, slobodna ekspanzija pokazuje raspodjelu impulsa u početnom kvantnom stanju. Raspodjela impulsa jedna je od kjučnih karakteristika svakog kvantnog stanja te se, primjerice, povijesno pokazala kao ključan potpis Bose-Einsteinove kondenzacije ili Fermijeve degeneracije u zatočenom hladnom plinu [150, 151]. Međutim, u radu ukazujemo kako za sustave s necjelobrojnom statistikom raspodjela impulsa nije prikladna opservabla. Naime, višeznačnost anyonske valne funkcije preslikava se i na višeznačnost raspodjele impulsa koja bi se dobila standardnom definicijom. Shvate li se anyoni kao Wilczekove kompozitne čestice, koje se sastoje od točkastog naboja i beskonačno uskog magnetskog toka, okomite komponente kinetičkog impulsa međusobno ne komutiraju te ne mogu biti dijagonalizirane u istoj

bazi. Kao rješenje predlažemo uvođenje tzv. *raspodjele kvaziimpulsa*, za koju pokazujemo da je vremenski neovisna te poprima očekivani oblik u bozonskoj/fermionskoj granici ili granici velikih vremena. Slaganje eksplicitno pokazujemo za sustav dva anyona zatočena u harmoničkom potencijalu. Uporabom Monte-Carlo integracije dobivamo i konkretan oblik raspodjele kvaziimpulsa za sustav od 20 anyona u harmoničkoj klopci, iz kojega se jasno vidi utjecaj statističkog parametra α. Nadalje, pokazujemo ovisnost dvočestičnih korelacija u sustavu anyona u ovisnosti o statističkom parametru. Konačno, dajemo prijedlog eksperimentalne implementacije ovakvog sustava s ultrahladnim atomskim plinovima.

3 Potraga za sintetskim magnetizmom

Dijelovi ovoga poglavlja objavljeni su i u sljedećim radovima:

- T. Dubček, K. Lelas, D. Jukić, R. Pezer, M. Soljačić, and H. Buljan,
  New J. Phys. **17**, 125002 (2015).

- K. Lelas, N. Drpić, T. Dubček, D. Jukić, R. Pezer, and H. Buljan,
  New J. Phys. **18**, 095002 (2016).

- T. Dubček, N. Šantić, D. Jukić, D. Aumiler, T. Ban, and H. Buljan,
  Phys. Rev. A **89**, 063415 (2014).

- N. Šantić, T. Dubček, D. Aumiler, H. Buljan, and T. Ban,
  Sci. Rep. **5**, 13485 (2015).

- N. Šantić, T. Dubček, D. Aumiler, H. Buljan, and T. Ban,
  Opt. Soc. Am. B **34**, 1264 (2017).

Magnetizam i magnetske pojave privlačile su ljudsku pozornost još od davnina. Nakon što je u devetnaestom stoljeću zaokružena Maxwellova klasična teorija elektromagnetizma, otkriće kvantne mehanike dovelo je do novih mogućnosti i pitanja. Još i danas, neka od njih nisu u potpunosti razjašnjena. Kvantni simulatori i sintetski magnetizam otvaraju put proučavanju kvantnih magnetskih pojava. Vrlo često, ključni korak na tome putu jest odabir prikladne metode za stvaranje sintetskog magnetizma koja će omogućiti realizaciju ciljanih složenih pojava. S takvom motivacijom, u ovome poglavlju, razmatraju se i

predlažu nove metode za uspostavu sintetskog magnetizma u fotoničkim i atomskim sustavima [3–7].

3.1 Rešetkom-potpomognuto tuneliranje u fotoničkoj rešetci

Sintetski magnetizam u fotoničkim sustavima pokazao se kao jedinstven alat za realizaciju topoloških stanja i faza [28–31, 33, 34, 36, 37, 41–44, 100, 105, 160]. Bitan je stoga razvoj metoda za postizanje sintetskih magnetskih polja u konkretnim sustavima o kojima se radi. Strategije bazirane na modulaciji, magneto-optičkom vezanju ili posebnim geometrijama, dosad su korištene za vezane optičke rezonatore, fotoničke kristale i metamaterijale. Međutim, metoda koja bi omogućila postizanje uskladljivih kompleksnih matričnih elemenata tuneliranja za optičke rešetke nije razvijena.

U ovom radu, uvodimo jednu takvu metodu—tzv. *rešetkom-potpomognuto tuneliranje* [3], te predlažemo njegovu implementaciju u optički induciranim fotoničkim rešetkama [161–165]. Metoda je inspirirana prethodno spomenutim laserski-potpomognutim tuneliranjem u optičkim rešetkama [24, 25]. Uspostavu sintetskog magnetizma pokazujemo direktnom usporedbom evolucije u kontinuiranoj fotoničkoj rešetci s dinamikom u diskretnoj rešetci s netrivijalnim fazama matričnih elemenata tuneliranja. Točnije, pokazujemo da jedno i dvodimenzionalne fotoničke rešetke mogu dovesti do tzv. *konične difrakcije* [37, 167]—potpisa realizacije Harper-Hofstadterovog hamiltonijana.

3.2 Laserski-potpomognuto tuneliranje u TG plinu

Uvođenje međudjelovanja u kvantne sustave često dovodi do jako-koreliranih višečestičnih stanja. Međudjelovanje može znatno obogatiti proizlazeću fiziku, te uzrokovati zanimljive posljedice. U okviru topoloških stanja, primjerice, pokazano je da interakcije mogu dovesti i do faznih prijelaza. Nedavnim eksperimentalnim napretkom u kontroli atomskih plinova, u kojima se međudjelovanje može mijenjati korištenjem raspršenja svjetlosti, omogućena je koherentna manipulacija višečestičnim stanjima i njihovom dimamikom. Sintetski magnetizam, međutim, u ovim sustavima uglavnom se uvodi nekim oblikom periodičnog tjeranja [23, 24, 26], što u kombinaciji s međudjelovanjem tijekom evolucije dovodi do termalizacije na efektivno beskonačnoj temperaturi [170–175]. Posljedice kombinacije međudjelovanja i periodičkog tjeranja, stoga, mogu imati značajan utjecaj

na primjenjivost uobičajenih metoda za stvaranje sintetskog magnetizma u kvantnim sustavima.

U ovom radu proučavamo metodu laserski-potpomognutog tuneliranja za stvaranje sintetskih magnetskih polja u jednodimenzionalnim bozonskim plinovima s kontaktnim interakcijama—tzv. Tonks-Girardeau plinovima [4]. Poglavlje započinjemo s uvođenjem posljedica koje međudjelovanje i periodičko tjeranje imaju u kvantnim višečestičnim sustavima. Zatim slijedi razmatranje utjecaja na sintetski magnetizam u jako međudjelujućim bozonskim plinovima, gdje pokazujemo da stroboskopska dinamika Tonks-Girardeau plina s laserski-potpomognutim tuneliranjem efektivno realizira osnovno stanje jednodimenzionalnih neprobojnih bozona na diskretnoj rešetci s netrivijalnim fazama preskoka.

3.3 Sintetska Lorentzova sila za hladni plin

Većina metoda za stvaranje sintetskih magnetskih polja za atome dizajnirana je korištenjem adijabatske evolucije u ultrahladnim kvantno-degeneriranim atomskim plinovima, a sintetski magnetizam u klasičnim sustavima gotovo je u potpunosti zanemaren. Međutim, i među klasičnim sustavima s magnetskim interakcijama javljaju se primjeri koji su dovoljno složeni da predviđanje njihova ponašanja postaje prezahtjevno i za najjača super-računala. Primjerice, kompleksni astrofizički objekti ili plazme. U klasičnim atomskim plinovima, shema za stvaranje sintetskog magnetskog polja mora biti primjenjiva na atome s relativno velikim brzinama, zbog čega su standardne metode vezane uz adijabatsku evoluciju ograničene. Nadalje, zbog relativno velikih volumena koje zauzimaju , magnetska sila mora biti relativno uniformna i jaka na područjima od barem nekoliko kubnih milimetara. S druge strane, zbog relativno velikih temperatura, spontana emisija fotona prihvatljiva je.

S ovim smjernicama, predlažemo metodu za stvaranje sintetske Lorentzove sile koja se zasniva na Dopplerovom efektu i tlaku zračenja [5]. Ovaj teorijski prijedlog popraćen je suradnjom s eksperimentalnom grupom na Institutu za fiziku, iz koje proizlazi ekperimentalna potvrda sintetičke Loretzove sile [6, 7]. U ovom radu, kratko dajemo pregled glavnih ideja, te zatim i rezultata spomenute suradnje.

4 Zaključak

Ovaj rad teorijski se bavi problemom sintetskih magnetskih polja za atome i fotone. Doprinos je okrenut u dva smjera. Prvi dio rada usredotočen je na ulogu sintetskog magnetizma u istraživanju topoloških faza [1, 2]. U posljednje vrijeme ovo područje izaziva veliko zanimanje, ponajprije zbog fascinantnih pojava kao što su zaštićena rubna stanja i necjelobrojni kvantni brojevi. Vjerojatno ključna karakteristika upravo je njihova robusnost, koja je posebice od značaja za primjenu u kvantnom računanju. Razmatrali smo dva sustava u kojima se javljaju teško dostižni topološki fenomeni, te njihovu vezu sa (sintetskim) magnetizmom. Koristeći prednosti sintetskih magnetskih polja, pokazali smo kako se topološke faze koje u protivnom zahtjevaju komplicirane prostorne grupe i zbog toga su teško dohvatljive, mogu realizirati u jednostavnim rešetkama. Točnije, predložili smo eksperimentalnu realizaciju Weylovih točaka, te vezanih pojava, u optičkoj rešetci s laserski-potpomognutim tuneliranjem [1]. Također, razmotrili smo i realizaciju te detekciju stanja s necjelobrojnom statistikom u hladnom atomskom oblaku. Pokazali smo kako se uobičajenim metodama i razumijevanju mora oprezno pristupati pri istraživanju topoloških stanja uz pomoć kvantne simulacije i sintetskog magnetizma. Ultrahladni atomski sustavi tako naglašavaju zanimljive aspekte vezane uz izvlačenje relevantnih opservabli kod necjelobrojne statistike. Točnije, ukazali smo kako raspodjela impulsa, jedan od ključnih potpisa kvantnih stanja, nije primjerena opservabla u sustavu anyona, u kojem okomite komponente kinetičkog impulsa ne komutiraju [2]. Predložili smo alternativnu opservablu koja u granicama odgovara ispravnoj raspodjeli, te pokazali kako se necjelobrojna statistika može raspoznati i iz dvočestičnih korelacija anyona u harmoničkom oscilatoru.

Drugi dio rada bavi se prijedlozima novih metoda za uvođenje sintetskog magnetizma u atomskim i fotoničkim sustavima [3–7]. Pokazali smo da povlačenje analogija između različitih fizikalnih sustava može dovesti do novih ideja u sintetskom magnetizmu, što otvara put prema zanimljivim topološkim fazama i drugim pojavama. Predložili smo tzv. rešetkom-potpomognuto tuneliranje kao način za uvođenje podesivih sintetskih magnetskih polja u fotoničkim rešetkama [3]. Potvrdili smo ispravnost ove metode direktnom usporedbom propagacije svijetlosti u kontinuiranom sustavu, u kojemu dolazi do konične difrakcije, i evolucije u diskretnom modelu s netrivijalnim fazama preskoka. Naglasili smo kako ovakav pristup vodi na mogućnost generalnog preslikavanja širenja svjetlosti u dielektričnim

strukturama na intrigantne diskretne modele, kao što je Harper-Hofstadterov hamilto-nijan. Isti pristup omogućio nam je ispitivanje primjenjivosti laserski-potpomognutog tuneliranja u prisustvu jakih interakcija, što smo i potvrdili za slučaju Tonks-Girardeau plina u jednodimenzionalnoj rešetci [4]. Konačno, proširili smo koncept simulacije i na klasične, a ne kvantne, sustave u prisustvu sintetskog magnetizma. Dali smo prijedlog metode za stvaranje sintetske Lorentzove sile u klasičnim hladnim atomskim plinovima, koja se zasniva na Dopplerovom efektu i tlaku zračenja kod dvokoračnih dvofotonskih prijelaza, čime se postiže sila okomita na brzinu [5]. Teorijski prijedlog popraćen je su-radnjom s eksperimentalnom grupom, čime je ideja dokazana za hladni atomski plin u magneto-optičkoj zamci [6, 7].

Bibliography

[1] T. Dubček, C. J. Kennedy, L. Lu, W. Ketterle, M. Soljačić, and H. Buljan, "Weyl Points in Three-Dimensional Optical Lattices: Synthetic Magnetic Monopoles in Momentum Space," Physical Review Letters **114**, 1–5 (2015).

[2] T. Dubček, B. Klajn, R. Pezer, H. Buljan, and D. Jukić, "Quasimomentum distribution and expansion of an anyonic gas," Physical Review A Rapid Communication, accepted for publication .

[3] T. Dubček, K. Lelas, D. Jukić, R. Pezer, M. Soljačić, and H. Buljan, "The Harper-Hofstadter Hamiltonian and conical diffraction in photonic lattices with grating assisted tunneling," New Journal of Physics **17**, 125002 (2015).

[4] K. Lelas, N. Drpić, T. Dubček, D. Jukić, R. Pezer, and H. Buljan, "Laser assisted tunneling in a Tonks-Girardeau gas," New Journal of Physics **18**, 095002 (2016).

[5] T. Dubček, N. Šantić, D. Jukić, D. Aumiler, T. Ban, and H. Buljan, "Synthetic Lorentz force in classical atomic gases via Doppler effect and radiation pressure," Physical Review A **063415**, 2–6 (2014).

[6] N. Šantić, T. Dubček, D. Aumiler, H. Buljan, T. Ban, N. Šantic, T. Dubcek, D. Aumiler, H. Buljan, and T. Ban, "Experimental Demonstration of a Synthetic Lorentz Force by Using Radiation Pressure," Scientific Reports **5**, 1–8 (2015).

[7] N. Šantić, T. Dubček, D. Aumiler, H. Buljan, and T. Ban, "Synthetic Lorentz force in an expanding cold atomic gas," Journal of the Optical Society of America B **34**, 1264–1269 (2017).

[8] R. Feynman, "Simulating physics with computers," International journal of theoretical physics **21**, 467–488 (1982).

[9] I. Bloch, J. Dalibard, and W. Zwerger, "Many-body physics with ultracold gases," Reviews of Modern Physics **80**, 885–964 (2008).

[10] I. Bloch, J. Dalibard, and S. Nascimbène, "Quantum simulations with ultracold quantum gases," Nature Physics **8**, 267–276 (2012).

[11] J. D. Joannopoulos, S. G. Johnson, J. N. Winn, and R. D. Meade, *Photonic Crystals : Molding the Flow of Light (Second Edition).* (Princeton University Press, 2008) p. 446.

[12] A. Aspuru-Guzik and P. Walther, "Photonic quantum simulators," Nature Physics **8**, 285–291 (2012).

[13] C. Noh and D. G. Angelakis, "Quantum simulations and many-body physics with light," Reports on Progress in Physics **016401**, 16401 (2016).

[14] X.-G. Wen, "Topological order: from long-range entangled quantum matter to an unification of light and electrons," arXiv:1210.1281 [cond-mat.str-el] (2012).

[15] Y. Aharonov and D. Bohm, "Significance of Electromagnetic Potentials in the Quantum Theory," Physical Review **115**, 485–491 (1959).

[16] J. M. Luttinger, "The effect of a magnetic field on electrons in a periodic potential," Physical Review **84**, 814–817 (1951).

[17] K. Madison, F. Chevy, and W. Wohlleben, "Vortex formation in a stirred Bose-Einstein condensate," Physical review letters **84**, 806–809 (2000).

[18] J. R. Abo-Shaeer, C. Raman, J. M. Vogels, and W. Ketterle, "Observation of vortex lattices in Bose-Einstein condensates." Science **292**, 476–479 (2001).

[19] J. Dalibard, F. Gerbier, G. Juzeliunas, and P. Öhberg, "Coll.: artificial gauge potentials for neutral atoms," Reviews of Modern Physics **83**, 1523 (2011).

[20] M. V. Berry, "Quantal Phase Factors Accompanying Adiabatic Changes," Proceedings of the Royal Society A: Mathematical, Physical and Engineering Sciences **392**, 45–57 (1984).

[21] R. Dum and M. Olshanii, "Gauge Structures in Atom-Laser Interaction: Bloch Oscillations in a Dark Lattice," Physical Review Letters **76**, 1788–1791 (1996).

[22] Y.-J. Lin, R. L. Compton, K. Jiménez-García, J. V. Porto, and I. B. Spielman, "Synthetic magnetic fields for ultracold neutral atoms," Nature **462**, 628 (2009).

[23] J. Struck, C. Olschlager, M. Weinberg, P. Hauke, J. Simonet, A. Eckardt, M. Lewenstein, K. Sengstock, and P. Windpassinger, "Tunable gauge potential for neutral and spinless particles in driven optical lattices," Physical Review Letters **108**, 225304 (2012).

[24] H. Miyake, G. A. Siviloglou, C. J. Kennedy, W. C. Burton, and W. Ketterle, "Realizing the harper hamiltonian with laser-assisted tunneling in optical lattices," Physical Review Letters **111**, 185302 (2013).

[25] M. Aidelsburger, M. Atala, M. Lohse, J. T. Barreiro, B. Paredes, and I. Bloch, "Realization of the Hofstadter Hamiltonian with ultracold atoms in optical lattices," Physical Review Letters **111**, 1–5 (2013).

[26] M. Aidelsburger, M. Atala, S. Nascimbène, S. Trotzky, Y.-A. Chen, and I. Bloch, "Experimental realization of strong effective magnetic fields in an optical lattice," Physical Review Letters **107**, 255301 (2011).

[27] M. Aidelsburger, M. Lohse, C. Schweizer, M. Atala, J. T. Barreiro, S. Nascimbène, N. R. Cooper, I. Bloch, and N. Goldman, "Measuring the Chern number of Hofstadter bands with ultracold bosonic atoms," Nature Physics **11**, 162–166 (2014).

[28] M. Hafezi, E. A. Demler, M. D. Lukin, and J. M. Taylor, "Robust optical delay lines with topological protection," Nature Physics **7**, 907–912 (2011).

[29] R. O. Umucalilar and I. Carusotto, "Artificial gauge field for photons in coupled cavity arrays," Physical Review A - Atomic, Molecular, and Optical Physics **84**, 1–8 (2011).

[30] K. Fang, Z. Yu, and S. Fan, "Realizing effective magnetic field for photons by controlling the phase of dynamic modulation," Nature Photonics **6**, 782–787 (2012).

[31] M. Hafezi, S. Mittal, J. Fan, A. Migdall, and J. M. Taylor, "Imaging topological edge states in silicon photonics," Nature Photonics **7**, 1001 (2013).

[32] S. Longhi, "Bloch dynamics of light waves in helical optical waveguide arrays," Physical Review B **76**, 195119 (2007).

[33] M. C. Rechtsman, J. M. Zeuner, Y. Plotnik, Y. Lumer, S. Nolte, M. Segev, and A. Szameit, "Photonic Floquet Topological Insulators," Nature **496**, 196–200 (2013).

[34] M. C. Rechtsman, J. M. Zeuner, A. Tünnermann, S. Nolte, M. Segev, and A. Szameit, "Strain-induced pseudomagnetic field and photonic Landau levels in dielectric structures," Nature Photonics **7**, 153–158 (2013).

[35] H. Schomerus and N. Y. Halpern, "Parity anomaly and landau-level lasing in strained photonic honeycomb lattices," Physical Review Letters **110**, 013903 (2013).

[36] A. B. Khanikaev, S. Hossein Mousavi, W.-K. Tse, M. Kargarian, A. H. MacDonald, and G. Shvets, "Photonic topological insulators," Nature Materials **12**, 233–239 (2012).

[37] J. M. Zeuner, N. K. Efremidis, R. Keil, F. Dreisow, D. N. Christodoulides, A. Tünnermann, S. Nolte, and A. Szameit, "Optical analogues for massless Dirac particles and conical diffraction in one dimension," Physical Review Letters **109**, 1–5 (2012).

[38] M. Hafezi, "Synthetic Gauge Fields With Photons," International Journal of Modern Physics B **28**, 1441002 (2014).

[39] N. Westerberg, C. Maitland, D. Faccio, K. Wilson, P. Öhberg, and E. M. Wright, "Synthetic magnetism for photon fluids," Physical Review A **94**, 1–8 (2016).

[40] I. Carusotto and C. Ciuti, "Quantum fluids of light," Reviews of Modern Physics **85**, 299–366 (2013).

[41] F. D. M. Haldane and S. Raghu, "Possible realization of directional optical waveguides in photonic crystals with broken time-reversal symmetry," Physical Review Letters **100**, 1–4 (2008).

[42] S. Raghu and F. D. M. Haldane, "Analogs of quantum-Hall-effect edge states in photonic crystals," Physical Review A **78**, 033834 (2008).

[43] Z. Wang, Y. D. Chong, J. D. Joannopoulos, and M. Soljačić, "Reflection-free one-way edge modes in a gyromagnetic photonic crystal," Physical Review Letters **100**, 1–4 (2008).

[44] Z. Wang, Y. Chong, J. D. Joannopoulos, and M. Soljačić, "Observation of unidirectional backscattering-immune topological electromagnetic states," Nature **461**, 772–775 (2009).

[45] G. Floquet, "Sur les équations différentielles linéaires à coefficients périodiques," Annales scientifiques de l'École Normale Supérieure **12**, 47–88 (1883).

[46] F. Casas, J. a. Oteo, and J. Ros, "Floquet theory: exponential perturbative treatment," Journal of Physics A: Mathematical and General **34**, 3379 (2001).

[47] N. Goldman, J. Dalibard, M. Aidelsburger, and N. R. Cooper, "Periodically driven quantum matter: The case of resonant modulations," Physical Review A - Atomic, Molecular, and Optical Physics **91**, 1–16 (2015).

[48] A. Eckardt, "Colloquium: Atomic quantum gases in periodically driven optical lattices," Reviews of Modern Physics **89**, 1–30 (2017).

[49] W. Magnus, "On the exponential solution of differential equations for a linear operator," Communications on pure and applied mathematics **VII**, 649–673 (1954).

[50] S. Blanes, F. Casas, J. A. Oteo, and J. Ros, "A pedagogical approach to the Magnus expansion," European Journal of Physics **31**, 907–918 (2010).

[51] L. Landau, "Theory of phase transformations," Physikalische Zeitschrift der Sowjetunion **11**, 26 (1937).

[52] V. Ginzburg and L. Landau, "On the Theory of superconductivity," Soviet Physics Journal of Experimental and Theoretical Physics **20**, 1064–1082 (1950).

[53] V. L. Berezinskii, "Destruction of long-range order in one-dimensional and two-dimensional systems having a continuous symmetry group I. classical systems," Sov. Phys. Journal of Experimental and Theoretical Physics **32**, 493 (1971).

[54] J. M. Kosterlitz and D. J. Thouless, "Ordering, metastability and phase transitions in two-dimensional systems," Journal of Physics C: Solid State Physics **6**, 1181–1203 (1973).

[55] J. G. Bednorz and K. A. Müller, "Possible high Tc superconductivity in the Ba-La-Cu-O system," Zeitschrift für Physik B Condensed Matter **64**, 189–193 (1986).

[56] T. Ando, Y. Matsumoto, and Y. Uemura, "Theory of Hall Effect in a Two-Dimensional Electron System," Journal of the Physical Society of Japan **39**, 279–288 (1975).

[57] K. V. Klitzing, G. Dorda, and M. Pepper, "New method for high-accuracy determination of the fine-structure constant based on quantized hall resistance," Physical Review Letters **45**, 494–497 (1980).

[58] D. J. Thouless, M. Kohmoto, M. P. Nightingale, and M. Den Nijs, "Quantized hall conductance in a two-Dimensional periodic potential," Physical Review Letters **49**, 405–408 (1982).

[59] C. L. Kane and E. J. Mele, "Z2 topological order and the quantum spin hall effect," Physical Review Letters **95**, 146802 (2005).

[60] L. Fu, C. L. Kane, and E. J. Mele, "Topological Insulators in Three Dimensions," Physical Review Letters **98**, 106803 (2007).

[61] R. Roy, "Topological phases and the quantum spin Hall effect in three dimensions," Physical Review B - Condensed Matter and Materials Physics **79**, 195322 (2009).

[62] M. Koenig, S. Wiedmann, C. Bruene, A. Roth, H. Buhmann, L. W. Molenkamp, X.-L. Qi, and S.-C. Zhang, "Quantum Spin Hall Insulator State in HgTe Quantum Wells," **766** (2007).

[63] B. A. Bernevig, T. L. Hughes, and S.-C. Zhang, "Quantum Spin Hall Effect and Topological Phase Transition in HgTe Quantum Wells," Science **314**, 1757–61 (2007).

[64] M. Z. Hasan and C. L. Kane, "Colloquium: Topological insulators," Reviews of Modern Physics **82**, 3045–3067 (2010).

[65] X.-L. Qi and S.-C. Zhang, "Topological insulators and superconductors," Reviews of Modern Physics **83**, 1057–1110 (2011).

[66] T. Stanescu, *Introduction to Topological Quantum Matter and Quantum Computation* (CRC Press, Boca Raton, 2016) p. 394.

[67] D. C. Tsui, H. L. Stormer, and A. C. Gossard, "Two-dimensional magnetotransport in the extreme quantum limit," Physical Review Letters **48**, 1559–1562 (1982).

[68] R. Laughlin, "Quantized motion of three two-dimensional electrons in a strong magnetic field," Physical Review B **27**, 3383–3389 (1983).

[69] H. L. Stormer and D. C. Tsui, "The quantized Hall effect." Science **220**, 1241–1246 (1983).

[70] A. Kitaev, "Anyons in an exactly solved model and beyond," Annals of Physics **321**, 2–111 (2006).

[71] C. Balz, B. Lake, J. Reuther, H. Luetkens, R. Schönemann, T. Herrmannsdörfer, Y. Singh, A. T. M. Nazmul Islam, E. M. Wheeler, J. A. Rodriguez-Rivera, T. Guidi, G. G. Simeoni, C. Baines, and H. Ryll, "Physical realization of a quantum spin liquid based on a complex frustration mechanism," Nature Physics **12**, 942–949 (2016).

[72] A. Kitaev, "Fault-tolerant quantum computation by anyons," Annals of Physics **303**, 2–30 (2003).

[73] C. Nayak, S. H. Simon, A. Stern, M. Freedman, and S. Das Sarma, "Non-Abelian anyons and topological quantum computation," Reviews of Modern Physics **80**, 1083–1159 (2008).

[74] A. Stern and N. H. Lindner, "Topological Quantum Computation–From Basic Concepts to First Experiments," Science **339**, 1179–1184 (2013).

[75] T. Senthil, "Symmetry-Protected Topological Phases of Quantum Matter," Annual Review of Condensed Matter Physics **6**, 299–324 (2015).

[76] Y. Ando, "Topological Insulator Materials," Journal of the Physical Society of Japan **82**, 102001 (2013).

[77] M. Sato and Y. Ando, "Topological superconductors: a review," Reports on Progress in Physics **80**, 076501 (2017).

[78] N. P. Armitage, E. J. Mele, and A. Vishwanath, "Weyl and Dirac Semimetals in Three Dimensional Solids," arXiv:1705.01111 [cond-mat.str-el] (2017).

[79] A. A. Burkov, "Topological Semimetals," Nature Publishing Group **15**, 1145–1148 (2016).

[80] D. R. Hofstadter, "Energy levels and wave functions of Bloch electrons in rational and irrational magnetic fields," Physical Review B **14**, 2239–2249 (1976).

[81] L. Lu, J. D. Joannopoulos, and M. Soljačić, "Topological states in photonic systems," Nature Physics **12**, 626–629 (2016).

[82] S. D. Huber, "Topological mechanics," Nature Physics **12**, 621–623 (2016).

[83] X.-G. Wen, "Zoo of quantum-topological phases of matter," arXiv:1610.03911 [cond-mat.str-el] (2016).

[84] M. Nakahara, *Geometry, topology, and physics* (Institute of Physics Pub, 2003) p. 573.

[85] I. M. Lifshitz, "Anomalies of electron characteristics of a metal in the high pressure region," Soviet Physics Journal of Experimental and Theoretical Physics **11**, 1130–1135 (1960).

[86] P. Pancharatnam, "Generalized theory of interference, and its applications," Resonance, Journal of science **44**, 247 (1956).

[87] M. Born and V. Fock, "Beweis des Adiabatensatzes," Zeitschrift fur Physik **51**, 165–180 (1928).

[88] B. Simon, "Holonomy, the Quantum Adiabatic Theorem, and Berry's Phase," **51**, 2167–2170 (1983).

[89] Y. Aharonov and J. Anandan, "Phase Change during a Cycle Quantum Evolution," Physical Review Letters **58**, 1593–1596 (1987).

[90] J. Samuel and R. Bhandari, "General Setting for Berry Phase," Physical Review Letters **60**, 2339–2342 (1988).

[91] A. Uhlmann, "Parallel transport and quantum holonomy along density operators," Reports on Mathematical Physics **24**, 229–240 (1986).

[92] F. Wilczek and A. Zee, "Appearance of gauge structure in simple dynamical systems," Physical Review Letters **52**, 2111–2114 (1984).

[93] J. Zak, "Berrys phase for energy bands in solids," Physical Review Letters **62**, 2747–2750 (1989).

[94] D. Xiao, M. C. Chang, and Q. Niu, "Berry phase effects on electronic properties," Reviews of Modern Physics **82**, 1959–2007 (2010).

[95] L. Fu and C. L. Kane, "Time reversal polarization and a Z2 adiabatic spin pump," Physical Review B - Condensed Matter and Materials Physics **74**, 195312 (2006).

[96] R. B. Laughlin, "Anomalous quantum Hall effect: An incompressible quantum fluid with fractionally charged excitations," Physical Review Letters **50**, 1395–1398 (1983).

[97] C.-X. Liu, S.-C. Zhang, and X.-L. Qi, "The Quantum Anomalous Hall Effect: Theory and Experiment," Annual Review of Condensed Matter Physics **7**, 301–321 (2016).

[98] Y.-J. Lin and I. B. Spielman, "Synthetic gauge potentials for ultracold neutral atoms," Journal of Physics B: Atomic, Molecular and Optical Physics **49**, 183001 (2016).

[99] A. M. Turner and A. Vishwanath, "Beyond Band Insulators: Topology of Semi-metals and Interacting Phases," arXiv:1301.0330 [cond-mat.str-el] (2013).

[100] L. Lu, L. Fu, J. D. Joannopoulos, and M. Soljačić, "Weyl points and line nodes in gyroid photonic crystals," Nature Photonics **7**, 294 (2013).

[101] H. Weyl, "Elektron und Gravitation. I," Zeitschrift für Physik **56**, 330–352 (1929).

[102] S. L. Adler, "Axial-vector vertex in spinor electrodynamics," Physical Review **177**, 2426–2438 (1969).

[103] J. S. Bell and R. Jackiw, "A PCAC puzzle: π0-γγ in the σ-model," Il Nuovo Cimento A **60**, 47–61 (1969).

[104] N. Goldman, J. C. Budich, and P. Zoller, "Topological quantum matter with ultracold gases in optical lattices," Nature Physics **12**, 639–645 (2016).

[105] L. Lu, J. D. Joannopoulos, and M. Soljačić, "Topological photonics," Nature Photonics **8**, 821 (2014).

[106] L. Lu, Z. Wang, D. Ye, L. Ran, L. Fu, J. D. Joannopoulos, and M. Solja i, "Experimental observation of Weyl points," Science **349**, 622–624 (2015).

[107] Z. Lan, N. Goldman, A. Bermudez, W. Lu, and P. Åhberg, "Dirac-Weyl fermions with arbitrary spin in two-dimensional optical superlattices," Physical Review B - Condensed Matter and Materials Physics **84**, 1–16 (2011).

[108] J. H. Jiang, "Tunable topological Weyl semimetal from simple-cubic lattices with staggered fluxes," Physical Review A - Atomic, Molecular, and Optical Physics **85**, 1–7 (2012).

[109] S. Ganeshan and S. Das Sarma, "Constructing a Weyl semimetal by stacking one-dimensional topological phases," Physical Review B - Condensed Matter and Materials Physics **91**, 1–11 (2015).

[110] B. M. Anderson, G. Juzeliunas, V. M. Galitski, and I. B. Spielman, "Synthetic 3D spin-orbit coupling," Physical Review Letters **108**, 1–5 (2012).

[111] S.-Y. Xu, N. Alidoust, I. Belopolski, Z. Yuan, G. Bian, T.-R. Chang, H. Zheng, V. N. Strocov, D. S. Sanchez, G. Chang, C. Zhang, D. Mou, Y. Wu, L. Huang, C.-C. Lee, S.-M. Huang, B. Wang, A. Bansil, H.-T. Jeng, T. Neupert, A. Kaminski, H. Lin, S. Jia, and M. Zahid Hasan, "Discovery of a Weyl fermion state with Fermi arcs in niobium arsenide," Nature Physics **11**, 748–754 (2015).

[112] B. Q. Lv, N. Xu, H. M. Weng, J. Z. Ma, P. Richard, X. C. Huang, L. X. Zhao, G. F. Chen, C. E. Matt, F. Bisti, V. N. Strocov, J. Mesot, Z. Fang, X. Dai, T. Qian,

M. Shi, and H. Ding, "Observation of Weyl nodes in TaAs," Nature Physics **11**, 724–727 (2015).

[113] D. Jaksch and P. Zoller, "Creation of effective magnetic fields in optical lattices: the Hofstadter butterfly for cold neutral atoms," New Journal of Physics **5**, 56 (2003).

[114] A. R. Kolovsky, "Creating artificial magnetic fields for cold atoms by photon-assisted tunneling," Europhysics Letters **93**, 20003 (2011).

[115] H. Miyake, *[Thesis] Probing and Preparing Novel States of Quantum Degenerate Rubidium Atoms in Optical Lattices*, June (Massachusetts Institute of Technology, Cambridge, US, 2013) p. 146.

[116] P. Hosur and X. Qi, "Recent developments in transport phenomena in Weyl semimetals," Comptes Rendus Physique **14**, 857–870 (2013).

[117] G. Jotzu, M. Messer, R. Desbuquois, M. Lebrat, T. Uehlinger, D. Greif, and T. Esslinger, "Experimental realization of the topological Haldane model with ultracold fermions," Nature **515**, 237–240 (2014).

[118] N. Goldman, J. Dalibard, A. Dauphin, F. Gerbier, M. Lewenstein, P. Zoller, and I. B. Spielman, "Direct imaging of topological edge states in cold-atom systems," Proceedings of the National Academy of Sciences **110**, 6736–6741 (2013).

[119] L. Tarruell, D. Greif, T. Uehlinger, G. Jotzu, and T. Esslinger, "Creating, moving and merging Dirac points with a Fermi gas in a tunable honeycomb lattice," Nature **483**, 302–305 (2012).

[120] P. T. Ernst, S. Götze, J. S. Krauser, K. Pyka, D.-S. Lühmann, D. Pfannkuche, and K. Sengstock, "Probing superfluids in optical lattices by momentum-resolved Bragg spectroscopy," Nature Physics **6**, 56–61 (2010).

[121] C. J. Kennedy, G. A. Siviloglou, H. Miyake, W. C. Burton, and W. Ketterle, "Spin-Orbit coupling and quantum spin hall effect for neutral atoms without spin flips," Physical Review Letters **111**, 1–5 (2013).

[122] C. J. Kennedy, W. C. Burton, W. C. Chung, and W. Ketterle, "Observation of Bose-Einstein Condensation in a Strong Synthetic Magnetic Field," Nature Physics **11**, 859–864 (2015).

[123] F. Wilczek, "Quantum mechanics of fractional-spin particles," Physical Review Letters **49**, 957–959 (1982).

[124] J. M. Leinaas and J. Myrheim, "On the theory of identical particles," Il Nuovo Cimento B Series 11 **37**, 1–23 (1977).

[125] D. Arovas, J. R. Schrieffer, and F. Wilczek, "Fractional statistics and the quantum Hall effect," Physical Review Letters **53**, 722–723 (1984).

[126] B. I. Halperin, "Statistics of quasiparticles and the hierarchy of fractional quantized hall states," Physical Review Letters **52**, 1583–1586 (1984).

[127] Z. Hadzibabic, P. Krüger, M. Cheneau, B. Battelier, and J. Dalibard, "Berezinskii–Kosterlitz–Thouless crossover in a trapped atomic gas," Nature **441**, 1118–1121 (2006).

[128] B. Paredes, P. Zoller, and J. I. Cirac, "Fractional quantum Hall regime of a gas of ultracold atoms," Solid State Communications **127**, 155–162 (2003).

[129] L.-M. Duan, E. Demler, and M. D. Lukin, "Controlling Spin Exchange Interactions of Ultracold Atoms in Optical Lattices," Physical Review Letters **91**, 090402 (2003).

[130] M. Aguado, G. K. Brennen, F. Verstraete, and J. I. Cirac, "Creation, manipulation, and detection of abelian and non-abelian anyons in optical lattices," Physical Review Letters **101**, 1–4 (2008).

[131] Y. Zhang, G. J. Sreejith, N. D. Gemelke, and J. K. Jain, "Fractional angular momentum in cold-atom systems," Physical Review Letters **113**, 1–5 (2014).

[132] M. Burrello and A. Trombettoni, "Non-abelian anyons from degenerate landau levels of ultracold atoms in artificial gauge potentials," Physical Review Letters **105**, 1–4 (2010).

[133] T. A. Sedrakyan, V. M. Galitski, and A. Kamenev, "Statistical Transmutation in Floquet Driven Optical Lattices," Physical Review Letters **115**, 1–5 (2015).

[134] M. T. Batchelor, X. W. Guan, and N. Oelkers, "One-dimensional interacting anyon gas: Low-energy properties and Haldane exclusion statistics," Physical Review Letters **96**, 1–4 (2006).

[135] O. I. Pâĉtu, V. E. Korepin, and D. V. Averin, "Correlation functions of one-dimensional Lieb–Liniger anyons," Journal of Physics A: Mathematical and Theoretical **40**, 14963–14984 (2007).

[136] R. Santachiara and P. Calabrese, "One-particle density matrix and momentum distribution function of one-dimensional anyon gases," Journal of Statistical Mechanics: Theory and Experiment **06**, 5 (2008).

[137] A. del Campo, "Fermionization and bosonization of expanding one-dimensional anyonic fluids," Physical Review A **78**, 045602 (2008).

[138] Y. Hao, Y. Zhang, and S. Chen, "Ground-state properties of one-dimensional anyon gases," Physical Review A - Atomic, Molecular, and Optical Physics **78**, 1–6 (2008).

[139] T. Keilmann, S. Lanzmich, I. McCulloch, and M. Roncaglia, "Statistically induced phase transitions and anyons in 1D optical lattices." Nature communications **2**, 361 (2011).

[140] G. Tang, S. Eggert, and A. Pelster, "Ground-state properties of anyons in a one-dimensional lattice," New Journal of Physics **17**, 123016 (2015).

[141] S. Greschner and L. Santos, "Anyon Hubbard Model in One-Dimensional Optical Lattices," Physical Review Letters **115**, 1–5 (2015).

[142] C. Sträter, S. C. Srivastava, and A. Eckardt, "Floquet realization and signatures of one-dimensional anyons in an optical lattice," Physical Review Letters **117**, 1–5 (2016).

[143] A. Micheli, G. K. Brennen, and P. Zoller, "A toolbox for lattice-spin models with polar molecules," Nature Physics **2**, 341–347 (2006).

[144] S. Longhi and G. Della Valle, "Anyons in one-dimensional lattices: a photonic realization." Optics letters **37**, 2160–2 (2012).

[145] E. Kapit, M. Hafezi, and S. H. Simon, "Induced self-stabilization in fractional quantum Hall states of light," Physical Review X **4**, 1–11 (2014).

[146] E. Kapit, P. Ginsparg, and E. Mueller, "Non-abelian braiding of lattice bosons," Physical Review Letters **108**, 1–5 (2012).

[147] T. Graß, B. Juliá-Díaz, and M. Lewenstein, "Topological phases in small quantum Hall samples," Physical Review A - Atomic, Molecular, and Optical Physics **89**, 1–12 (2014).

[148] N. R. Cooper and S. H. Simon, "Signatures of fractional exclusion statistics in the spectroscopy of quantum hall droplets," Physical Review Letters **114**, 1–5 (2015).

[149] D. Lundholm and N. Rougerie, "Emergence of Fractional Statistics for Tracer Particles in a Laughlin Liquid," Physical Review Letters **116**, 1–6 (2016).

[150] E. A. Cornell and C. E. Wieman, "Nobel lecture: Bose-Einstein condensation in a dilute gas, the first 70 years and some recent experiments," (2002).

[151] B. DeMarco, "Onset of Fermi Degeneracy in a Trapped Atomic Gas," Science **285**, 1703–1706 (1999).

[152] H. R. Lewis and W. B. Riesenfeld, "An Exact Quantum Theory of the Time-Dependent Harmonic Oscillator and of a Charged Particle in a Time-Dependent Electromagnetic Field," Journal of Mathematical Physics **10**, 1458 (1969).

[153] A. Minguzzi and D. M. Gangardt, "Exact coherent states of a harmonically confined tonks-girardeau gas," Physical Review Letters **94**, 1–4 (2005).

[154] Y. S. Wu, "Multiparticle quantum mechanics obeying fractional statistics," Physical Review Letters **53**, 111–114 (1984).

[155] W.-H. Huang, "Statistical interparticle potential between two anyons," Physical Review B - Condensed Matter and Materials Physics **52**, 90–92 (1995).

[156] F. Mancarella, A. Trombettoni, and G. Mussardo, "Statistical mechanics of an ideal gas of non-Abelian anyons," Nuclear Physics B **867**, 950–976 (2013).

[157] S. C. Morampudi, A. M. Turner, F. Pollmann, and F. Wilczek, "Statistics of Fractionalized Excitations through Threshold Spectroscopy," Physical Review Letters **118**, 1–6 (2017).

[158] J. D. Jackson, *Classical Electrodynamics* (Wiley, 1998) p. 808.

[159] U. J. Wiese, "Ultracold Quantum Gases and Lattice Systems: Quantum Simulation of Lattice Gauge Theories," arXiv:1305.1602 [quant-ph] (2013).

[160] Y. E. Kraus, Y. Lahini, Z. Ringel, M. Verbin, and O. Zilberberg, "Topological States and Adiabatic Pumping in Quasicrystals," Physical Review Letters **109**, 1–5 (2012).

[161] N. K. Efremidis, S. Sears, D. N. Christodoulides, J. W. Fleischer, and M. Segev, "Discrete solitons in photorefractive optically induced photonic lattices," Physical Review E **66**, 046602 (2002).

[162] J. W. Fleischer, M. Segev, N. K. Efremidis, and D. N. Christodoulides, "Observation of two-dimensional discrete solitons in optically induced nonlinear photonic lattices," Nature **422**, 147–150 (2003).

[163] J. W. Fleischer, T. Carmon, M. Segev, N. K. Efremidis, and D. N. Christodoulides, "Observation of Discrete Solitons in Optically Induced Real Time Waveguide Arrays," Physical Review Letters **90**, 023902 (2003).

[164] D. Neshev, E. Ostrovskaya, W. Krolikowski, and Y. Kivshar, "Spatial solitons in optically induced gratings," Optics Letters **28**, 710–712 (2003).

[165] J. W. Fleischer, G. Bartal, O. Cohen, T. Schwartz, O. Manela, B. Freedman, M. Segev, H. Buljan, and N. K. Efremidis, "Spatial photonics in nonlinear waveguide arrays," Optics Express **13**, 1780 (2005).

[166] D. N. Christodoulides, F. Lederer, and Y. Silberberg, "Discretizing light behaviour in linear and nonlinear waveguide lattices," Nature **424**, 817–823 (2003).

[167] O. Peleg, G. Bartal, B. Freedman, O. Manela, M. Segev, and D. N. Christodoulides, "Conical Diffraction and Gap Solitons in Honeycomb Photonic Lattices," Physical Review Letters **98**, 103901 (2007).

[168] M. V. Berry, "Conical diffraction asymptotics: fine structure of Poggendorff rings and axial spike," Journal of Optics A: Pure and Applied Optics **6**, 289 (2004).

[169] M. G. Tarallo, A. Alberti, N. Poli, M. L. Chiofalo, F. Y. Wang, and G. M. Tino, "Delocalization-enhanced Bloch oscillations and driven resonant tunneling in optical lattices for precision force measurements," Physical Review A **86**, 033615 (2012).

[170] M. Rigol, V. Dunjko, and M. Olshanii, "Thermalization and its mechanism for generic isolated quantum systems," Nature **452**, 854–858 (2008).

[171] L. D'Alessio and A. Polkovnikov, "Many-body energy localization transition in periodically driven systems," Annals of Physics **333**, 19–33 (2013).

[172] L. D'Alessio and M. Rigol, "Long-time behavior of isolated periodically driven interacting lattice systems," Physical Review X **4**, 1–11 (2014).

[173] M. Bukov, S. Gopalakrishnan, M. Knap, and E. Demler, "Prethermal floquet steady states and instabilities in the periodically driven, weakly interacting bose-hubbard model," Physical Review Letters **115**, 1–6 (2015).

[174] T. Kuwahara, T. Mori, and K. Saito, "Floquet-Magnus theory and generic transient dynamics in periodically driven many-body quantum systems," Annals of Physics **367**, 96–124 (2016).

[175] A. Eckardt and E. Anisimovas, "High-frequency approximation for periodically driven quantum systems from a Floquet-space perspective," New Journal of Physics **17**, 93039 (2015).

[176] R. Nandkishore and D. A. Huse, "Many-Body Localization and Thermalization in Quantum Statistical Mechanics," Annual Review of Condensed Matter Physics **6**, 15–38 (2015).

[177] A. Lazarides, A. Das, and R. Moessner, "Equilibrium states of generic quantum systems subject to periodic driving," Physical Review E - Statistical, Nonlinear, and Soft Matter Physics **90**, 1–6 (2014).

[178] M. Girardeau, "Relationship between Systems of Impenetrable Bosons and Fermions in One Dimension," Journal of Mathematical Physics **1**, 516–523 (1960).

[179] M. D. Girardeau and E. M. Wright, "Dark solitons in a one-dimensional condensate of hard core bosons," Physical Review Letters **84**, 5691–5694 (2000).

[180] A. Lenard, "Momentum Distribution in the Ground State of the One-Dimensional System of Impenetrable Bosons," Journal of Mathematical Physics **5**, 930–943 (1964).

[181] R. Pezer and H. Buljan, "Momentum distribution dynamics of a Tonks-Girardeau gas: Bragg reflections of a quantum many-body wavepacket," Conference on Quantum Electronics and Laser Science - Technical Digest Series **240403**, 1–4 (2007).

[182] M. Bukov and A. Polkovnikov, "Stroboscopic versus nonstroboscopic dynamics in the Floquet realization of the Harper-Hofstadter Hamiltonian," Physical Review A - Atomic, Molecular, and Optical Physics **90**, 1–9 (2014).

[183] P. Jordan and E. Wigner, "Über das Paulische Äquivalenzverbot," Zeitschrift für Physik **47**, 631–651 (1928).

[184] M. Rigol and A. Muramatsu, "Emergence of quasicondensates of hard-core bosons at finite momentum," Physical Review Letters **93**, 230404 (2004).

[185] M. Rigol and A. Muramatsu, "Fermionization in an expanding 1D gas of hard-core bosons," Physical Review Letters **94**, 1–4 (2005).

[186] F. Meinert, M. J. J. Mark, K. Lauber, A. J. J. Daley, and H.-C. Nägerl, "Floquet Engineering of Correlated Tunneling in the Bose-Hubbard Model with Ultracold Atoms," Physical Review Letters **116**, 1–5 (2016).

[187] Á. Rapp, X. Deng, L. Santos, A. Rapp, X. Deng, and L. Santos, "Ultracold lattice gases with periodically modulated interactions," Physical Review Letters **109**, 1–5 (2012).

[188] H. Metcalf and P. van der Straten, "Laser cooling and trapping of atoms," Journal of the Optical Society of America B **20**, 887–908 (2003).

CHAPTER 6

Curriculum vitae

Tena Dubček was born on March 25, 1990 in Zagreb (Croatia). In 2013, she obtained her Master's degree in Physics from the Department of Physics, Faculty of Science, University of Zagreb, as first in class, for which she received the Commendation of the Faculty of Science for outstanding achievements. Since 2014, she stayed to work as a research and teaching assistant, in the group of Hrvoje Buljan. She spent the year 2016/17 as a Fulbright researcher at Massachusetts Institute of Technology (USA), in the group of Marin Soljačić and John Joannopoulos. She co-authored 6 papers in journals cited in the Web of Science and one which is currently under review, being the first author on four of them. She presented her work at more than 10 international scientific conferences or workshops, also receiving awards for her presentations. She participated in the organization of the international Workshop on topological and synthetic gauge fields for atoms and photons (Zagreb, 2015), and several outreach programs of the Physics department, where she also founded and is currently organizing the weekly Seminars of doctoral students. In 2012, she received the CERN studentship, awarded to a single student from Croatia. She is the recipient of the Faculty Council recognition for achievements in scientific and professional work, awarded by the Faculty of Science of the University of Zagreb (2016), and the Fulbright scholarship, awarded by the U.S. Department of State's Bureau of Educational and Cultural Affairs (2016). In 2017, she was awarded the national scholarship "For women in Science".

List of publications:

- <u>T. Dubček</u>, B. Klajn, R. Pezer, H. Buljan, and D. Jukić,
  Phys. Rev. A Rapid Comm., accepted for publication.

- N. Šantić, <u>T. Dubček</u>, D. Aumiler, H. Buljan, and T. Ban,
  Opt. Soc. Am. B **34**, 1264 (2017).

- L. Jing, Y. Shen, <u>T. Dubček</u>, J. Peurifoy, S. Skirlo, Y. LeCun, M. Tegmark, and
  M. Soljačić, arXiv:1612.05231 (2016).

- K. Lelas, N. Drpić, <u>T. Dubček</u>, D. Jukić, R. Pezer, and H. Buljan,
  New J. Phys. **18**, 095002 (2016).

- <u>T. Dubček</u>, K. Lelas, D. Jukić, R. Pezer, M. Soljačić, and H. Buljan,
  New J. Phys. **17**, 125002 (2015).

- N. Šantić, <u>T. Dubček</u>, D. Aumiler, H. Buljan, and T. Ban,
  Sci. Rep. **5**, 13485 (2015).

- <u>T. Dubček</u>, C. J. Kennedy, L. Lu, W. Ketterle, M. Soljačić, and H. Buljan,
  Phys. Rev. Lett. **114**, 225301 (2015).

- <u>T. Dubček</u>, N. Šantić, D. Jukić, D. Aumiler, T. Ban, and H. Buljan,
  Phys. Rev. A **89**, 063415 (2014).

Hrvoje Buljan is a Professor at the Physics department of the University of Zagreb. His main research interests are in (nonlinear) optics and photonics, graphene plasmonics and ultracold atomic gases. He is a co-author of 65 publications, with more than 2300 citations, and he has been invited to give more than 40 invited talks at conferences, workshops, scientific institutes and universities around the world. He has mentored 3 defended PhD theses, with 3 additional underway, as well as more than 28 diploma theses. He leads/lead 8 grants (5MEUR project funded by the European Structural and Investment Funds 2017, Scientific Center of Excellence for Quantum and Complex Systems and Representations of the Lie Algebra 2015, Pseudomagnetic forces and fields for atoms and photons funded by the Unity through Knowledge Fund 2013, Nonlinear phenomena and wave dynamics in photonic systems funded by the Ministry of Science in Croatia 2007), and participated in others. In 1995, he was awarded Rector's Award by the Rector of the University of Zagreb. He co-authored the most cited Phys. Rev. B paper published in 2009 (according to WoS). He is the recipient of the Annual State Award for Science, awarded by the Croatian parliament (2010).

Marin Soljačić is Professor of Physics at Massachusetts Institute of Technology (USA). His main research interests are in electromagnetic phenomena, focusing on nanophotonics, non-linear optics, and wireless power transfer. He is a co-author of more than 200 scientific articles, more than 100 issued US patents, and he has been invited to give more than 100 invited talks at conferences and universities around the world. He is the recipient of the Adolph Lomb medal from the Optical Society of America (2005), and the TR35 award of the Technology Review magazine (2006). In 2008, he was awarded a MacArthur fellowship "genius" grant. He is an international member of the Croatian Academy of Engineering since 2009. In 2011 he became a Young Global Leader (YGL) of the World Economic Forum. In 2014, he was awarded Blavatnik National Award, as well as Invented Here! (Boston Patent Law Association). In 2017, he was awarded "The Order of the Croatian Daystar, with the image of Ruđer Bošković", the Croatian President's top medal for Science. In 2017, the Croatian President also awarded him with "The Order of the Croatian Interlace" medal.